"INTERACTION OF DROPS FALLING INTO VOLATILE LIQUIDS"

by

GORDON POOL

Submitted for the Degree of

DOCTOR OF PHILOSOPHY

at the University of Aston in Birmingham

July 1980

INTERACTION OF DROPS FALLING INTO VOLATILE LIQUIDS

GORDON POOL

Submitted for the Degree of PhD July 1980

SUMMARY

The incidence of explosive melt-coolant interactions (MCIs) has prompted widespread research in an attempt to explain their cause. The conditions under which such explosions may occur is the subject of the present work.

Experiments have been performed both in the laboratory and in the field using different melts and usually water as the coolant. On the small scale, molten tin, lead, aluminium and copper metals have been dropped in small, reproducibly-sized quantities ($\simeq$0.25 g), into perspex containers of water and occasionally different coolants. Other melts used have been molten sodium chloride and copper (I) iodide. In the field, larger amounts of melt (up to 5 kg) have been poured into mild steel containers of water. The melts have included copper, iron, nickel, magnox and sodium chloride.

Photographic techniques were used to observe the MCIs and in addition, a hydrophone has monitored pressure fluctuations in the coolant on the small scale. The photographic techniques were three-fold: high speed photography, stroboscopically illuminated photography and short exposure, spark-illuminated photography.

The effect of a pressure pulse within the coolant was also studied for both small and large melt masses. The result was very often an explosion under otherwise non-explosive conditions.

Also,observation was made of a spark-induced steam bubble generated in water at different temperatures. This may help to throw light on the existence of a coolant critical temperature above which explosions fail to occur.

MELT
COOLANT
THERMAL
EXPLOSIONS
SAFETY

ACKNOWLEDGMENTS

I would like to express my gratitude to Professor F M Page and Professor W O Alexander for their kind help during my research at Aston. I also thank the Health and Safety Executive for sponsoring my work, and the many staff and students within the Department of Chemistry whose friendship and assistance have proven invaluable.

LIST OF TABLES

LIST OF FIGURES

LIST OF PLATES

LIST OF CONTENTS

CHAPTER ONE

INTRODUCTION

There are times when it proves necessary to cool down one liquid in another on an industrial scale. In by far the majority of cases, the cooling process takes place without any violent disturbance to the system. Occasionally, however, the conditions are such that a more rapid interaction may occur and this is explosive in nature.

The hot liquid, sometimes called the melt, can be at a high enough temperature to cause coolant to vaporise. Whereas this vaporisation usually occurs at the boundary between the two liquids, it is possible for vapour to be generated within the melt after liquid coolant has penetrated the boundary. As water, for example, increases its volume by over twelve hundred times on changing into steam, a phase change within the melt would cause it to break up extensively. Add to this the fact that such a transformation occurs in the order of a thousandth of a second by virtue of the heattransfer rates involved, and it is easy to see why such an event is called a 'vapour explosion'.

A number of systems exist which are liable to produce explosive melt-coolant interactions (MCI's) but by far the most widespread is the quenching of molten metals in water. Historically, a number of incidents have occurred. During the early days of

smelting at Coalbrookdale[1], near Ironbridge, the Old Furnace exploded after a cloudburst caused a pool dam to break and flood it. Although there was no loss of life, all buildings in the area were destroyed. Another explosion, this time at Sheffield,[2] caused at least fifteen fatalities, many of them young children.

Modern metallurgical processes also bring molten metal and water into close proximity. Metal is sometimes melted in water-cooled furnaces and also solidified, a technique known as continuous casting. The continuous casting process demands that metals be cooled rapidly to maintain good grain structure and composition. It is in operation all over the world and rarely causes any danger. A mould keeps the two liquids apart but any fracture can lead to them mixing and becoming potentially explosive.

During the period 1950-1960, reports were received from the USA, Spain and the UK describing explosions which had occurred during the continuous casting of aluminium. These explosions resulted from the accidental mixing of molten aluminium and water and some of them were so violent as to be called catastrophic. They resulted in fatalities, in serious injuries and in hundreds of thousands of pounds worth of damage to plants and buildings. In spite of the fact that accurate statistics are not available, some indication of the hazard and the damage caused can be given. A Japanese professor[3] at the University of Toyama quoted 261 known explosions in Japan during the 36 years from 1935 to 1970. These explosions resulted in 80 fatalities and 800 injuries. The

Japanese reports refer to liquid slag and water explosions as well as to liquid metal and water explosions.

The Aluminium Association of America collected such records as they could find[4] for the period 1944-75. The list is acknowledged to be incomplete, and, since members of the Association could more easily obtain information from their own industry, it is concerned primarily with aluminium explosions. It does, however, include iron, steel, copper, magnesium and zinc. This list recorded 75 explosions in North America during the 31 years and shows that 32 people were killed and 300 injured.

In the UK, despite restricted notification of accidents, there were 327 reported explosions of molten metal in 1975.

The kind of damage that may result from an explosive MCI may be illustrated by a liquid steel and water explosion in Quebec[5]. The incident occurred when about 45 kg of liquid steel fell into a trough containing about 350 litres of water. The explosion cracked the concrete floor of the building which was half a metre thick and damaged adjacent furnaces. A 60 m section of exterior wall opposite to the furnace and a 15 m section at the end of the building 50 m from the furnace had to be rebuilt. Another 300 m of wall (just under half a metre thick) needed repair as did a short section of wall at the corner diagonally opposite to and 200 m from the trough. In addition to this, skylights were raised over a 5000 m^2 area, the metal frames buckled and 6000

panes of glass were broken. The shock wave accompanying the explosion damaged a boiler house located 23 m from the building. Witte et al[6] have obtained some heat transfer data from this incident and their calculations have produced the high rate of 10^{10} BTU/Hr/ft^2. They compare this to the heat transfer rate during boiling which rarely exceeds 10^7 BTU/Hr/ft^2.

An aluminium explosion may be quoted[7] in which the explosive force was estimated as the equivalent of 250 kg of TNT in which the whole foundry was wrecked, five persons were killed and 33 injured. On the other hand, the result of the interaction between molten metal and cooling water may be so trivial as hardly to warrant the term 'explosion' and such incidents are often described by the term 'sputtering'. But even this small sputtering may result in burning injuries or in the loss of an eye.

The most recent major incident in the UK occurred at Scunthorpe[8] in 1975. The accident happened at the British Steel Corporation's plant and a total of 11 people were killed. The incident occurred because of the failure of a blast furnace cooling pipe and the water found its way, via a tortuous path, into an insulated rail torpedo containing some 200 tons of molten steel. On seeing the water running into the torpedo, the shift manager ordered a shunting engine to be brought to remove the torpedo. When the engine started to pull the steel container, a violent explosion occurred which ejected 180 tons of molten steel into the environment. The explosion is thought to have resulted from the

intermixing of molten steel and water when the initial surge on moving disturbed the slag layer which was separating the two liquids.

The overall scope of the hazard in the UK is evident from the fact that some 40 to 50 million tonnes of metal are melted annually and it is to be remembered that cooling water is extensively used in the melting and treating of these considerable quantities of metal.

It was with a view to minimising the risks involved in the melting and treating of metals that the Americans initiated a research programme designed to identify the conditions which gave rise to catastrophic explosions when molten aluminium came into contact with cooling water. The first empirical work was published in 1957 by Long[9]. Early research was concentrated upon aluminium because the explosive nature of the finely divided metal was well-known. However, Long's extensive series of experiments soon established that a vapour-explosion was very different to a so-called dust explosion.

He carried out a comprehensive set of 880 tests during which he dropped quantities of molten aluminium into a welded steel tank containing coolant water. In order to estimate the conditions which favour an explosive interaction, Long varied metal temperature, dropping height, water depth and water temperature. His results indicated that for aluminium, an explosion

occurred only after the metal had spread onto the container base, not as it fell through the water. Subsequent work has shown that some metals do explode as they fall through the water but others will only after they have fallen onto an independent surface.

Amongst other things, Long concluded that water became trapped between the container base and the metal, and it was the rapid vaporisation of this coolant which constituted an explosion. His entrapment hypothesis was supported by the experimental observation that a smooth surface to the container succeeded in suppressing an explosion, whilst an oxide covered surface encouraged one.

His other major discovery was that coolant temperature tended to determine whether an interaction was violent or not. Warm water (60-100^{o}C) did not sustain any explosions whereas cool water (0-50^{o}C) did. These phenomena, together with others such as the degree of breakup of the aluminium before coolant entry (ie the drop height) served to enable Long to formulate certain criteria which, when abided by, would minimise the dangers associated with aluminium casting.

From this moment on, an interest had been stimulated amongst researchers throughout the world and programmes of investigation were sponsored to confirm and extend the initial observations on the aluminium/water system. Working with large masses of the

metal (between 4.5 and 18 kg), Laber and Lemmon[10] obtained results very similar to those of Long. The base involvement has led two German scientists, Maischak and Feige[11], to propose a possible chemical explanation for the explosions. Their theory is that the base contaminants are very often oxygen-containing compounds such as rust and calcium hydroxide which on reduction by aluminium can create local temperatures high enough to generate hydrogen gas:

$$Fe_2O_3 + 2Al \longrightarrow Al_2O_3 + 2Fe \quad \text{exothermic}$$

$$2Al + 3H_2O \longrightarrow Al_2O_3 + 3H_2 \quad \text{exothermic}$$

The hydrogen gas explodes on ignition in air.

However, the widely held belief of workers researching all fields of MCI systems is that an explosion is essentially a physical phenomenon and not chemical. Epstein[12] has studied the kinetics involved if such an explosion were chemical in nature. His calculations indicated that the only way in which the very short reaction times associated with an explosion could be explained was to assume that every water molecule striking the melt surface reacted to form oxide and liberate hydrogen gas. Undoubtedly this is a limiting case kinetically, that would be a highly improbable event in nature.

Many workers since Long have investigated molten metal-water

explosions. They have used various quantities of metal (ranging from small droplets as used by Brauer et al[13] and Flory et al[14] to the previously mentioned large masses) and also different types of metal. Over the years, it has become clear that MCIs of an explosive kind may result from every molten metal and water under appropriate thermal conditions. The work undertaken by Genco and Lemmon[15] using molten aluminium, molten pig iron and molten slag was intended to observe industrially commonplace materials, whereas Witte et al[16] have extended the range of melts to molten zinc, molten bismuth, molten tin and mercury. Genco and Lemmon[15] determined a ratio of coolant weight to melt weight of between 1:10 and 1:5 as being most explosive. Witte et al concluded that the rapid heat transfer requiring substantial melt surface area enhancement was the key to explosive interaction. They also considered that the collapse of the coolant vapour layer surrounding the melt was the indirect cause of the breakup.

More recently, the copper-water system has been assessed by Zyszkowski[17]. His work was with small amounts of molten copper and his conclusions were that forces produced on the molten interior of a solidifying drop help it to fragment.

Bradley and Witte[18] have performed experiments using hot molten jets of metal sprayed into cool water. They argue that such an arrangement ensures a reproducible sample configuration and relative velocity between melt and coolant. They employed

a high speed photographic technique to observe an interaction as did Paoli and Mesler[19] who looked at lead cooling in water at framing rates up to 8000 f/s.

Although the molten metal-water system is the most prevalent for violent interaction, it is by no means the only one. Jennings[20] quotes several examples where hot and cold liquids became intermixed with disastrous results. One incident concerned the loading of a road tanker with hot tar at a temperature a little below 100°C. When the barrel was approximately half full, the pump failed and the tar line to the barrel was blown out with steam in accordance with normal practice. In order to fill his tanker barrel with tar, the driver went to another site to have the barrel topped up. Here, however, the tar was at a temperature around 150°C and a few seconds after filling commenced, the hot tar erupted from the barrel manhole. The accident was attributed to the steam condensate which had settled on the surface of the first batch of tar and when the fresh hot tar was pumped on top of it, the water became entrapped and evaporated forming enormous volumes of steam which ejected the tar out of the tank.

Another example quoted concerned a process in which an oil of density less than one which contained small quantities of water, was being treated in a vessel to drive off the water vapour prior to carrying out a reaction. The water and oil were immiscible and the water thus tended to settle at the base of

the tank. The process was commenced and the heating fluid in the heater coils was around 250°C. It was noticed during the early stages of the process that the manhole was partly open and after heating for some time the operator noticed he had neglected to start the agitator. On doing this, large quantities of oil were ejected with considerable force and the ejection continued until only approximately one quarter of the original contents were left in the vessel. It was assumed that the accident was caused by the stratification of the oil and water which allowed the oil to be heated to high temperatures without affecting the water layer. The starting of the agitator broke up the separate layers and forcibly mixed the hot oil with the water to produce a vapour explosion. It was stated that even if the agitator had not been started, the result would have been the same on the basis that at some stage, conduction across the interface would have raised the water temperature sufficiently to induce boiling and the associated disturbance resulting from the boiling would have produced the necessary intermixing of oil and water.

A similar incident was described by Keey[21] at a Chemical Engineering Symposium in 1977. In this case, an accident took place at a New Zealand works involved in greasemaking, the re-refining of used oils and other allied operations, in which an explosion occurred in one of the vessels used for drying waste oils. The result of this was an intense fire which destroyed the factory and killed five process workers. The process of re-refining the used oil consisted of heating the oil up to 220°C

to drive off water and the light hydrocarbon fractions. At the time of the incident the vapour scrubbing system was being tested and the vessel was charged with about 7500 litres of wet waste oil. The heating system was started the following day and after the contents had reached 102°C, the plant was shut down owing to a fault in the scrubbing system. It took five days to repair the fault and the vessel was left charged with oil. On the sixth day the drying process was restarted and when the oil was at about 177-180°C, the vessel exploded. The accident was assumed to be due to the separation of oil and water with the result that about 60 litres of water became covered by a thick sludge of poor thermal conductivity. It was estimated that on the basis of thermal conduction, the water would have reached its critical flashing condition at the time of the incident. The pressure produced by the explosion was estimated at 80 atmospheres with only 20 atmospheres being required to burst the vessel.

In the oil and natural gas industries, only a few incidents have been reported. Hughes[22] documents several instances where large heavy oil storage tanks were destroyed by the sudden vaporisation of water which had become entrapped in the hot oil. The water was believed to have entered the storage tanks through open roof vents or through condensation of water vapour in the air which enters the tank during tank breathing and pump-out periods. In one of the incidents, the oil was heated to around 137°C when the tank erupted.

Liquified natural gas spillages onto water constitute another system capable of producing explosions. This time, the water is the 'melt' and the LNG the coolant. The US Bureau of Mines first recognised the problem when they carried out a series of investigatory experiments. During these[23], two unexpected explosions occurred with no sign of ignition of the vapour. The first incident was on a relatively small scale with an explosion occurring approximately 3 seconds after the LNG-water contact which destroyed the apparatus. The second incident involved pouring about 70 gallons of LNG onto water. The explosion produced little damage to the container but was esimtated to have been equal to about 1 stick of dynamite. Enger and Hartman[24,25] have simulated mild explosions using LNG which is a mixture of hydrocarbons with boiling points ranging from -161°C (methane) to -11°C (isobutane). They observe stable film boiling between the LNG and water at first but as the lighter hydrocarbon fractions boil off, this changes to transition boiling with minor explosions accompanying it. When the water temperature was low, ice formed and explosions failed to occur. In the molten metal-water system the analogy may be drawn with hot water enabling metal solidification before film boiling breaks down. Workers such as Boyle[26], Rausch and Levine[27] and Katz and Sliepcevich[28] propose that the explosions may be explained by sudden vaporisation of superheated LNG. They observe that the LNG/water interface lacks nucleation sites so that superheating may readily take place. Board et al[29] have noted that freon and R-22 gas spread easily on cold water providing favourable conditions under

which the temperature of spontaneous nucleation of liquid approaches the temperature of homogeneous nucleation of liquid.

Enger and Hartman[30] have attributed this phenomenon to other explosions which occurred experimentally at the Bayou Long Waterway in Louisiana in 1956 and at Amarillo, Texas. The most documented incident seems to be that which occurred during the freezedown of the Transco frozen in-ground storage cavern at Hackensack, New Jersey in 1965. Here, a large cavern, approximately 56.6×10^3 m^3 was being prepared to store LNG. The system adopted was to grout the lower part of the cavern and freeze-seal the upper part by spraying with LNG. It was discovered that water was leaking into the lower part of the cavern at a rate of 50 gallons per minute but it was assumed that the LNG would freeze the cavern sufficiently quickly to prevent further leakage of water. This did not happen and a series of explosions shook the cavern roof and forced open all the safety vents. During these explosions (of which 10 occurred during the first 3 days) the cavern pressure rose from an average 2 inches of water to 15 inches of water within a few seconds.

A third industry susceptible to explosive MCIs is the paper and pulp industry. It has a long history of industrial accidents in the soda recovery operation of the pulp making process. In 1955, Sallock[31] reported an incident in a soda recovery furnace which caused extensive damage to the dissolving tank (4.3 m diameter by 3.6 m high), which was vented to the atmosphere

through a 1 m diameter stack. This explosion was attributed to the inadequacy of the smelt shattering spray equipment to deal with overload surges of smelt when the boiler was incorrectly operated. This resulted in large build-ups of smelt dropping into green-liquor with a resultant explosive MCI. Further investigations by Nelson and Kennedy[32,33] on similar incidents led them to believe that the explosions were definitely physical and not chemical in nature. In 1962, as a result of the increased frequency and severity of these recovery boiler explosions, the Black Liquor Recovery Boiler Advisory Committee (BLRBAC) was set up to try and improve the safety of these operations. In 1970, Osborne[34] reported on the problem of failed boiler tubes which allowed water to come into direct contact with molten smelt. Taylor and Gardner[35] give a comprehensive survey of the causes of boiler incidents and quote a total of 59 accidents resulting from smelt-water explosions between 1948 and 1973.

In the nuclear industry, water cooled research reactors have in the past been subject to destructive MCIs. The first accident involved the Canadian NRX Reactor at Chalk River in 1952. Hurst[36] notes that the damage resulted from a failure in the shut-down rod system due to operating errors and mechanical defects. The incident was a direct cause of either a uranium-steam or a uranium-water interaction of a non-chemical nature.

In 1954, the BORAX 1 reactor was being used at the Argonne

National Reactor Testing Station in Idaho to investigate safety factors. On being subjected to severe thermal conditions, a thermal explosion occurred which resulted in the complete destruction of the reactor vessel with the bunker housing also being breached. An area of more than 800 metres was contaminated on the downwind side of the reactor building. Whilst instrumentation did not record the full transient conditions, an estimate of the internal pressure generated of 690 atmospheres was made from the damage caused. Analysis of film records suggests that the work done by the explosion was equivalent to somewhere between 6 and 17 lbs of TNT. This time, the interaction was thought to be between the molten fuel plates (made of a uranium-aluminium alloy) and the circulating water.

A similar accident to the BORAX 1 reactor incident occurred on the same site some six years later in 1961. It involved the SL-1 reactor[38,39] which was an experimental, lower power, natural circulation boiling water reactor. It is believed that the withdrawal of a control rod led to a nuclear excursion, fuel element failure and a violent interaction between molten fuel and water. Once again, it was a uranium-aluminium alloy which interacted with water in the reactor. Such a system has been discussed by workers such as Thompson[40], Hatfield[41] and Hurst[36].

A fourth occurrence[42] within a nuclear reactor took place in 1962 in the SPERT ID reactor, once again in the USA. This again

was a small, natural circulation boiling water reactor but this time, the core was immersed in an open tank of water and not contained in an enclosed vessel. As reported by Miller et al[43] the explosion was extremely rapid with only a small quantity of aluminium oxide being subsequently collected. This further emphasises the likelihood that such a thermal explosion is of a physical nature. Elgert et al[44] had previously monitored aluminium-water interactions in a sealed container. Their high pressure values (23000 psi) and rapid time scale (1-3 ms) together with the small amount of aluminium oxide retrieved (0.2%) serve as confirmatory evidence of a purely physical phenomenon.

In the more modern liquid metal fast breeder reactors, the possibility exists of some sort of violent MCI. This time, the uranium fuel elements may overheat and fuse a layer of oxide on their surface. This, in turn, may come into contact with liquid sodium metal which is used to efficiently remove heat from the system. As yet, no accidents have been reported but programmes of experimental investigation[31,40,41,45-53] are being conducted to minimise the risk of large-scale radioactive contamination which might result from an explosive MCI in a LMFBR.

As a final example of an explosive MCI, Colgate and Sigurgeissen[54] have proposed that the famous Krakatoa incident which devastated an area of the South Seas was, in part,

a consequence of hot and cold liquids intermixing. It is difficult to explain the extensive amount of damage which resulted by a volcanic eruption alone. What may have happened, is that molten lava and sea water were brought into contact with one another to create a huge explosion.

Whilst research to date has been far-reaching, the exact way in which an explosive MCI occurs, that is to say how coolant becomes intimately mixed with the melt, has yet to be fully understood. Some mathematical modelling has been attempted together with lengthy computer programs[55,56] to try and predict all explosive conditions. These attempts do not as yet consider all possible events in a melt-coolant situation.

The work undertaken and reported in this thesis was sponsored in the hope that a better understanding of the conditions under which an explosive MCI occurs might be determined. Work was chiefly carried out using the molten metal-water system as it is by far the most commonplace situation arising on an industrial scale. As mentioned previously, the physical parameters involved in an MCI are many, so by a variety of monitoring techniques, it was intended to assess their relevance to the explosive situation. Both small-scale and large-scale investigations have been made using different metals and sometimes alternative coolants. These have been observed photographically and monitored hydrophonically, and the results have been interpreted in an attempt to improve the understanding of MCIs in general. The

experiments have considered the high melting point metals such as copper, aluminium and iron as well as the lower melting point metals, such as tin and lead. Besides the natural mixing of melt in coolant, some work was carried out during which a pressure pulse was applied to the system to see if there was any modification of the cooling process.

CHAPTER TWO

THEORETICAL ASPECTS

In this Chapter, consideration is given to some of the theoretical aspects which are of relevance to explosive MCIs. Firstly, an account is presented of how a coolant such as water behaves when it is heated up by a hot surface. Such a temperature rise may cause a change of phase in the coolant and create substantial disturbances near to the hot surface (in the case of MCIs, the melt surface). The manner in which such disturbances produce explosions has provided a number of theories and these are discussed in Section 2.2. Section 2.3 outlines the objectives of the present work.

2.1 Coolant Characteristics at Elevated Temperatures

When a surface is exposed to a liquid and maintained at a temperature above the saturation temperature of the liquid, boiling may occur, and the heat flux will depend upon the difference in temperature between the surface and the saturation temperature. The curve which relates heat flux to this temperature difference is known as a boiling curve. Such a curve is traced in Fig 1.

In the region labelled 'convective heat transfer', free-convection currents are responsible for the motion of the fluid

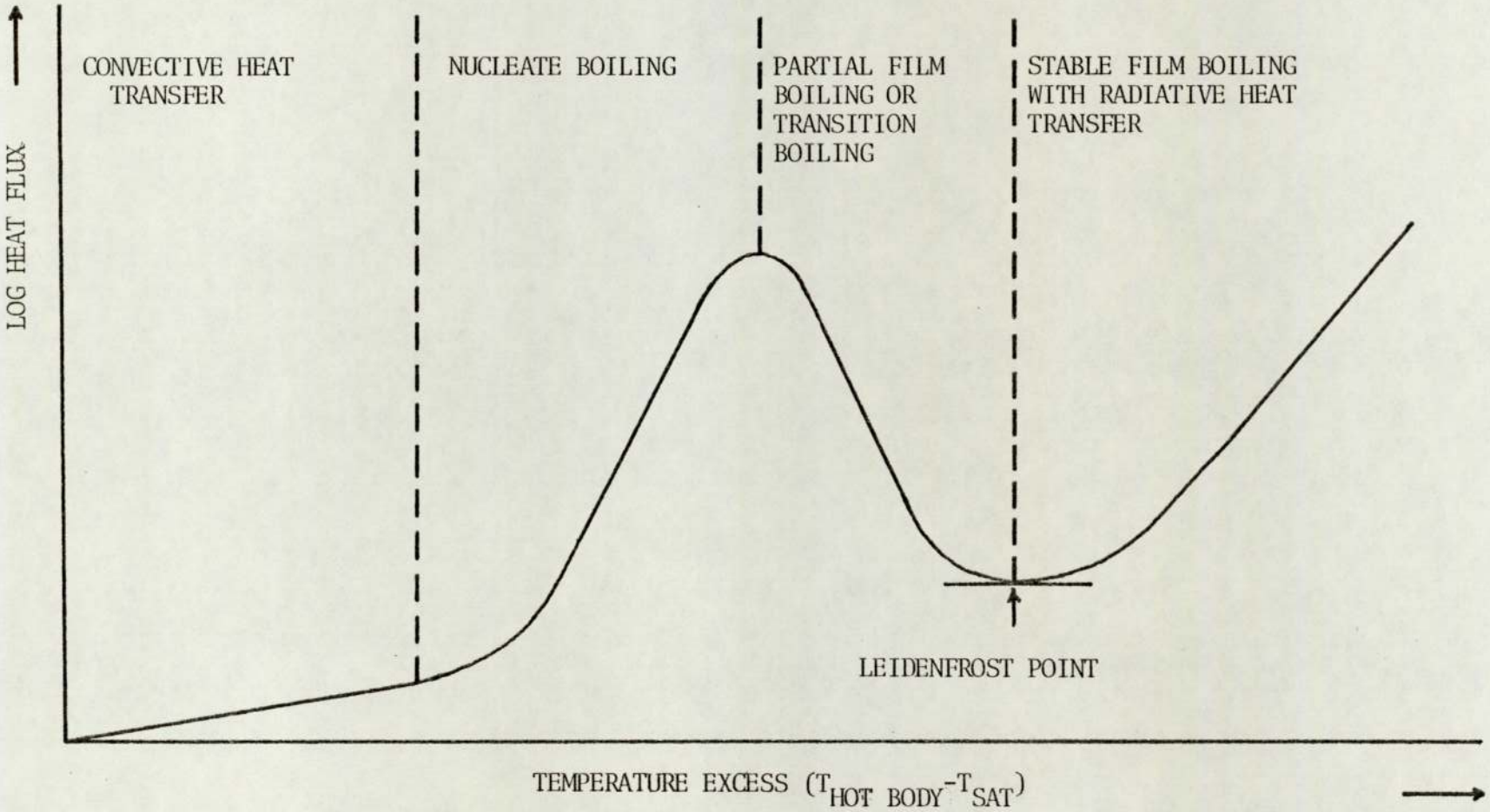

Fig 1 A typical boiling curve for a liquid showing how the heat transferred from a hot body varies with temperature difference

near the surface. At this stage, no vapour bubbles are present in the liquid. When first they do appear (moving along the curve) they are dissipated in the liquid after leaving the heating surface. These bubbles act as agitators of the liquid and serve to assist the transfer of heat to it. Their formation, as outlined by Cole[56], may be due to small impurities in the liquid (such as dust or dissolved gas) or small imperfections on the heating surface. By carrying out a simple force balance (see Fig 2) on a bubble radius r in a liquid of surface tension, σ, the vapour pressure inside and the liquid pressure outside are related by:

$$r^2 (P_V - P_L) = 2\sigma r$$

$$P_V - P_L = \frac{2\sigma}{r} \qquad \ldots(2.1)$$

This result implies that for $r \rightarrow 0$, $(P_V - P_L) \rightarrow \infty$, ie a bubble can never be created.

Let us assume that the temperature of the vapour inside the bubble is the saturation temperature corresponding to the pressure, P_V. If the liquid is at the saturation temperature corresponding to the pressure P_L, it is below the temperature inside the bubble. Consequently, heat must be conducted out of the bubble, the vapour inside must condense, and the bubble must collapse. This is the phenomenon which takes place when

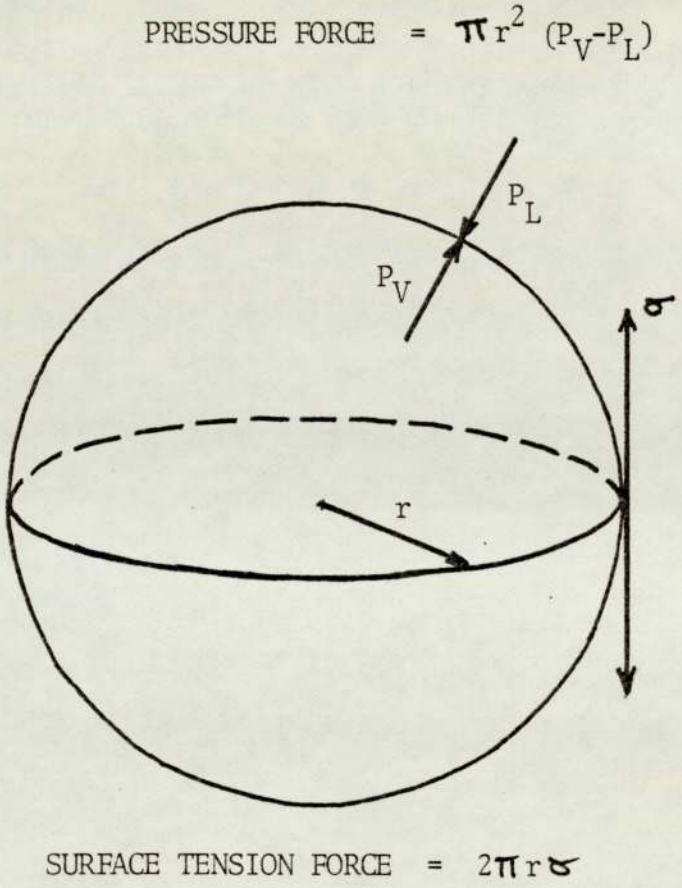

Fig 2 Force balance on a vapour bubble

bubbles collapse on the heating surface or in the body of fluid. In order for the bubbles to grow and escape from the heating surface, they must receive heat from the liquid. For this to happen, the liquid must be in a superheated condition (Wismer[57]) so that the temperature of the liquid exceeds that of the vapour within a bubble. This is a metastable state for the liquid[58-60] but it is observed experimentally (Rogers and Mesler[61]). The large heat transfer rates associated with nucleate boiling are brought about by microconvection in the superheated liquid sublayer. The strong agitating action of the vapour bubbles[62,63] created enables a calculation of heat flux to be made (Zuber[64,65]).

Zuber's formula is:

$$Q/A = K\Delta T^n \qquad \ldots(2.2)$$

where: Q/A is the heat transferred per unit area

K is a constant (it includes such constants as the Reynolds number and the Prandtl number)

ΔT is the superheat temperature difference

n may take the value of 3 to 24 for the same solid-liquid combination at constant pressure depending upon the solid surface roughness, ie nucleating characteristics

At some point, the efficiency with which vapour bubbles take

heat away from the heating surface reaches a maximum. Whereas before, fresh liquid took the place of departing vapour bubbles, now bubbles are formed so rapidly as to prevent this. Instead, the bubbles start to coalesce and partial film boiling or transition boiling commences. This highly unstable boiling regime has been described by Berenson[66] as 'a combination of unstable film boiling and unstable nucleate boiling alternately existing'. (Also Bankoff and Mehra[67]). Conflict has arisen as to whether there is any physical contact between the heating surface and the liquid during transition boiling. The photographic observation by Westwater and Santangelo[68] indicates no contact whereas work carried out by Bradfield[69] on quenching heated solid spheres indicates that there is. Indeed, Bradfield goes on to suggest that there is even contact during film boiling.

As may be seen from the boiling curve, heat flux decreases during transition boiling as the temperature of the heating surface increases. On reaching the minimum heat flux value, the so-called Leidenfrost[70] point, the formation of a stable vapour blanket over the heating surface takes place. A rise in surface temperature now produces a rise in heat flux across the vapour layer. The heat is transferred from the heating surface first to vapour molecules which then condense at the liquid-vapour interface and serve to raise the liquid temperature. Only at much higher temperatures does

the heat transfer process become modified to permit a radiative mechanism. The temperature at which stable film boiling begins is sometimes called the foam limit of the liquid (Spiegler et al[71]).

Heat transfer during stable film boiling is less than that during nucleate boiling because the vapour film tends to act as an insulator separating the heating surface from the liquid. Once a film has been formed, heat is transferred independently of the surface material, cleanliness and roughness providing the film thickness is greater than the roughness height (Berenson[66]). Formulae for the calculation of heat flux during stable film boiling have been derived by Bromley[72] (horizontal tube heating surface), Berenson[73] (horizontal plate heating surface) and Hsu and Westwater[74] (vertical plate heating surface).

Sometimes the terms 'subcooling' and 'saturated boiling' are used. Subcooling refers to the difference in temperature between the saturation temperature of the liquid and its bulk temperature. When the bulk temperature of the liquid is less than the saturation temperature 'subcooled boiling' takes place. When there is no subcooling, ie all of the liquid is at saturation temperature, 'saturated boiling' occurs. The temperature difference between the heating surface and the liquid's boiling point is often referred to as the superheat.

Many workers[75,76] have observed the manner in which a hot solid sphere is quenched in water. Thermocouples are incorporated into the spheres so that a temperature-time plot may be made. High speed photography has also been used to monitor the different boiling regimes. Walford[77], in carrying out quenching experiments on a nickel sphere in water, has identified an 'expansion cavity' phenomenon in slightly subcooled coolant (80-95°C). A large spherical shell was formed around the sphere which collapsed and reformed after liquid-solid contact had been made. He also found that heat flux across the vapour interface increased by 30% when the sphere's surface was oxidised. Witte and Stevens[78] cooled a hot silver sphere in water and noticed a pulsation boiling effect during the transition boiling regime.

Board et al[79] noted the existence of an oscillating vapour blanket around a foil heated by a ruby pulsed laser and cooled in water. Their oscillations occurred over a range of subcoolings and were of a frequency between 5 and 15 kz. The effect of vibration on the heat transfer in laminar film boiling has been observed by Burmeister[80]. Depending on their frequency, a substantial enhancement of heat flux occurs.

The addition of such substances as sodium hydroxide and oils to water may affect the cooling characteristics.

Paschkis[81-84] used such quenching solutions as well as pure water. By quenching in highly subcooled water, he noted a rise in the rate of heat transfer for a range of metal superheats. When a sodium hydroxide solution was used as coolant, transition boiling tended to replace the film boiling regime at higher metal temperatures. This was caused by solid sodium hydroxide forming on the metal surface and as it has poor thermal conductivity, the surface at which boiling occurred was at a lower temperature than the rest of the metal.

An explosive MCI is accompanied by high heat transfer rates from melt to coolant[16]. Such rates are considered to be attainable only after a significant increase in the surface area of the melt, ie after an initial break up or fragmentation of the hot fluid. A number of theories are outlined below which suggest mechanisms for fragmentation. They range from a physical pulling apart of a melt bolus (Section 2.2.1) either by an impact at the coolant surface or shear forces within the coolant to a very rapid formation of vapour from coolant trapped beneath the melt (Section 2.2.2); or even a combination of the two as in violent boiling (Section 2.2.3). While some theories are undoubtedly more likely than others for a particular melt-coolant system, it is unlikely that one theory alone prevails and a combination of theories is more probable to account for the necessary fragmentation of the melt.

2.2 Theories Regarding Explosive MCIs

2.2.1 Hydrodynamic Break Up

This means of fragmenting a molten substance as it comes into contact with a liquid coolant may be split into two general categories. These are impact break up and velocity break up and will be discussed separately.

Impact break up

When a bolus of hot melt falls onto the surface of a liquid coolant, the surface tension forces holding it together may be overcome by the inertia forces imposed by the coolant. Should this be the case, then some fragmentation of the melt into smaller quantities will occur. It is the geometric ratio between the inertia forces and the cohesive surface tension forces which determines such break up and this is called the Weber number.

$$We = \frac{\rho_c R V^2}{\sigma} \qquad \ldots(2.3)$$

$$= \frac{\text{inertia forces}}{\text{surface tension forces}}$$

where: ρ_c = coolant density

R = molten droplet radius

V = molten droplet velocity

σ = melt's surface tension

The demonstration that globules fragment into smaller, more stable sizes was made by Hinze[85,86]. Molten metal drop tests have also been conducted to determine the critical Weber number range. Mercury was dropped and the resulting fragmentation observed in the absence of heat transfer. Whilst a critical value for the Weber number of falling molten globules exists (it is approximately 8), the question still remains as to whether the rate of fragmentation is enough to account for the short energy release times required for an explosion.

Velocity break up

Fragmentation may result from a velocity differential existing between two fluids. Board and Hall[87] have results which are indicative of high heat transfer rates between melt and coolant arising from fine fragmentation. The fine break up was effected by a velocity differential which was created by a shock wave.

Ivins[88] has studied different modes of break up and his findings are tabulated below.

Table 1 Break up categories for fluid systems of differing relative velocities (Ivins[88])

Weber Number	Nature of Break Up
$\leqslant 8$	Stable
$8 < We \leqslant 30$	Aerodynamic bursting
$30 < We \leqslant 100$	Boundary layer stripping A
$100 < We < 1000$	Boundary layer stripping B
$10^3 < We < 10^5$	Boundary layer capillary wave stripping
$10^5 < We$	Taylor instability

These classifications may be described as follows:

(a) Aerodynamic bursting

Whilst in this Weber number range, differential velocities are still quite low, the dynamics of the system cause an initially spherical drop to become distorted into an umbrella shape which ultimately fragments into smaller drops[89]. The differential velocity determines the extent of fragmentation. When the differential is caused by a shock wave, then the minimum Weber number is found to be $\simeq 8$. By substituting this in equation (2.3) it can be deduced that the maximum size of a stable drop is given by:

$$r_{max} = \frac{8\sigma}{\rho_c V^2} \qquad \ldots(2.4)$$

(b) Boundary layer stripping

As the differential velocity between two fluids in a system increases, then the boundary region of the drop becomes affected. The result is that the fluid in this region is 'torn away' and subsequently breaks into smaller droplets. This 'stripping away' of the boundary layer is limited by the drop's surface tension. For Weber numbers between 30 and 100, a drop tends first to distort in shape and then undergo boundary layer stripping (type A). Drop systems with

Weber numbers in excess of 100 provide the conditions under which this boundary layer stripping takes place on an undistorted drop (type B).

(c) Capillary wave break up

At higher Weber numbers, the boundary layer of the drop creates surface waves by a mechanism known as the 'Kelvin-Helmholtz instability[90]'. As the amplitudes of these surface waves increase, drop fluid at the boundary is liable to break away into smaller droplets.

(d) Taylor instability[91]

For very high relative velocities with Weber number $> 10^5$, the boundary waves are formed by the acceleration of one fluid over the other. Fragmentation then occurs.

2.2.2 Coolant Entrapment

Long[1] invoked the coolant entrapment hypothesis after observing the way in which large masses of aluminium interacted with water contained in steel tanks. He maintained that explosions occurred after the melt had penetrated the water and come to rest on the tank base. His idea was that liquid water became trapped between the molten metal and container bottom. Rapid vaporisation of this coolant then

occurred with the result that the melt was fragmented and a shock wave propagated. Long performed experiments in which a large aluminium bolus fell onto a grid above the water tank and was broken up into smaller boli . These, on falling into the coolant, failed to explode because, according to Long, their bulk was insufficient to entrap water. On other occasions, he used greased or painted bases for the water tank, which, because they provided a non-wetting surface, helped prevent an aluminium-water explosion.

The way in which the container base affects cooling melt is still under investigation, but there is little doubt that a rusty tank bottom possesses a large number of nucleation sites. These would permit fragmentation of the melt by vaporising coolant at relatively small superheats.

2.2.3 Violent Boiling

When a sufficiently hot substance is introduced into a liquid coolant, it causes the coolant to boil. The process may be depicted graphically and is equivalent to traversing the boiling curve (Fig 1) from right to left.

Initially, a vapour film blankets the melt and this boiling regime is hydrodynamically 'quiet', ie there is little turbulence caused by it. As the heat transfer rate drops to the Leidenfrost point, the vapour film becomes unstable and

collapses. Cooling proceeds with the vapour film reforming and collapsing in the boiling regime known as 'transition boiling'. When nucleate boiling is attained, the level of hydrodynamic violence created by transition boiling decreases somewhat. Turbulence does still persist however as a result of the formation and collapse of bubbles at the coolant-melt interface. It is only when nucleation dies out and convective heat transfer takes over that much of the turbulence ceases.

Swift[92] first stated the violent boiling hypothesis. He argued that so long as the molten material remained liquid when the coolant entered the nucleate boiling regime, then the associated turbulent forces were sufficient to tear the melt apart.

The observations of workers such as Bradfield[69] and Witte and Stevens[78] give an idea of just how violent transition boiling can be. Bradfield observed the explosive formation of vapour when quenching a hot porous graphite cylinder in water. Witte and Stevens recorded a pulsation boiling phenomenon associated with transition boiling on a small hot copper sphere (1.9 cm diameter).

Indeed, the violence associated with the transition boiling regime increases as the degree of coolant subcooling increases. This may, in part, account for the probability of an explosive MCI decreasing as coolant temperature is raised. If the

violent boiling theory does hold for certain systems, then it is the intermittent nature of the vapour film during transition boiling which will tend to overcome the surface tension forces holding the mass together, and promote fragmentation.

2.2.4 Dissolved Gas

Epstein[93] proposed a fragmentation mechanism which relies upon the quantity of gas dissolved in the melt. On cooling down, supersaturation of the gas occurs and a resulting pressurisation in the melt causes a dispersal of small melt particles in the coolant. Two conditions are necessary:

(i) the melt can dissolve the gas without forming a stable phase, and

(ii) the solubility of gas in the melt increases with temperature.

Epstein's original experiment with atomic oxygen in silver tended to support the theory. He cited oxygen and hydrogen gas as having adequate solubility properties in metals to be appropriate in producing fragmentation.

However, Epstein was forced to modify his hypothesis when experiments performed by Shiralkar[94] tended to be contradictory. Shiralkar had observed fragmentation of tin in water despite having first degassed the metal sample

totally. The modification proposed by Epstein[95] stated, in effect, that the gas came from the coolant. Protons in water coolant were believed to diffuse through a melt oxide layer into the metal where they were subsequently reduced to hydrogen atoms. The melt in this vicinity becomes super-saturated with hydrogen and as the thermal wave moves inwards cooling the melt, the atoms recombine to form gaseous molecular hydrogen which is capable of tearing the melt apart. Calculations indicate that the build up of gas may occur in anything from 2-100 ms. Gunnerson and Cronenberg[46] have observed that because the solubility of inert gases is so low (10^{-6} molar fraction), this mechanism does not predominate in uranium dioxide fragmentation.

Another fragmentation mechanism based on dissolved gas in the melt has come from Buxton and Nelson[96]. Their sequence of events is not unlike Epstein's original postulate.

(i) A large quantity of dissolved gas should be present in the melt.

(ii) Supersaturation of the dissolved gases takes place on cooling.

(iii) Nucleation of these gases is initiated by an applied pressure transient.

(iv) Rapid growth of gas bubbles causes fragmentation.

This so-called 'impulse initiated gas release' differs from Eptsein's theory in one aspect. Epstein proposes that nucleation arises spontaneously from the latent gas pressure of dissolved gas. Buxton and Nelson argue that such large latent gas pressures occur in very few systems and consider nucleation to be initiated by a pressure wave.

2.2.5 Thermal Stress

Analysis of the heat transfer processes and calculation of the associated thermal stress in an aluminium-water system has been carried out by Hsaio et al[97]. Cronenberg et al[98] have treated the uranium dioxide-sodium system similarly. The stress in the solidifying melt was determined for two conditions:

(i) direct contact between the two liquids, and

(ii) assuming a nominal film boiling heat transfer coefficient.

In the aluminium-water system, the direct contact calculation led to physical stresses which were approximately two orders of magnitude more than those worked out assuming a film boiling heat transfer coefficient. With the uranium dioxide-

sodium system, there was little difference.

The surface tensile stresses calculated from direct contact between aluminium and water were in excess of the metal's yield strength, whereas the stresses resulting from an assumption of a film boiling heat transfer coefficient were significantly less. In the uranium dioxide-sodium case, both conditions gave surface tensile stresses greater than solid uranium dioxide's yield strength. Additional mathematics on the latter system indicated a peak stress being reached in about 50 ms. Experimental results produced by Armstrong et al[47,49] show good agreement here, with his peak stresses coming after between 30 and 80 ms. The conclusion which may be drawn from these mathematical analyses is that thermal stress fragmentation is very relevant in the uranium dioxide-sodium system, whereas the establishment of a vapour film is the governing factor with aluminium and water. Work by Knapp and Todreas[100] supports the thermal stress mechanism.

Doubt has been laid on the theory, however, with criticism of two points. The theory depends upon the pressurisation of the inner molten core due to a surface crust contraction in the melt to account for break up. Firstly, observation has been made by Swift and Baker[101] of fragmentation at times prior to the normal freezing of the uranium dioxide surface. Secondly, in metal porosity experiments undertaken by Fast[102],

the presence of nitrogen and hydrogen gas has been shown to induce fragmentation of solidifying molten iron samples. Similar tests without the gases failed to fragment the samples.

2.2.6 Coolant Entrainment

This theory is similar to that of coolant entrapment but relies on the coolant being encapsulated into the melt as the melt falls through it. Groenveld[103] outlines the way in which coolant may be entrained from a hydrodynamic viewpoint. He backs this up with highspeed film of the way water globules encapsulate a drop of hexane. Schins[104] proposes a model which takes into account the vast temperature difference involved in an MCI. His five stage process commences with direct contact between melt and coolant which heats a layer of coolant surrounding the melt. Then transient boiling of coolant commences which imparts a shock to the melt's surface. Vapour film collapse then initiates the cavitation of bubbles within the molten droplet. This in turn entrains coolant within the cavitating melt so that subsequent fragmentation is brought about. Such a model is proposed qualitatively and as yet no experimental results have succeeded in confirming it.

2.2.7 Internal Acoustic Cavitation

The theoretical model proposed by Kazimi[105] for fragmentation

considered the effect of surface boiling on the cooling molten drop. As film collapse occurs, fluctuating pressure waves are believed to be generated in the melt. During a negative pressure cycle, cavitation bubbles are created which to some extent collapse in the positive pressure cycle. Bernath[106] has produced a formula for calculating the minimum negative pressure threshold (P_{th}) for homogeneous cavitation.

$$P_{th} = \left[\frac{9.06\sigma^3/KT}{\ln\left(\frac{1.45\rho N^2\sigma^2}{P_{th}M^{3/2}RT}\right) - \frac{L}{KT}} \right]^{\frac{1}{2}} \qquad \ldots(2.5)$$

where: K = Boltzmann's constant

N = Avogadro's number

M = molecular weight

L = latent heat of vaporisation

R = gas constant

The implication is that for successful fragmentation, continued bubble growth must take place and therefore the rate of bubble growth must exceed the rate of bubble collapse. Kazimi proposes that realistically, cavitation inception occurs more readily because of the presence of impurities than in a theoretical prediction. Indeed, if the presence of dissolved gas is assumed in the melt (Cronenberg and Grolmes [107]), the threshold pressure for homogeneous cavitation may be calculated as follows:

$$P_{th} = \Delta P + \frac{4\sigma}{3\sqrt{3R_{gn}}} \left(1 + \Delta P \frac{R_{gn}}{2\sigma}\right)^{-\frac{1}{2}} \quad \ldots(2.6)$$

where: ΔP = difference between system and vapour pressure

R_{gn} = radius of the gas nuclei

This calculation is based on the assumption of equilibrium between pressure and surface tension forces (Flynn[108]).

Kazimi's theory is not far removed from the previously discussed gas release theories.

2.2.8 Vapour Bubble Collapse and Jet Formation

On changing from film boiling to transition boiling, bubbles of vapour are formed. These may expand and then collapse near a cooling melt's surface.

Such cavitation may be very damaging. Attention has focussed upon the maximum pressures which might be released as a result of cavity collapse. A simple water hammer treatment as outlined by Cook[109] gives the pressure rise associated with a conversion of kinetic energy to potential energy stored in the compressed liquid as:

$$P' = \rho C \Delta U \quad \ldots(2.7)$$

where: C is the acoustic velocity at the bubble wall

U is the bubble wall velocity

ρ is the liquid density

At minimum bubble radius, U = 0 and $\Delta U = U$. Cook used the value of U from the Rayleigh[110] analysis:

$$U^2 = \frac{2p_\infty}{3\rho} \left(\frac{R_o^3}{R^3} - 1\right) \qquad \ldots(2.8)$$

where: p_∞ is the pressure at infinity

R_o is the initial bubble radius

R is the bubble radius subsequently

Such a simple calculation cannot be expected to give even approximate results when the bubble wall velocity (U) approaches the acoustic velocity (C). The acoustic velocity is several thousand feet per second. Hence collapse pressures ranging up to 3×10^6 atms would be predicted for $U < C$. Such a treatment neglects compressibility, bubble contents and other effects during the collapse period. No adequate experimental determination of collapse pressure intensities has been made. Isolated indications such as that of Harrison[111] who reported pressure measurements in a liquid at a 10 cm distance from the collapse point giving peak values of up to 10 atms, do not provide convincing evidence of

the actual pressures developed and radiated.

The phenomenon of sonoluminescence[112] has been observed in hydrodynamically cavitating bubbles. A low intensity light emission from collapsing cavities is believed to be created by compressed gas becoming incandescent at bubble collapse.

The commonly held view at present is that the damage caused through cavitation is attributable to the impacts from pressure shock waves that radiate from the collapse centre of a small bubble. However, depending on the combination of initial cavity size, flow velocity and pressure gradients, collapse pressures may or may not be of a damaging magnitude. Furthermore, even though the collapse pressure is high, the collapse may not occur close enough to a boundary surface for the radiated wave to cause damage.

An alternative mechanism arises from the formation of microjets in a liquid. Two possible modes of the jet model are shown in Fig 3. The first suggestion of such jets was made by Kornfeld and Suvarov[113] and recent confirmatory work has been carried out by Ellis[114,115] and his co-workers. Photographs of collapsing bubbles in static fluids show distortion on collapse and these effects are exaggerated with pressure gradients or near boundary surfaces. Such a distortion is seen on occasions to lead to a microjet of liquid of very high velocity moving through the

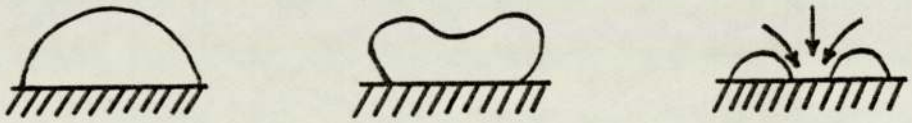

(a) HEMISPHERICAL BUBBLE ATTACHED TO WALL

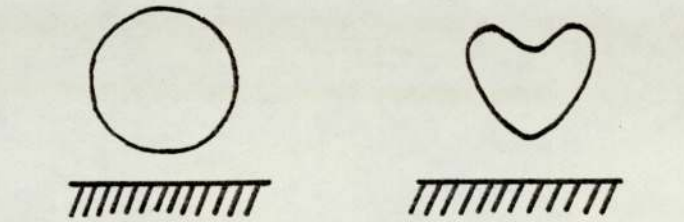

(b) BUBBLE COLLAPSING NEAR WALL

Fig 3 Schematic representation of microjet formation

interior of the cavity just before collapse. It is believed that such liquid jets may cause damage if collapse is close enough to a boundary.

Photographs of this phenomenon were taken by Shutler and Mesler[116] using an arrangement similar to Naudé and Ellis[115] and by Floreschuetz and Chao[117] who observed bubbles in a static subcooled boiling experiment. Gibson[118] followed up the work of Benjamin and Ellis[114] in the study of collapse near a wall. Numerical solutions to the equation of motion have been obtained by Plesset and Chapman[119] which show the time history of jet formation when a bubble collapses at or near a wall in a non-viscous incompressible liquid.

Board, Farmer and Poole[120] first proposed that jet formation resulting from a vapour bubble collapse may cause dispersion of the molten material in an MCI. Buchanan[121] suggested a model for thermal explosions taking jet formation into account and Buchanan and Dullforce[122] have supplied additional evidence.

Buchanan's model calls for a five stage process as follows:

Stage 1 The transition boiling regime permits molten material and coolant to come into contact and form a vapour bubble.

Stage 2 The bubble expands and collapses and in so doing a high velocity microjet is created and directed towards the molten material.

Stage 3 The powerful jet penetrates the molten material whose surface area is consequently increased very rapidly.

Stage 4 On penetrating and breaking up in the molten material, the microjet has heat transferred to it. As the surface area of melt is increasing, the total heat transfer rate is rapidly enhanced.

Stage 5 On being heated to a certain temperature, the jet suddenly vaporises, and a high pressure vapour bubble is formed. The rapid expansion of this bubble disperses the molten material into the coolant.

The process may now be repeated from Stage 2.

To give an idea of the velocities assumed by microjets in liquids, Plesset and Chapman's[119] numerical solutions give a value of 170 m sec^{-1} for a bubble collapsing near a solid boundary and 130 m sec^{-1} for one collapsing whilst in contact with a solid boundary. Hancox and Brunton[123] have reported that multiple impact by water travelling at 90 m sec^{-1}

can erode stainless steel, so that potentially, microjets are very damaging.

2.2.9 Spontaneous Nucleation

The spontaneous nucleation model as proposed by Fauske[48,49] considers that for a large scale vapour explosion to occur, the conditions for liquid-liquid contact must exist such that the contact interface temperature between the melt and coolant must exceed that for spontaneous nucleation of the coolant (T_{SN}). The contact interface temperature (T_I) in the absence of solidification of the melt may be calculated using:

$$\frac{T_I - T_c}{T_H - T_I} = \left[\frac{k_H \rho_H C_H}{k_c \rho_c C_c}\right]^{1/2} \qquad \ldots(2.9)$$

where: k is the thermal conductivity

ρ is the density

C is the specific heat capacity

T is the temperature

Subscripts: H the hot liquid

c the coolant

I the interface

To assess the temperature at which spontaneous nucleation occurs, Volmer's rate equation is used such that:

$$J = \text{const} \exp\left(\frac{-W}{kT}\right) \qquad \ldots(2.10)$$

where: J is the rate of bubble nucleation per unit volume

k is Boltzmann's constant

W is the reversible work of formation of a critical vapour embryo in the liquid and is given by

$$W = \frac{16\pi\sigma^3}{3(P_V - P_L)^2} \qquad \ldots(2.11)$$

where: σ is the surface tension of the pure liquid

P_V is the vapour pressure

P_L is the liquid pressure

The nucleation rate remains small until the temperature of the liquid reaches a critical value whereupon J increases rapidly. For vapour nucleation in the bulk of a pure liquid, this temperature limit is referred to as the homogeneous nucleation temperature, T_{HN}, and may be approximated to 90% of the thermodynamic critical temperature. When partial liquid-liquid contact occurs, the effect of wetting at the interface must be considered with equation (2.11) being multiplied by a wetting factor. Only for a high degree of non-wetting is T_{SN} significantly lower than T_{HN}.

Experimentally, there is a delay period from the time of melt-coolant contact to the onset of rapid vapour production and pressurisation. Henry and Fauske[124-126] tried to account for this in the context of the time required to attain T_{SN} from the onset of liquid-liquid contact. Whilst the time for the establishment of the interface temperature is 10^{-12} sec (calculated from the relaxation time for thermal vibrational propagation) Henry and Fauske proposed that vapour bubble nucleation can only proceed once a thermal layer has developed in the coolant phase thick enough to support the beginnings of a vapour bubble.

Board and Hall[127] consider that the Leidenfrost temperature for the coolant is a better indicator of a threshold temperature than T_{SN} for an energetic interaction. The Leidenfrost temperature is the temperature below which stable film boiling ceases in coolant. It is estimated as $^{27}/_{32}\ T_c$.

This estimation is made from Van der Waal's reduced equation of state for gases near their critical temperatures:

$$p' = \frac{8T'}{3(v' - 1/3)} - \frac{3}{(v')^2} \qquad \ldots(1)$$

where: $p' = \frac{p}{p_c}$, $v' = \frac{v}{v_c}$, $T' = \frac{T}{T_c}$,

and p is pressure, v is volume and T is temperature with the subscript c referring to the critical value.

The point of maximum superheat, T_m', is found by setting:

$$\left[\frac{dp'}{dv'}\right]_{T'} = 0$$

ie, this is the temperature at which there is no further volume change regardless of imposed pressure:

whence: $$\frac{8T_m'}{3(v_m - 1/3)^2} = \frac{6}{(v_m')^3} \qquad \ldots(2)$$

and substituting this condition in equation (1),

$$p_m' = \frac{1}{(v_m')^2}\left[\frac{2(3v_m' - 1)}{v_m'} - 3\right] \qquad \ldots(3)$$

Putting $p_m' = 0$

$$\frac{1}{(v_m')^2}\left[\frac{2(v_m' - 1)}{v_m'} - 3\right] = 0$$

$$\frac{2(v_m' - 1)}{(v_m')^3} - \frac{3}{(v_m')^2} = 0$$

$$\frac{2(3v_m' - 1) - 3v_m'}{(v_m')^3} = 0$$

$$2(3v_m' - 1) - 3v_m' = 0$$

$$3v_m' = 2$$

$$v_m' = {}^2/_3$$

Substituting in (2)

$$\frac{8T_m'}{3({}^2/_3 - {}^1/_3)^2} = \frac{6}{({}^2/_3)^3}$$

$$T_m' = \frac{3}{4} \cdot \frac{3}{9} \cdot \frac{27}{8} = \frac{81}{96} = \frac{27}{32}$$

Such an approximation has been experimentally verified for a number of liquids[27].

By and large, the spontaneous nucleation model has still to be worked out thoroughly, one reason being that nucleation characteristics, though well understood for liquid-solid interfaces, have still to be assessed properly in the case of liquid-liquid contact.

2.3 Objectives of the Present Work

The investigations outlined in this thesis are intended to add to the current knowledge about MCIs and present experimental evidence which may help to explain the way an explosive interaction is brought about.

An approach similar to that of Konuray[128] has been adopted so that preliminary experiments were designed to confirm the suitability of his system. Once this had been done, some higher melting point metals, namely copper and aluminium, were used to see whether they spontaneously exploded on being dropped into water. Also some high speed cine films were taken as this photographic technique has proved of use to other workers. In fact, an extension to the photographic work was made by taking some pictures using spark illumination. The advantage here is that not only is definition improved (35 mm format being used instead of 16 mm) but also the time scale involved is a great deal shorter. For example, one frame of a high speed film taken at 3000 frames per second is exposed for 133 μs whereas by using a spark for illumination an exposure of 35 μs is obtained.

The effect of a shock wave on a cooling melt droplet is investigated with the higher melting point metals. Board et al[86] have succeeded in promoting an explosive interaction with tin in water at 80°C in this way, so further work was

intended to supplement this. Indeed, as much experimental evidence to date has supported the vapour collapse theory for explosive initiation, an attempt to cause such collapse prematurely around cooling copper and aluminium drops would help to substantiate this hypothesis.

To broaden the scope of MCI research, different systems were studied. Alternative coolants to water were examined as were other types of melt. The molten sodium chloride and copper (I) iodide served as models for slag interaction with water which is of industrial significance.

Finally, more work was undertaken to lend support to the vapour collapse theory. A number of measurements were made of 'dwell time' which is the time taken for a molten droplet to explode after entering the coolant. This was carried out using water at different temperatures to find out what variation if any there was. Previous dwell time measurements had been made using larger melt masses of less reproducible shape and size. Any variation in dwell time with water temperature was thought to be a function of how the steam blanket surrounding a tin drop collapsed. Additional experimental work on spark generated steam bubbles was carried out to confirm whether the time taken for collapse was of a comparable order of magnitude.

The large scale work involved dropping a variety of materials into water and recording the events on film at high framing rates. Salts and high melting point metals were used so that a comparison might be made between the small and the large scale experiments.

CHAPTER THREE

EXPERIMENTAL SYSTEMS

Work was undertaken both on the small scale and the large scale. Small scale experiments were performed within the laboratory and used small quantities of melt (drops of approximately 0.25 g in weight). Large scale tests were carried out at an outdoor research station and here much larger quantities of melt were dropped (as much as 5 kg). Whilst no base effects were investigated on the small scale, they did prove relevant on the large scale.

3.1 Small Scale System

In the laboratory, an experimental arrangement was employed which meant that small, reproducible droplets of melt could be generated and observed as they fell into a coolant. The main coolant was ordinary tap water, but carbonated water was tried as well as certain organic liquids.

The furnaces used to heat the melt were of two types. The first, designed for use up to about 750^{o}C, heated a cylindrical chamber by means of an electrical winding around a ceramic former. This winding was capable of taking up to 5 amps direct current. The second, which was able to heat to 1500^{o}C, also heated a cylindrical chamber, this time by virtue of a higher

electrical current (up to 20 amps) passing through an array of silicon carbide heating elements. Both furnaces were surrounded by sufficient heat insulation to minimise heat loss and maintain a safe temperature on the outside. They were supported above the laboratory bench so that a coolant tank might be positioned beneath.

In the cylindrical heating chamber of a furnace, a melting tube would be placed which contained a quantity of solid metal or salt ready for melting. The melting tube was designed to produce droplets of a reasonable size (which were forced out by the mass of melt above) and be of sufficient length to contain an adequate supply of melt for an experiment. The eventual design of tube is shown in Fig 4. Such a tube was made from either graphite or pyrophyllite, both of which had disadvantages. Pyrophyllite is a fragile material which has to be handled carefully whereas graphite tends to erode at high temperatures giving a slightly less reproducible melt drop size.

Temperature control in the smaller furnace was accomplished by using a chromel alumel thermocouple wired to the furnace supply unit so as to maintain a required fuel temperature. In the larger furnace, a Pt/13% Rh thermocouple in a recrystallised alumina sheath was used and fitted into a machined recess in a melting tube within the furnace. The thermocouple was connected to a Eurotherm digital panel meter which displayed the temperature. In either case, the furnace was supported above

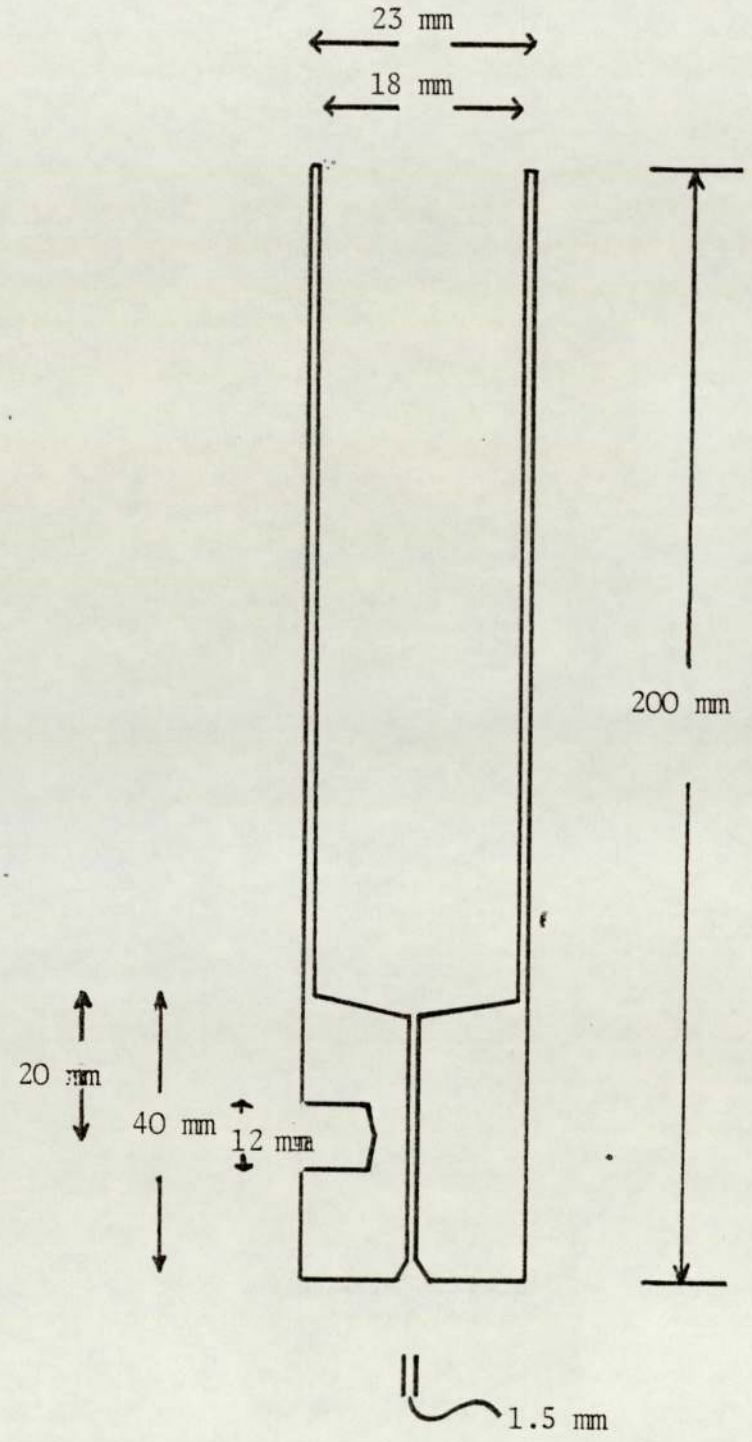

Fig 4 Melting tube design

bench level so that a coolant tank might be placed beneath.

Though experiments were performed with melt droplets falling through various air drops, an attempt to minimise the air drop was usually made so that little or no fragmentation was caused to the melt on impact with the coolant surface. The coolant tanks used were made from thin perspex sheet with cross-sectional area about 15 cms square. As metals with high melting points such as aluminium (mp 660^{o}C) and copper (mp 1083^{o}C) required a greater fall through water to lose their high heat content, longer tanks were used for these metals or a stainless steel base was placed inside a smaller tank.

For the measurement of pressure waves within the coolant, a standard measuring hydrophone type 8100 was placed in the coolant tank. This was capable of recording absolute sound measurements over a high frequency range (0.1 Hz to 200 kHz). The hydrophone was supplied by Brüel and Kjaer of Copenhagen and used lead zirconate titanate as the active sensing element with a temperature range of operation of -40 to +120^{o}C. It sensitivity was 26.6 μV per Nm^{-2}. In the earlier experiments, the recording of a typical pressure trace produced through the hydrophone was accomplished by using an assembly of electrical circuits (see Fig 5). Initially, when a drop of melt fell, it interrupted a narrow light beam which formed part of a photoelectric switching circuit (see RS applications sheet, RS/2056, circuit 6). This switched through a delay unit

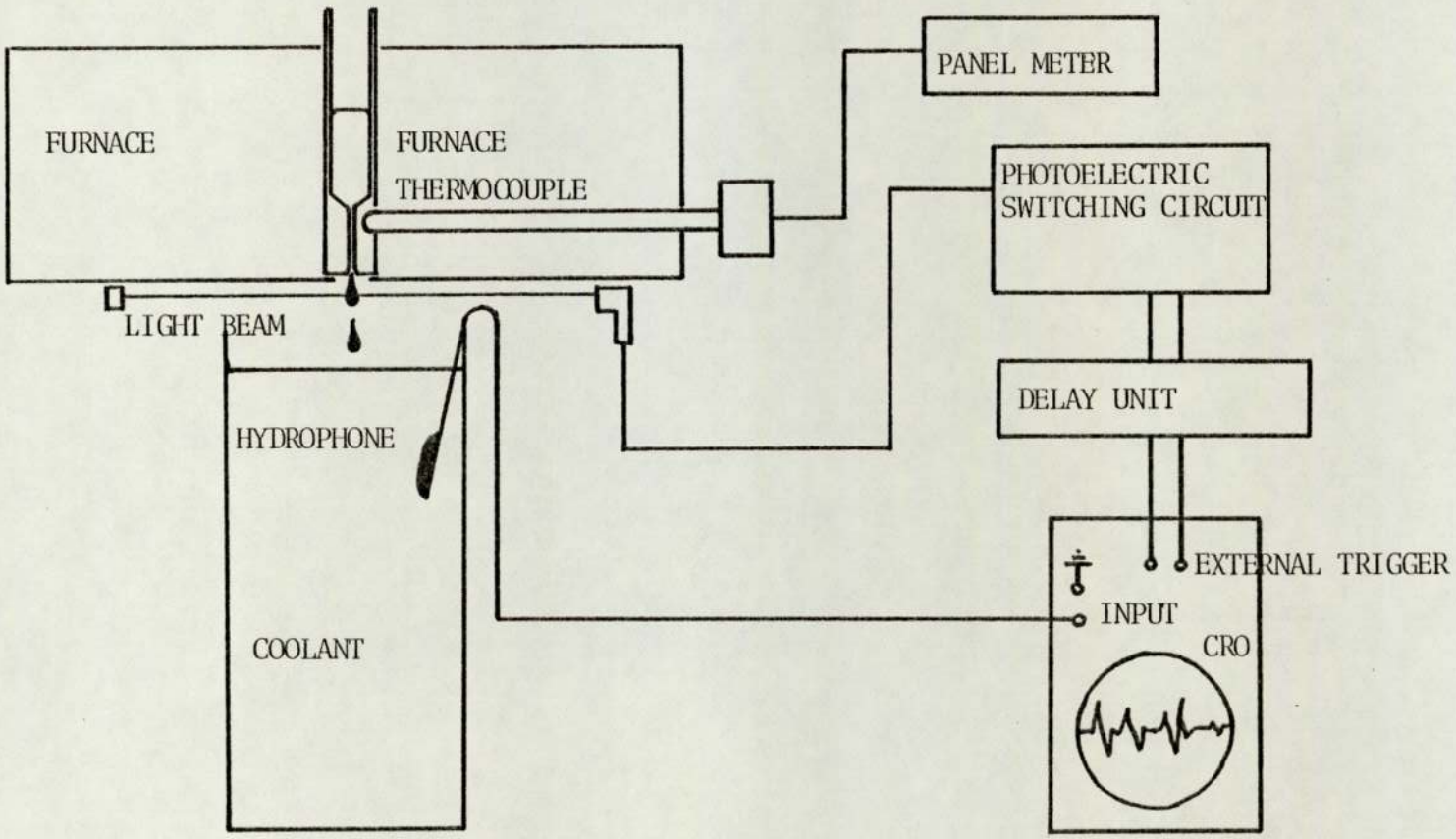

Fig 5 Schematic representation of small-scale hydrophonic monitoring of an MCI

(Venner electronics type EDTR/1/30/A/M) which caused a small electrical pulse to be generated and carried to the external trigger of a storage oscilloscope (Telequipment DM64). The pressure traces of a number of MCIs could then be superimposed and compared.

In later tests, a transient recorder (Datalab DL905) was used. When connected to the hydrophone directly, this device was able to store rapidly fluctuating pressure patterns over a preselected time period and then transfer the information to the CRO screen for detailed analysis. The potential generated by the hydrophone when subjected to an explosive MCI was sufficient to trigger the recorder. A feature of the recorder was its ability to store and display information prior to the trigger pulse which meant both pre- and post-explosion data could be gathered.

A number of photographic techniques were employed to observe small scale MCIs. These fell into three categories.

(1) High speed cinephotography
(2) Stroboscopically-illuminated photography
(3) Short exposure, spark-illuminated photography

(1) <u>High speed cinephotography</u>

Conventional cine cameras work by intermittently moving the

film past a shutter by mechanical means. Unfortunately, such a stop-go arrangement severely limits the framing rate of such a camera. To obtain high framing rates, three camera systems may be chosen from:

(a) A moving optical system which enables the image formed by the main lens to be held stationary with respect to the moving film with the shutter operated mechanically. Framing rates of between 18 and 15000 full frames per second may be achieved using this system. The camera used in the small scale observation work was a Hyspeed (supplied by John Hadland Photographic Instruments) and employed this type of system. It was fitted with a half-head height unit so that one conventional frame was split into two frames. Hence higher framing rates were obtainable.

(b) Multi-flash light systems whereby motion is arrested by the short duration of repeated illuminating flashes.

(c) A combination of a moving optical system and a stationary loop of film inside a drum. Synchronisation is important of the event and shutter system. However, very high framing rates are obtainable.

For a more thorough discussion of high speed photography, Chesterman's[129] treatise is recommended.

Initially, the high speed camera was connected to the photo-electric switching device previously mentioned. However, it was found that with high framing rates (>1000 frames sec^{-1}) the camera failed to reach full speed before the event took place. Therefore, in subsequent tests, a manual synchronisation was employed to make sure the full framing rate coincided with the required event. In later experiments, a timing light generator (supplied by John Hadland Photographic Instruments) was used. This exposed the edge of the 16 mm cine film to small regular pulses of light, provided by LEDs within the camera. Measurement on the processed film between the bright spots enabled an accurate value for framing rates to be calculated. The film used in the work was either Fuji RT400 16 mm colour reversal or Ilford Mark V 16 mm black and white negative film. Both types of film could be push processed in order that short exposures would provide satisfactory images. High intensity light units of 650 W and 1 kW were used to give adequate lighting both from the front and the back of the MCI (back lighting being through a diffusing screen).

(2) Stroboscopically illuminated photography

By this technique, it was possible to follow the path of a falling melt droplet as it progressed through the coolant. A stroboscope (Flash-tac transistorised model) was placed at the side of the coolant tank so that pulses of light were incident upon a droplet as it fell. In front of the tank a Minolta

SRT303 35 mm SLR camera was positioned so that it viewed the light reflected by the melt droplet. By keeping the shutter of the camera open as the drop fell, and suitably adjusting the aperture setting, an exposure was made onto the 35 mm film (Kodak Tri-X pan). This showed a clearly defined pattern of white spots of light from which the path of the melt droplet could be accurately determined.

Stroboscope flashing rates were varied for the particular melt density, eg for aluminium 2300 flashes min^{-1} were used and for copper 7500 flashes min^{-1} were used. As the higher melting point metals were observed, a long coolant tank was employed. However, because the stroboscope could only illuminate approximately 25 cm of coolant at a time, a cardboard shield was made to keep out any extraneous light. This was moved up and down so that any particular depth of coolant could be concentrated upon.

(3) Short exposure, spark illuminated photography

One of the ways in which the spark generator device (loaned by Culham Laboratories, Oxon) was used was to create a spark between two electrodes which then illuminated a melt droplet for a short period of time as it fell through the coolant. The illuminated droplet was photographed using the 35 mm Minolta camera onto Tri-X pan film.

The arrangement was designed so that the camera's shutter release

triggered the spark through its flash synchronising socket. Firing was manual and great care was taken with the spark generator as it was capable of giving a powerful electric shock. To determine the exact length of time which the spark illuminates for, a metal disc was calibrated around its edge and then mounted into the chuck of an electric drill. With the drill's motor turned on to a pre-selected speed, the spark was triggered through the camera and made to light up the disc edge. The photograph obtained showed a minimal but measurable blurring of the calibration marks and by calculation, the spark duration time was determined. As the electrodes in the spark generator were made of stainless steel, repeated discharges caused them to become pitted and erode slightly. When this happened their original shape was restored in the workshop but it meant that the spark duration time varied slightly from test to test. With this in mind, a number of calibration photographs were taken and the maximum duration time quoted.

Preliminary experiments were carried out to assess the thermocouple accuracy for measuring melt temperature. Cooling curves were plotted for metals of differing melting point, namely copper (1083^{o}C), aluminium (660^{o}C), lead (327^{o}C) and tin (232^{o}C), for the Pt/13% Rh thermocouple. Also, an experiment was undertaken to determine the depth of water at which superheated aluminium drops (drops heated well above the melting point) solidified. To do this, a gauze sheet was put into the coolant tank at different distances below the coolant surface.

When unsolidified aluminium fell onto the sheet, the square pattern was impregnated onto the melt surface. When an already solidified drop fell onto the gauze, no such pattern was seen.

A statistical experiment was performed to confirm the work of Konuray[128] which involved measuring the percentage disintegration of metal drops at different temperatures. The metal used was lead.

A variation of the coolant was made to see if explosive MCIs occurred in such liquids as carbonated water, formamide and propan-1-ol. The range of melts examined was extended to molten salts, in particular sodium chloride and copper (I) iodide.

To see how pressure pulses created within the coolant affected a cooling melt droplet, the spark generator previously mentioned was used. Broadly speaking, the generator is a large capacitor bank which can discharge large potential differences (up to 5 kV) between two electrodes. When the device was used in the laboratory, a cage was constructed around the high tension section to prevent any accidents. The electrodes were mounted in a perspex cooling tank (see Plate I) so that a spark discharge might be made beneath water. A high speed film of a cooling aluminium drop being subjected to a pressure wave was made and manual triggerings were carried out to observe the shock wave effect on both aluminium and copper drops.

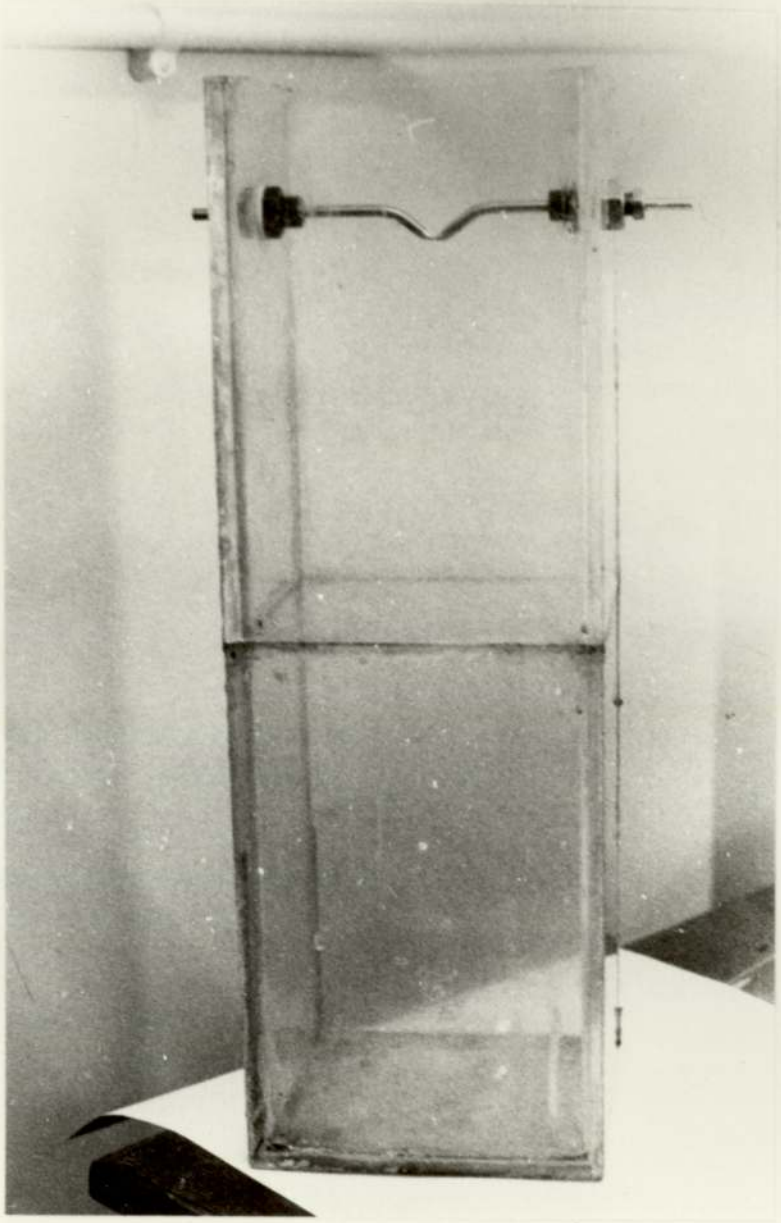

Plate I Perspex cooling tank modified to incorporate spark generator electrodes.

Measurements of 'dwell time' were made hydrophonically for tin drops at 500°C falling into water at various temperatures and exploding. The dwell time (or time taken for a drop to explode after hitting the coolant surface) is very small (in the order of 1-2 ms) but can be successfully recorded using the transient recorder apparatus.

Films were made of the way in which a spark generated steam bubble behaved when formed in water at different temperatures to simulate a vapour bubble growth and collapse cycle.

3.2 Large Scale

The purpose of carrying out tests using large quantities of melt (up to 5 kg) was to see if results gathered in the laboratory resembled those obtained in the field. The amounts of melt used in the large scale experiments were much more likely to be encountered industrially.

The reproducibility of drop masses and bolus shapes were much poorer in the field than in the laboratory. A tipping rig was used to pour melt into the coolant (see Plate II) with a crucible containing the melt clamped securely in a metal ring. The air drop through which the melt was poured could be varied as the legs supporting the tipping rig were replaceable by longer ones. The site where the tests took place (see Plate III) consisted of two bays built out of large concrete blocks which would withstand

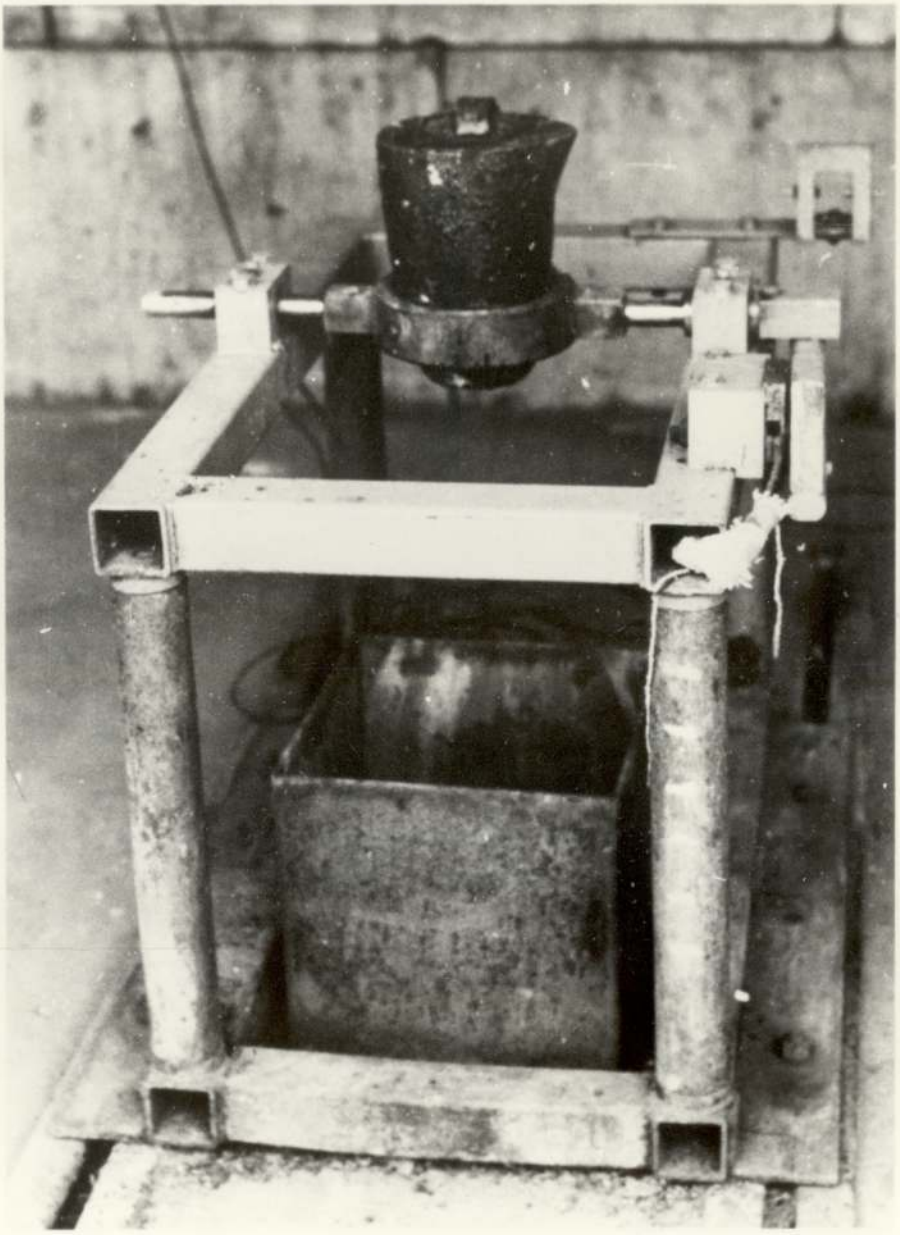

Plate II Tipping rig for large scale testing.

Plate III Large scale test site

a powerful explosion. In the left hand bay, solid metal or salt was melted in one of two ways. The first method was to heat it using a minitoroidal burner fired by a propane and oxygen gas mix which was positioned above the crucible and the hot flame played downwards. The crucible was supported beneath on an array of refractory bricks to minimise heat loss. Higher melting point substances were liquefied in this way. The second method of heating was with an electrical resistance furnace fired by silicon carbide rods which were capable of taking 30 amps of electricity. To make sure sufficient superheat had been given to the melt, a portable thermocouple was dipped in and the approximate temperature measured.

When the required temperature was reached, the melt was carried carefully into the right hand bay with tongs and secured to the tipping rig. The coolant tanks used in the field were made out of $\frac{1}{4}$" thick mild steel and usually had a perspex window at the front for visual observation of the cooling process. Although the majority of tests were carried out using a 1 ft^3 tank, larger ones were occasionally used. The bases were either left rusty or painted with a rustoleum paint to create a smooth surface. Before the tests took place, a safety plate was placed on top of the coolant tank to prevent any premature explosive interaction. This was then pulled clear just before a test. The pouring of the melt was triggered remotely when all personnel were at a safe distance.

The melts used were chiefly copper, iron, nickel, sodium chloride and magnox (a magnesium alloy). For some of the iron tests, the effect of a pressure wave in the coolant water was observed. To do this a small quantity of cordtex charge was stuck onto the side of the water tank. By carefully synchronising the time at which the charge was detonated, the shock wave was created as the iron bolus fell through the water.

Besides viewing the debris created by an MCI with the naked eye, the only monitoring of each test was by cine camera. One Bolex camera running at 32 frames per second was positioned about 5 metres from the tipping rig and a Hyspeed high speed camera shooting at framing rates of between 800 and 3000 frames per second was located at about 15 metres. This was sandbagged heavily for protection. To provide sufficient light for the high speed camera, a line of 20-30 flashbulbs mounted onto a backboard was used. This was fastened onto the tipping rig and an electrical pulse applied to the first bulb. With only a small distance between each bulb (<2 mm) the heat from the first bulb would then fire the next one. This process would be repeated along the line with the consequence that a high intensity light beam was created with a duration of 0.25-0.45 second . Careful synchronisation of the flash ignition, melt pour and camera trigger (carried out remotely) were vital for at 3000 frames per second, a 30 m reel of film takes only $1^{1}/3$ seconds to pass through the high speed camera.

CHAPTER FOUR

RESULTS

The results obtained are divided into those from the small scale laboratory work and those from the large scale field tests.

4.1 Small Scale

4.1.1 Thermocouple Accuracy

The accuracy of the Pt/13% Rh thermocouple used with the larger furnace and in the majority of experiments was tested by plotting cooling curves similar to that shown in Fig 6 for various metals. The results of such graphical analyses are shown in Table 2. A comparison between the melting points of the metals and the values deduced graphically shows that there is good agreement over a wide temperature range. The error in the melt temperatures recorded was therefore taken to be $\pm$ 15^{o}C.

The chromel alumel thermocouple used in some tin experiments was considered to have an accuracy of $\pm$ 10^{o}C.

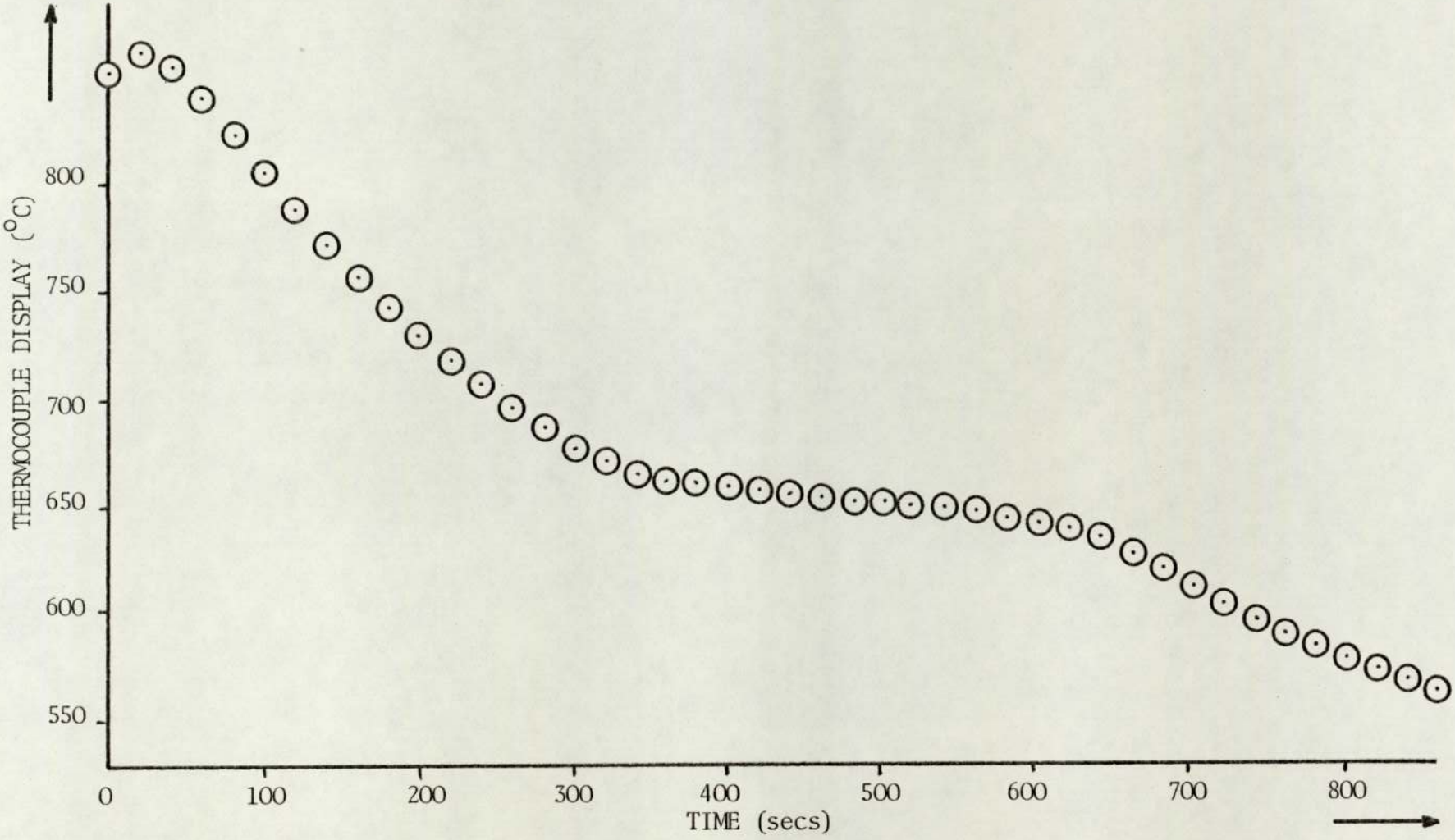

Fig 6 Cooling curve for aluminium

Table 2 Comparison between metal melting points and figures shown using Pt/13% Rh thermocouple with Eurotherm panel meter

Panel Meter Reading, °C (from graph)	Actual Figure, °C	Fixed Point
247	232	Melting point of tin
322	327	Melting point of lead
653	660	Melting point of aluminium
1068	1083	Melting point of copper

4.1.2 Percentage Disintegration and Drop Size Reproducibility

The results of work carried out by Konuray[128] included graphs showing the percentage disintegration of tin drops in water as a function of their temperature. Percentage disintegration is a measure of how much a melt fragments on interacting with a coolant. Some workers have sieved the debris created by an MCI and weighed the small fragments. This weight was compared to the initial melt mass to calculate the percentage disintegration.

Mathematically,

$$\text{Percentage Disintegration} = \frac{M_E}{M_T} \times 100 \qquad \ldots(4.1)$$

where: M_E is the mass of disintegrated drops

M_T is the total mass of drops

As indicated by Konuray[128] there is another way to determine percentage disintegration. This is by dropping a number of molten drops and counting how many explosively interact with the coolant. Such an approach does not take any partial disintegration or incomplete fragmentation of drops into account. It yields values for the percentage disintegration which are higher than those obtained by the weighing method. However, the trends remain the same in either method so to try and confirm some of Konuray's[128] data, lead drops at

various temperatures were observed falling into water and a plot of percentage disintegration (calculated by counting the exploding drops) against metal temperature was drawn (see Fig 7). The plot is very similar to that obtained by Konuray[128], with a maximum value for percentage disintegration at approximately 500°C.

To ensure that each lead drop was of a reproducible mass, drops which had not fragmented were weighed and a histogram drawn of drop weight spread (see Fig 8).

4.1.3 MCIs for Aluminium and Copper

Aluminium and copper drops were observed as they interacted with water as coolant in the free-contacting mode. This means that the way in which melt and coolant were brought together was by melt falling freely through coolant and not being influenced by a third body, ie a base. Aluminium was heated as high as 1285°C and copper as high as 1400°C but no explosions occurred and hence no spongy debris was produced.

The aluminium drops were seen to fall in three different ways. Firstly, a drop would penetrate the water and acquire a steam envelope around it. On falling, the drop flattened out somewhat and on subsequent examination, a solid disc-like shape was found. Another way in which a drop behaved was to fall to about 5 cm water depth, and assume a distinctly spherical

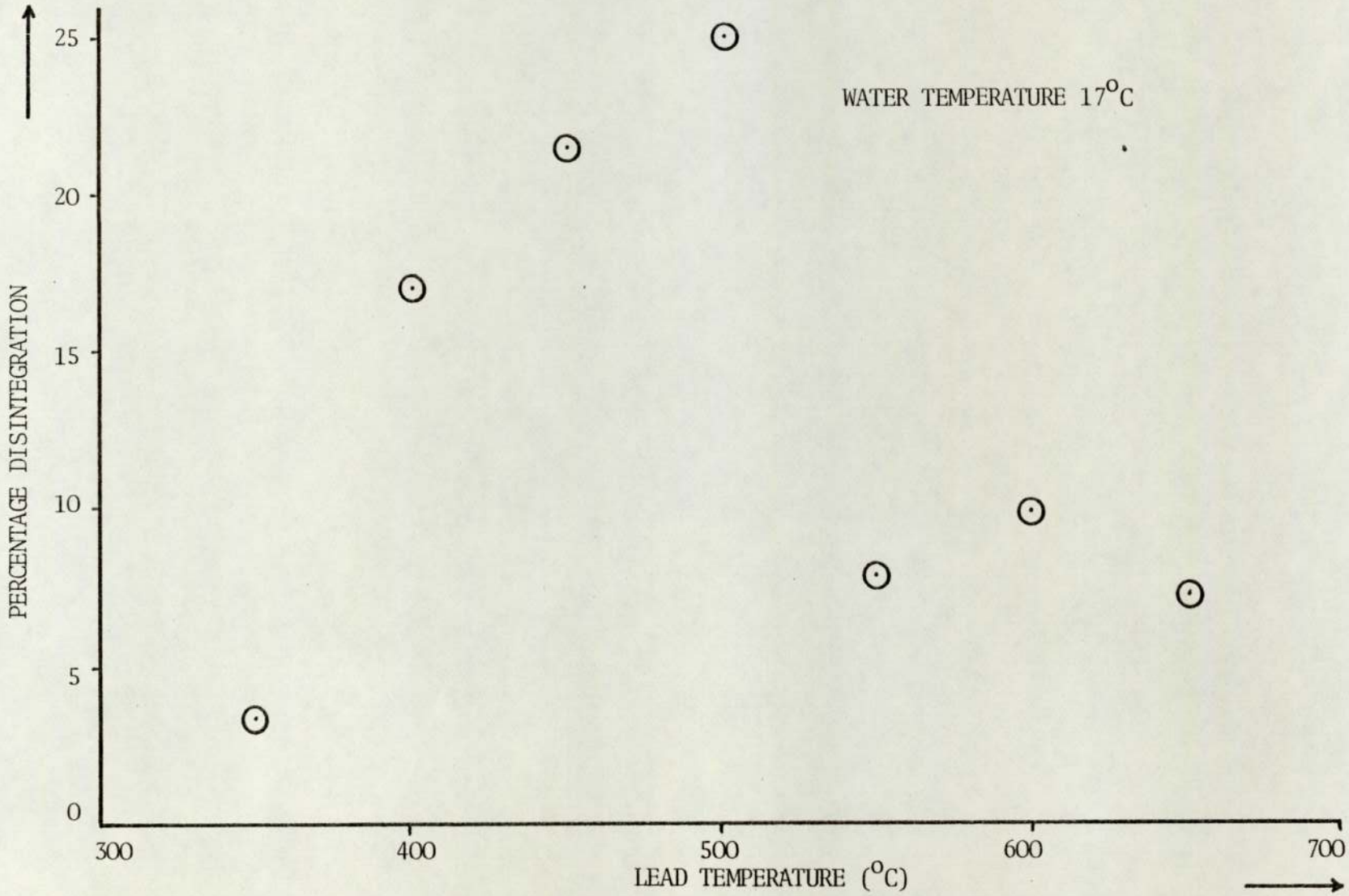

Fig 7 Percentage disintegration as a function of metal temperature for lead drops

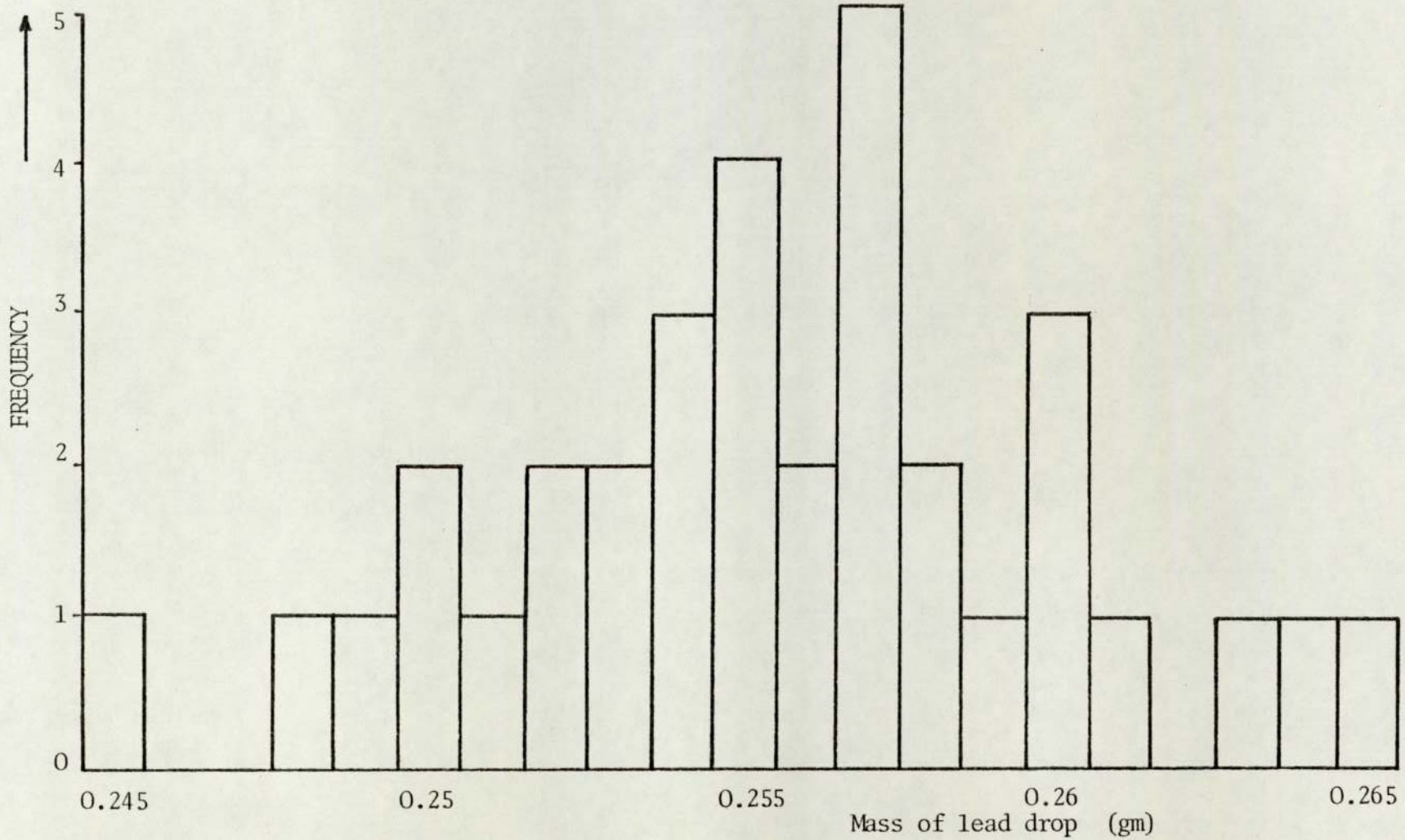

Fig 8 Weight distribution of lead drops

shape. It would then hover at this water depth with a pronounced hissing noise clearly audible. The sphere would drop after a short time, (approximately 10 seconds) and the spheroidal shape was retained on solidification. The aluminium sphere had small holes in it and its centre, whilst not completely hollow, contained only small amounts of rather gritty metal. The final way in which an aluminium drop fell was with a minor interaction with the coolant water. Examination of such a solidified drop revealed that some surface 'blistering' had occurred and yet this was insufficient to blow apart the metaldroplet.

The copper drops also fell through water in three ways. The majority fell through the coolant surrounded by a vapour blanket which persisted to approximately a 60 cm depth of water. The solid copper droplets were smooth and regularly shaped with no sign of coolant interaction. Some drops, however, fell and assumed a spheroidal shape. On cutting one of these solidified drops open, its centre was seen to be hollow (see Plate IV). Occasionally, a drop would fall with no real explosive activity but with definite coolant interaction. Such drops (see Plate V) possessed cavities which contained gritty copper debris yet much of the drop was still complete.

4.1.4 Stroboscopically Illuminated Photographs

Konuray[128] had also used a photographic technique which

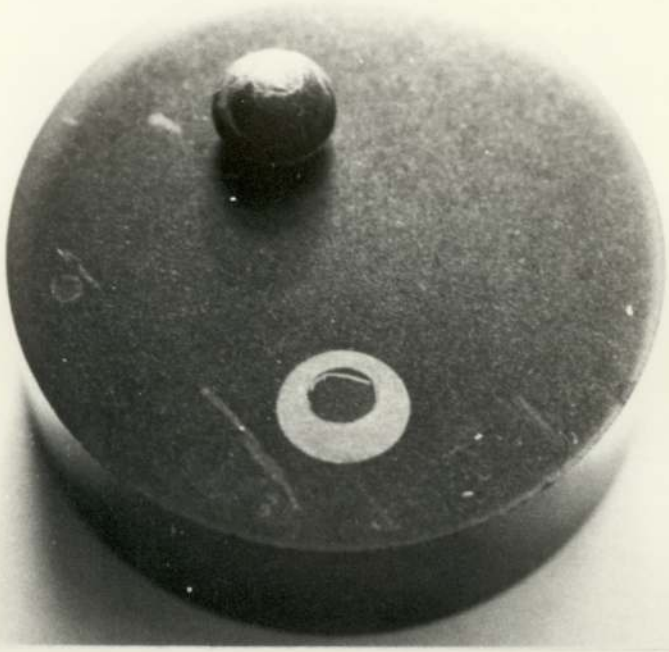

Plate IV Solid sphere of copper together with a similar sphere in cross-section.

Plate V Partially fragmented copper drops together with some showing no signs of fragmentation.

employed a stroboscope to illuminate the path of a tin drop falling through water. He noticed a deviation in the way the drop fell through water which was warm enough to prevent an explosive interaction. He explained this behaviour by assuming that a vapour bubble collapse had taken place which imparted a force to the droplet causing it to deviate from its vertical fall.

Experiments have been performed to find out how molten aluminium and copper behave on falling through water. The stroboscope was again used to help trace the metal drop's path through the coolant. With such high melting point metals, however, a long tank was used as a high heat flux capable of sustaining stable film boiling around the drops was envisaged.

Photographs taken at the start of the droplet's fall showed no significant deviation (see Plate VI). It was not until the drops had fallen to a water depth of approximately 60 cm that any sign of deviation occurred (see Plate VII).

4.1.5 Melt Solidification

A simple series of experiments was carried out with aluminium drops falling through a measured water depth and coming to rest on a gauze base plate. The aluminium was heated to the required temperature and then the aperture at the bottom of the melting tube carefully unplugged with a tungsten rod so as

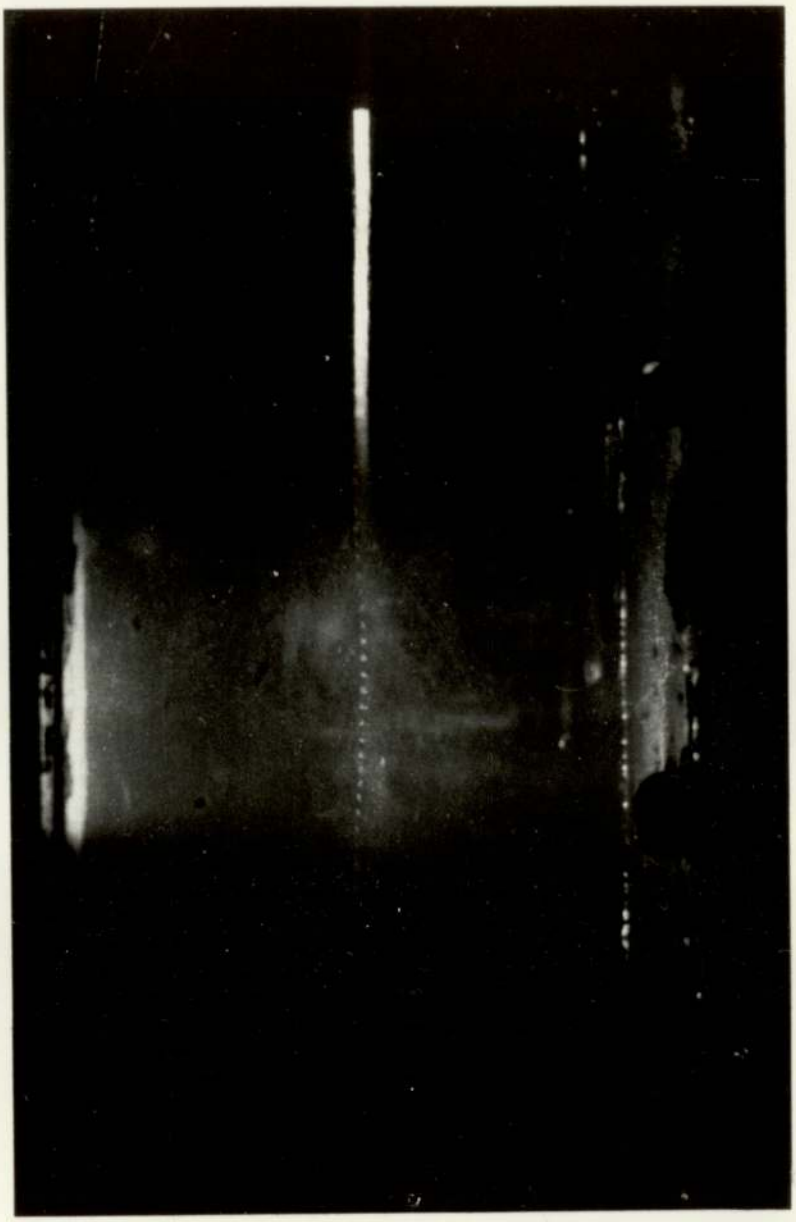

Plate VI Photograph of a copper drop (1200^{o}C) falling directly into water (15^{o}C) under stroboscopic illumination (7500 flashes per min.)

Plate VII Aluminium drops (950°C) deviating at a water depth of approximately 60 cm. Stroboscopic set at 2300 flashes per min.

to make discrete droplets of metal fall through 15 cm of air and into the coolant tank. The results are summarised in Table 3. It shows that even with a substantial superheat, the aluminium drops were solid well before they had fallen through 40 cm of water.

An example of the gauze imprints on the melt droplets is shown in Plate VIII.

Some of the solidified aluminium drops showed signs of minor surface interaction with the coolant water. Their surface had small 'blisters' where some of the water may have been entrained on falling. Whenever such a drop was seen, it had always solidified when others may not have. This indicates that when a small MCI takes place, heat is transferred more rapidly to solidify the melt a great deal more quickly.

4.1.6 Short Exposure, Spark Illuminated Photography

As outlined in the experimental procedure, a calibrated disc was mounted in a drill chuck, spun by the drill motor and photographed using a spark created to try and determine the time for which the spark lasted. The speed of the motor was found by lighting the rotating disc with the stroboscope whose flashing rate was variable. By altering the flashing rate so that the disc appeared stationary, an accurate value for the speed of rotation was found to be 2920 revs min^{-1}.

Plate VIII Aluminium droplets showing the marks left after falling onto a submerged gauze plate.

Table 3 Data showing the depth of water at which aluminium drops solidify

Aluminium Temperature, ^{o}C	Number of drops	Spread of masses, g	Water Temperature, ^{o}C	Water depth, cm	Number of drops solidified (with no gauze markings)
900	10	0.35-0.46	27	20	5
900	10	0.40-0.51	34	25	9
1115	10	0.58-0.65	31	25	1
1220	10	0.35-0.44	31	25	8
1285	10	0.49-0.57	31	35	10

After a series of photographs were taken of the spark illuminated disc, the maximum blurring of the calibration marks (spaced 1 cm apart) was 0.088 cm. The calculation of the time the spark must last to provide such a blur is as follows:

Speed of rotation of disc	=	2920 rpm ($\pm$ 90 rpm)
Diameter of disc	=	16 cm ($\pm$ 0.1 cm)
1 revolution of disc	=	16π cm
Circumference of disc travels at		2446.3 cm sec^{-1}
Time taken to travel 0.088 cm	=	35.97μs ($\pm$ 1.12μs)

This is the time for which the spark lasts.

With the spark triggered by the Minolta 35 mm camera release, a number of short exposure photographs were taken both of tin drops and aluminium drops. Previously, some photographs were taken using the $^1/_{1000}$ sec setting on the camera but the definition was not very good (see Plate IX). Once the aperture setting had been optimised (by running a trial length of film at different f-numbers) each exposure provided a satisfactory result. A selection of the photographs taken is shown in Plates X to XII.

These show an aluminium drop which has just dropped beneath the water surface and two separate tin drops, one having completely exploded and the other partially

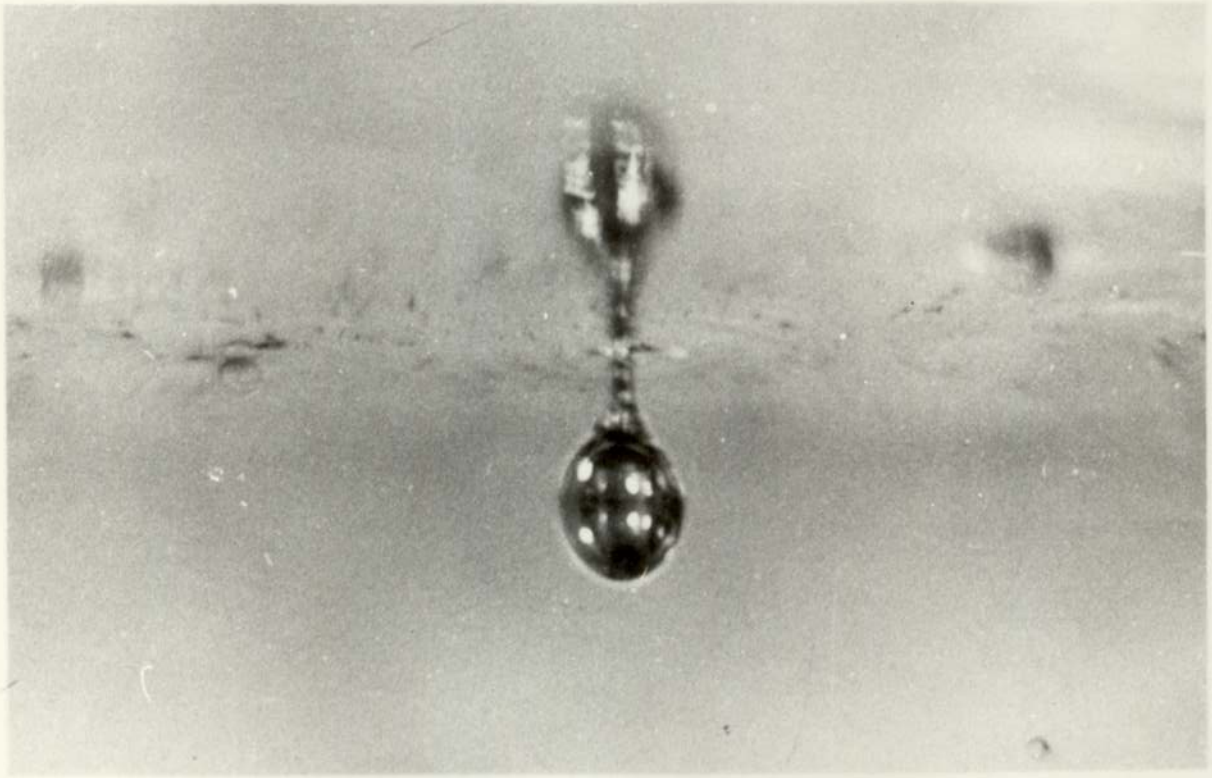

Plate IX An aluminium drop photographed just after water entry. Shutter speed 1 ms.

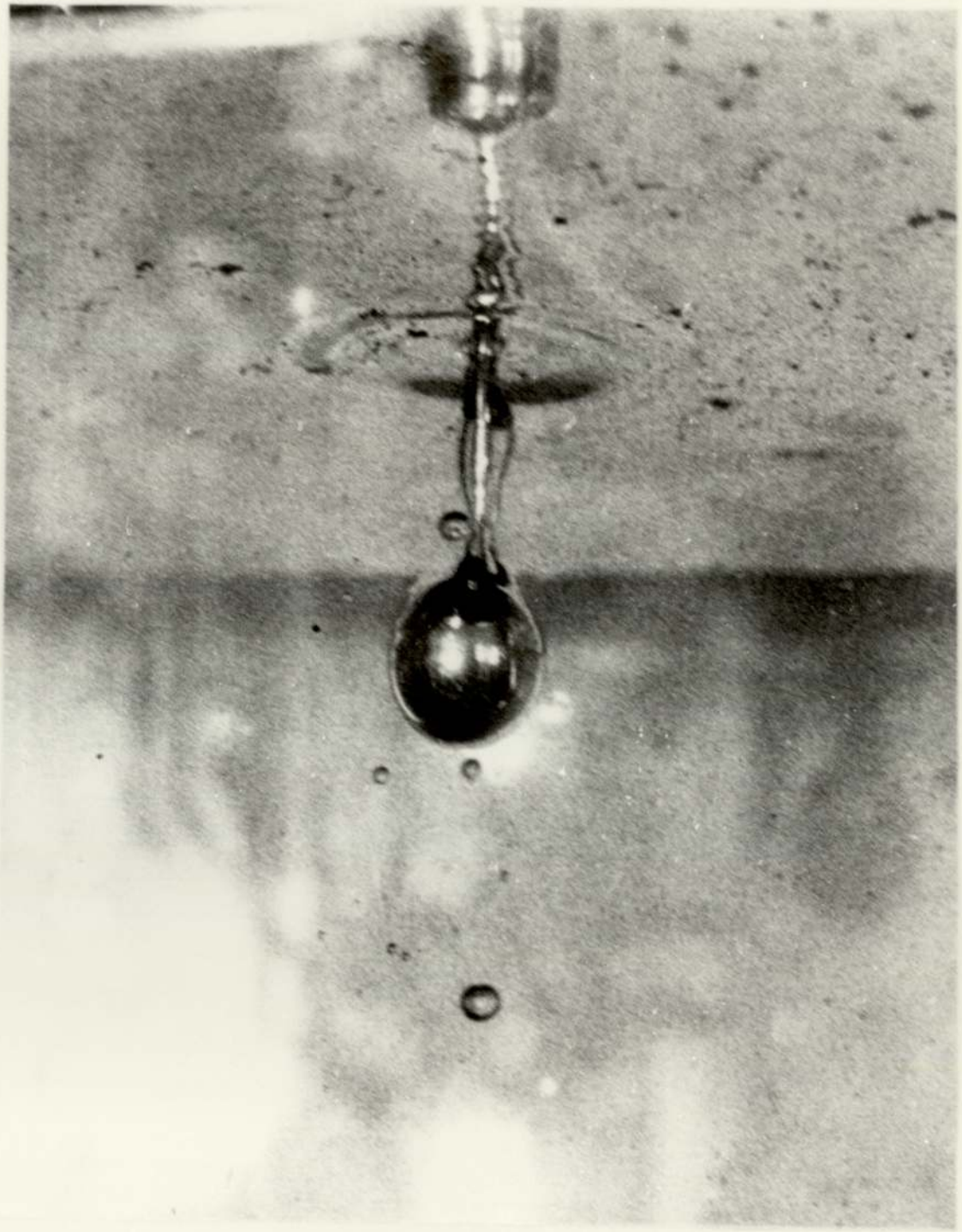

Plate X Short exposure photograph of an aluminium drop just beneath the water surface.

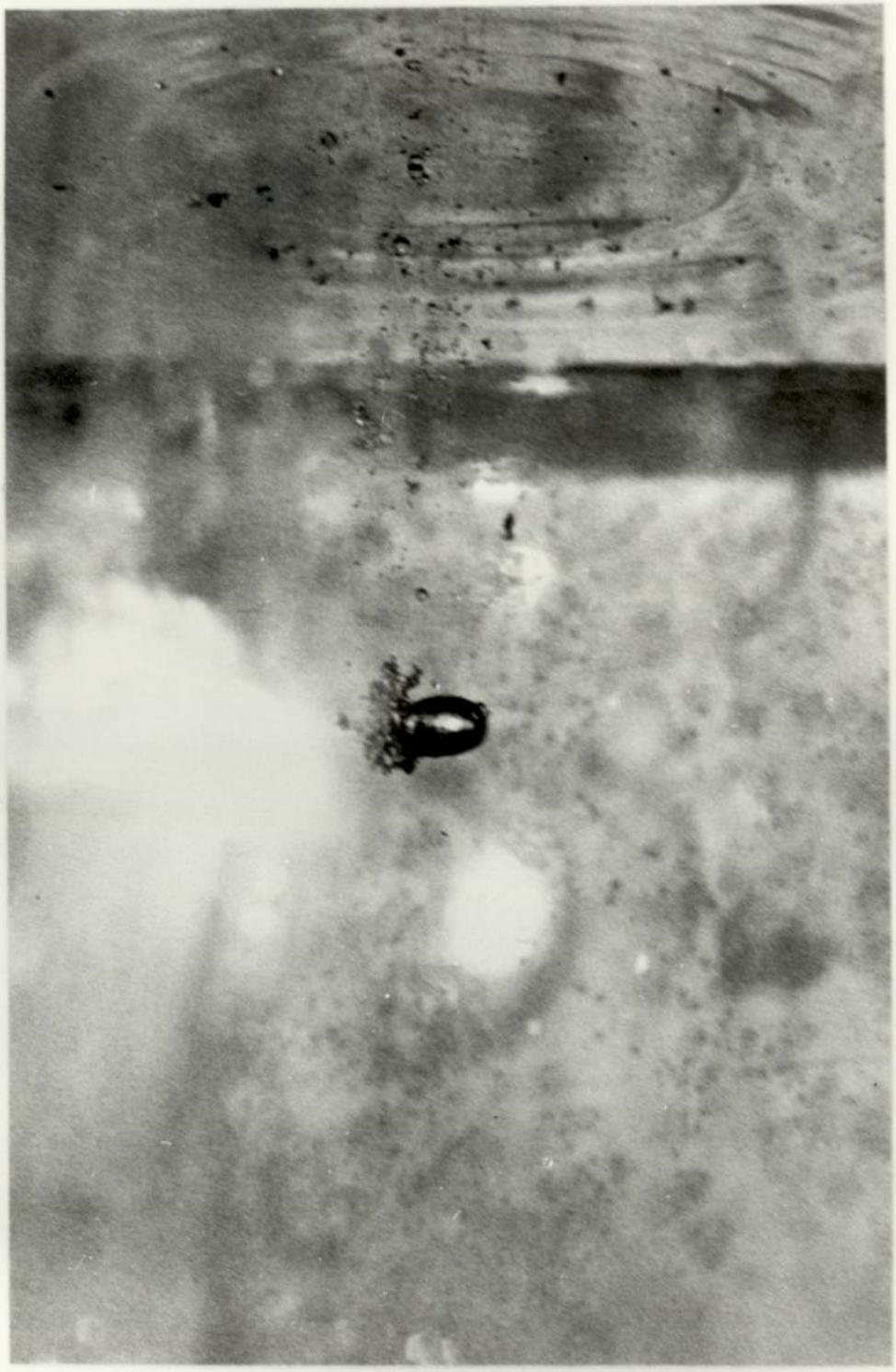

Plate XI Short exposure of a tin drop showing partial fragmentation.

Plate XII Short exposure photograph of a tin drop showing complete fragmentation.

4.1.7 The Effect of a Shock Wave

As there was no sign of explosive fragmentation when copper and aluminium drops fell through water, it was decided to see whether a shock wave or pressure pulse within the coolant altered the cooling process. Board et al[86,130] had observed that a mechanical disturbance applied to a crucible of molten tin cooling in water at 80°C provided an explosion. The belief was that the boiling regime in the coolant surrounding the metal was changed and liquid-liquid contact brought about.

The spark generator instrument provided the shock wave in the coolant. On discharging a high potential difference (usually 3 kV) between the two submerged electrodes, a steam bubble was formed very rapidly which gave an associated pressure wave within the water. Both copper drops and aluminium drops fell past the electrodes at which time a shock wave was generated and its effect on the cooling melt recorded.

Many of the aluminium drops which came under the influence of the shock wave exploded to give finely divided gritty debris (see Plate XIII). Some fragmented completely whilst others broke up partially but still formed spongy debris.

When hot copper drops (at approximately 1300°C) were

Plate XIII Aluminium droplets both complete and fragmented by a pressure pulse within the coolant.

subjected to a pressure pulse as they fell through water, no conventional explosions were produced. Instead, many of the drops broke up into small spherically-shaped particles of metal which bore no resemblance to gritty debris.

On one occasion, a high speed film was made of an aluminium drop falling through water and coming under the influence of a shock wave. Measurements were taken from the projected film of the area of the vapour blanket surrounding the droplet as it fell. It was found that after the shock wave was propagated the area increased significantly. A graph was plotted of the increase in vapour film thickness as a function of time, assuming a spheroidal shape for the cooling droplet. This graph is shown in Fig 9.

4.1.8 Coolants Other than Water

Experiments were carried out to find out whether coolants other than water were capable of sustaining an explosion with molten tin. Formamide was chosen as one coolant because it had certain properties which were similar to water (melting point 2.6^{o}C, boiling point 111^{o}C, surface tension 58.2 dynes/cm at 20^{o}C). A large number of 25 gm quantities of tin at different superheats were poured into formamide at various temperatures from an ordinary silica crucible and numerous 0.25 gm masses were dropped into the coolant. Whilst minor break up was occasionally observed, no clear fragmentation

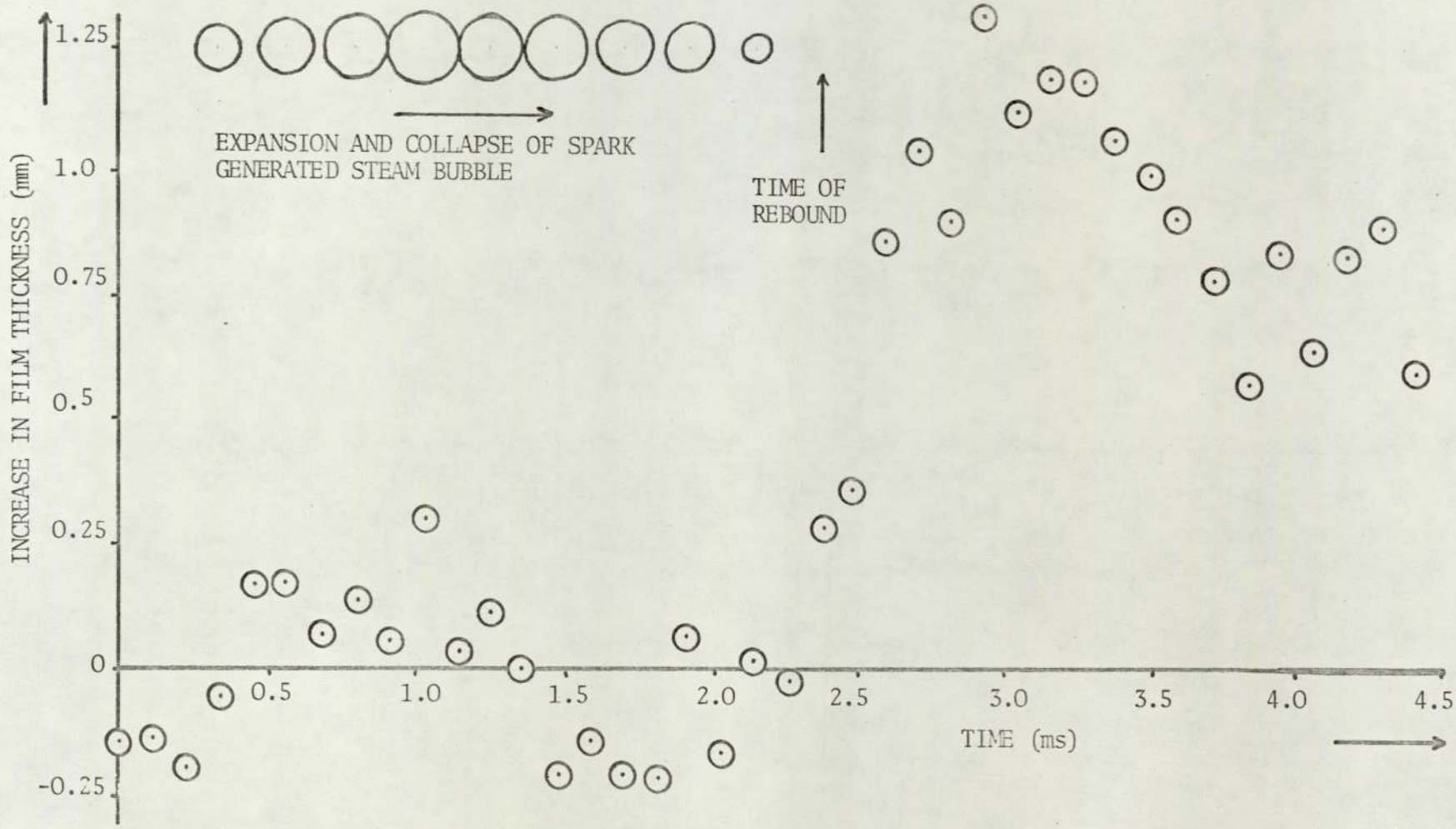

Fig 9 The effect of a spark generated pressure wave on the apparent thickness of a film of vapour surrounding an aluminium drop cooling in water

occurred as a result of an explosive interaction. The same was true of propan-1-ol as coolant. The small droplets of tin examined after falling through either coolant did not have the familiar pear drop shape formed after a non-explosive MCI with water (see Plate XIV). They were more of a disc shape suggesting perhaps that they had remained molten for longer than in water.

Some experiments involving the use of water carbonated by passing carbon dioxide gas through it for fifteen minutes were performed. It was found that tin drops at 500°C (the melt temperature providing the maximum percentage disintegration in water) failed to explode in carbonated water at room temperature. To see whether explosions occurred at lower coolant temperature, the carbonated water was cooled down. Even though the coolant temperature was as low as 2°C, no tin drops exploded and once again the shape of the solidified metal was disc-like.

4.1.9 Molten Salts as Melts

To try and determine how some slags might react when cooled in water, preliminary experiments were performed using molten sodium chloride and molten copper (I) iodide as melt . Molten sodium chloride formed well-defined drops when heated to over 900°C (the melting point of sodium chloride is 801°C). The average mass of such drops was found to be approximately

Plate XIV Pear shaped tin drops cooled in water alongside the disc-shaped drops formed on cooling in carbonated water.

0.1 gm by weighing some which had been cooled in propan-1-ol coolant (see Plate XV). Over a water temperature range of 0 to 85°C, molten salt exploded very soon after penetrating the water surface. The interactions were very noisy and as the droplets broke up, they dissolved in the water. However, at water temperatures in excess of 85°C, no such explosions occurred. Indeed, a drop would fall into the coolant and rise up to float on the surface of the water, suspended on a film of steam. Once the initially cherry red glow of a molten drop had disappeared, the drop would fall and dissolve in the coolant. The temperature of the drop had presumably fallen below the Leidenfrost temperature, the minimum temperature at which stable film boiling of coolant could be sustained.

Copper (I) iodide also broke up on falling through cool water. Drops formed readily at 800°C and the debris was finely divided (see Plate XV). Once again hot water suppressed any explosive activity. Some disproportionation of the copper (I) iodide was apparent after melting, with black iodine particles covering the drops.

4.1.10 High Speed Film Analysis

An example of a short sequence of cine film recording a tin drop as it fell through water is shown in Plate XVI. The half head height attachment provides two thinner frames to one

Plate XV Spherically shaped salt droplets (left) and fragments of copper (I) iodide droplets.

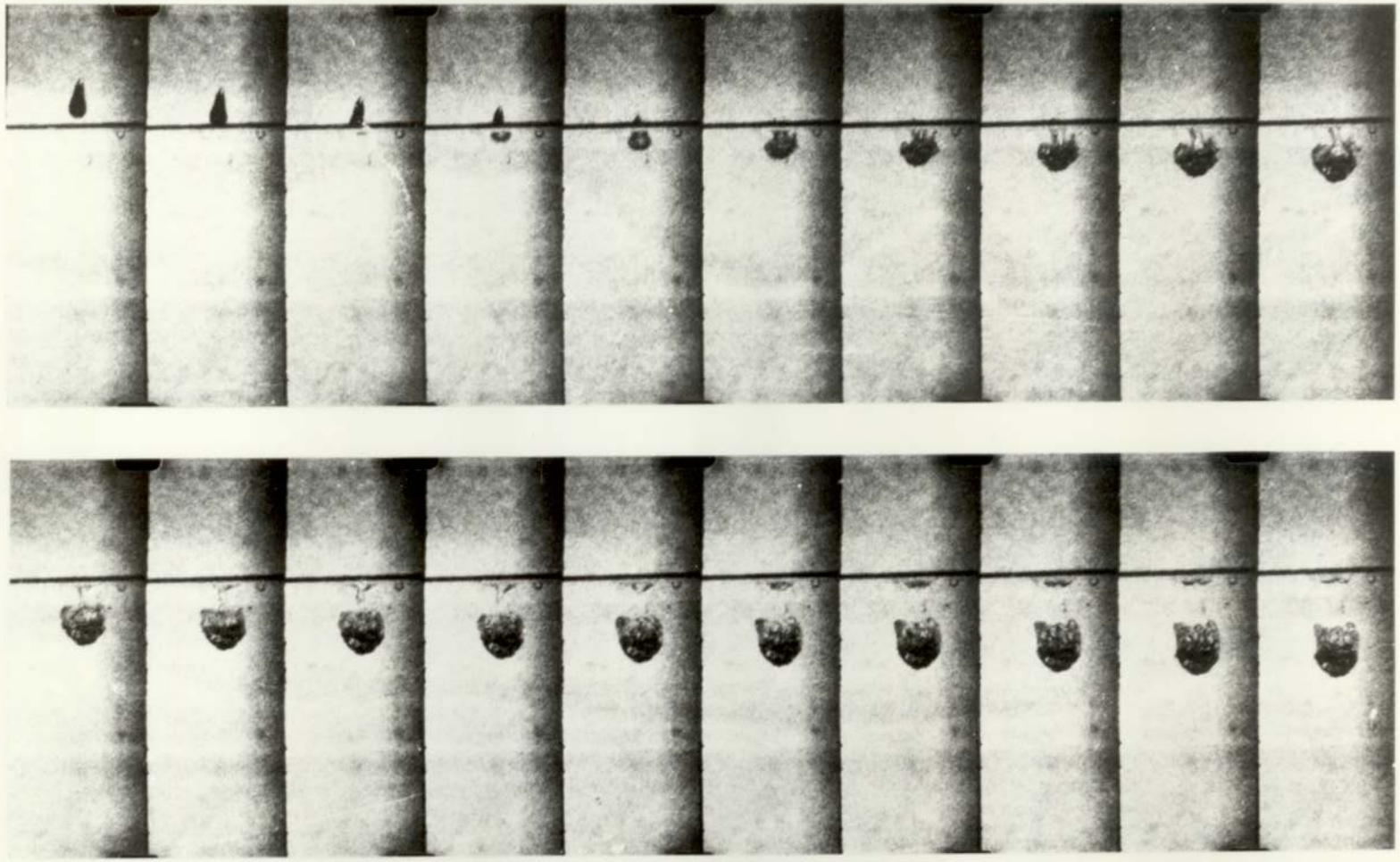

Plate XVI A sequence of cine film (shot at 1400 frames per second) showing a tin drop falling into water

conventional 16 mm frame. The film has been push processed to cope with the short-time exposures of high speed cinematography, and this unfortunately gives a grainy, less well defined image. The film sequence shown in Plate XVI was shot at 1400 frames per second which corresponds to an exposure of 0.29 ms per frame. An examination of other sequences of high speed film has shown that the explosive trigger is not captured using this technique as the time scale is too long. What does show up is the way in which a tin drop, on falling through water, builds up an envelope of steam around it of similar shape. In addition, drops very often rotated somewhat after entering the coolant (cf the spinning lead drops observed by Konuray[128]).

4.1.11 Recording of Pressure Waves

When tin drops explode in water, pressure waves are generated within the coolant. A hydrophonic measuring technique was employed to monitor these waves and to see whether the pressure patterns altered as melt temperature and coolant temperature changed. The initial experiments used a fast time sweep on a storage oscilloscope to record the data. A polaroid snapshot of the trace was then taken as a permanent record. One drawback of this system was that the pattern was stored by virtue of the cathode ray oscilloscope screen's phosphorescence. Very often the electron beam fluctuated so rapidly that the phosphorescence did not truly

record the trace. However, a number of traces were recorded of the pressure waves created by tin drops falling at different temperatures into water. Some of these traces are shown in Figs 10 to 12. Each photograph shows the superimposed traces resulting from ten drops falling into the coolant. For tin with a relatively low superheat, there is a spread of time over which pressure waves are produced. At higher tin temperatures (500 and 600°C) this spread is reduced as each drop falling into the water explodes. Also, the higher the tin temperature the greater the explosive pressure wave generated. A comparison of the traces in Figs 11 and 12 reveals that the pressure intensity associated with the hotter melt is much larger.

Later experiments were performed using a transient recorder. This was capable of storing 1024 equally spaced measurements over a predetermined time span and displaying them subsequently on a cathode ray oscilloscope screen. As the instrument was capable of storing pre-trigger signal information, it was discovered that a definite time period between a tin drop hitting the water surface and exploding was measurable. This 'dwell time' was measured for various water temperatures and found to increase as water temperature was increased (see Fig 13). A pressure pattern is shown in Fig 14 and the dwell time is marked. The reproducibility of the size of the tin drops is shown by histogram in Fig 15.

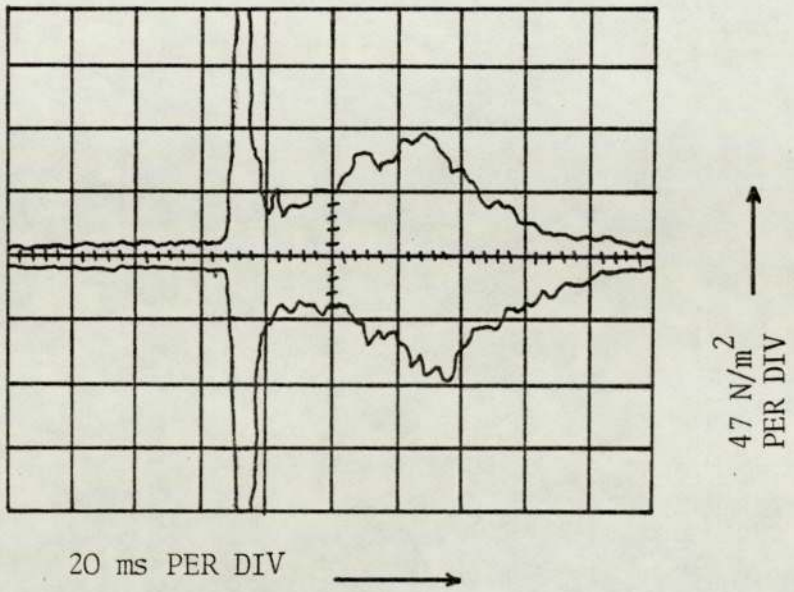

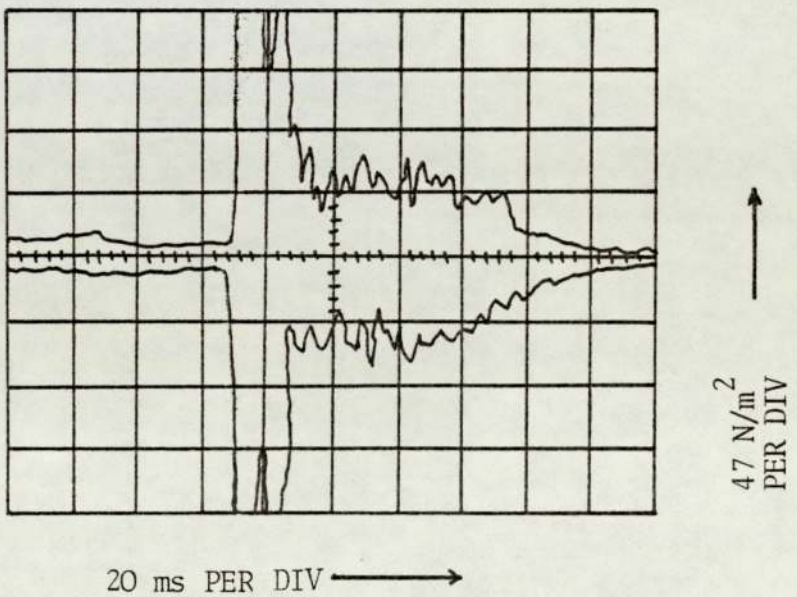

Fig 10 Two traces showing the pressure wave monitored when tin drops at 400°C fell into water at 25°C

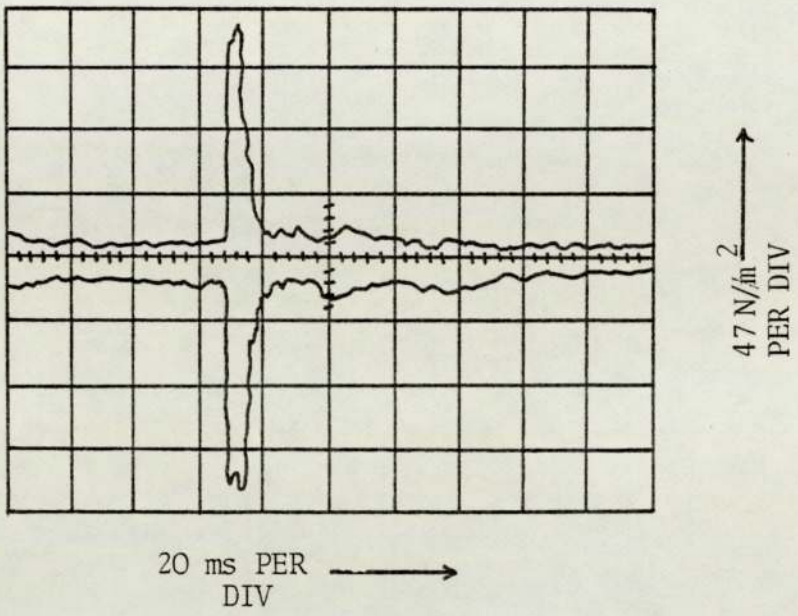

Fig 11 Pressure wave trace recorded when tin drops fell at 500°C into water at 25°C

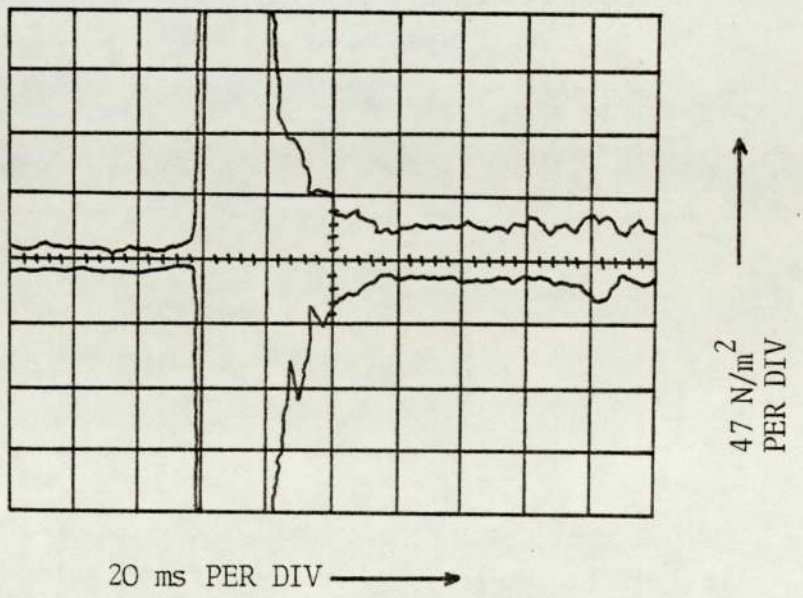

Fig 12 Pressure wave trace recorded when tin drops at 600°C fell into water at 25°C

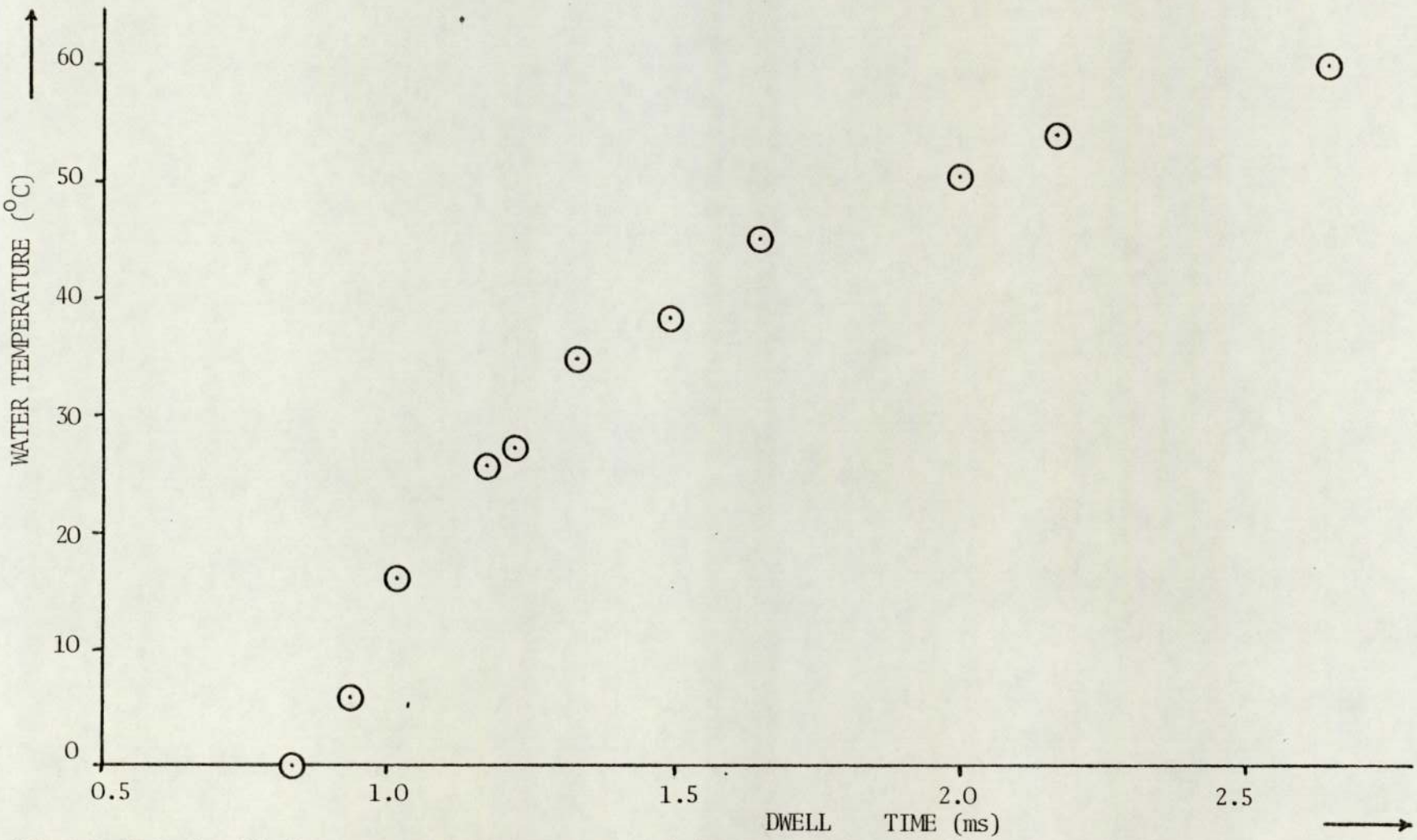

Fig 13 Relationship between water temperature and dwell time for tin drops falling through 6 cm into water

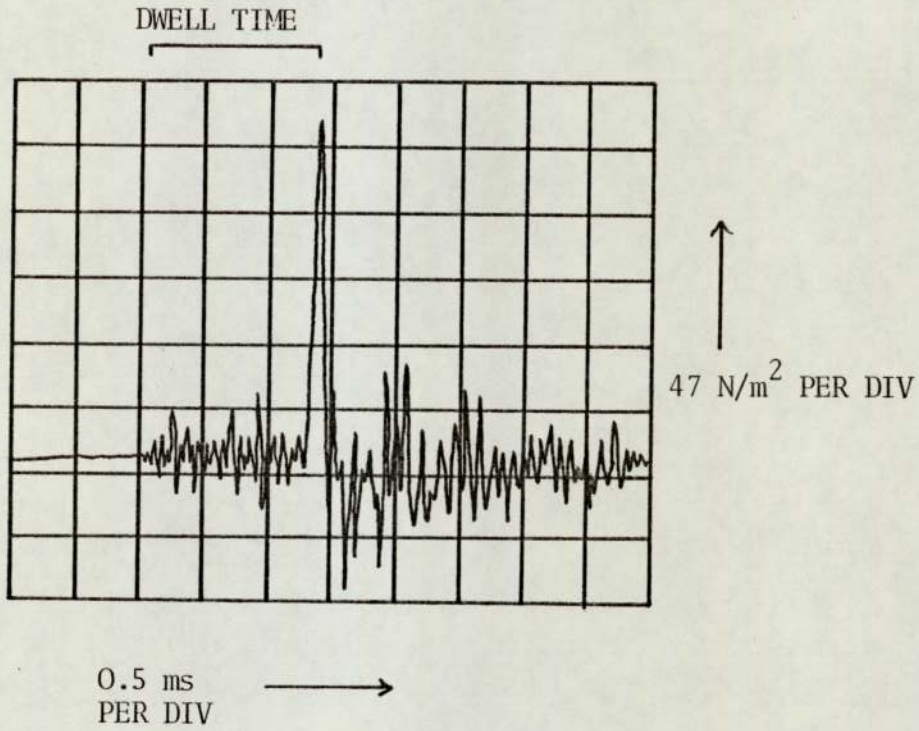

Fig 14 Pressure wave monitored using the transient recorder showing dwell time

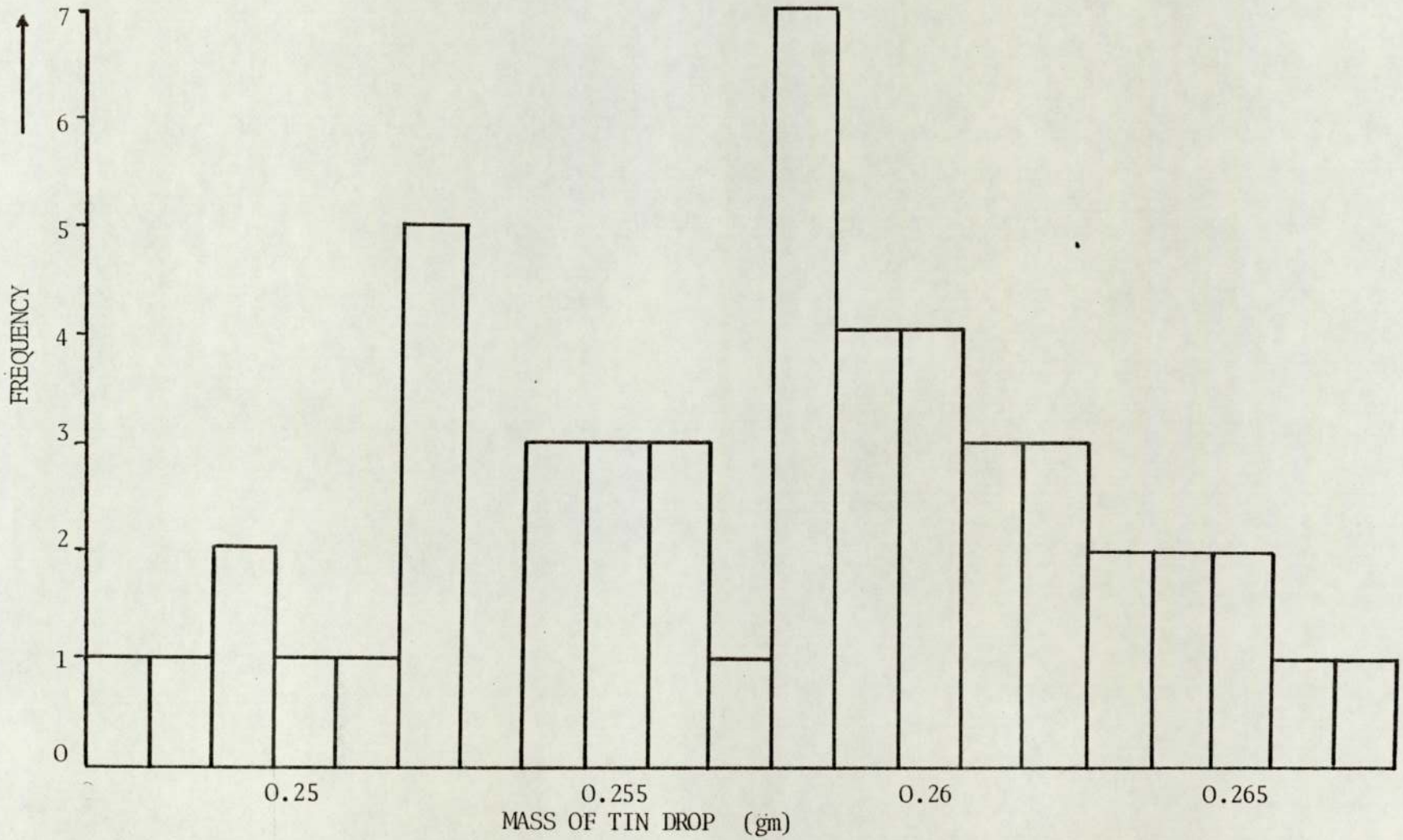

Fig 15 Weight distribution of tin drops

4.1.12 Steam Bubble Generation

High speed films were taken showing the way in which a steam bubble behaves when generated by a spark discharge in water at various temperatures. The bubbles which formed in cooler water expanded and collapsed with the time taken to do so increasing with water temperature. At a high water temperature ($88^{o}C$), a steam bubble formed slowly and collapsed sluggishly. Indeed, the shape of the bubble was far less regular than the shape of those created in cooler water. Also at lower temperatures, a number of 'rebound bubbles' were produced after the first bubble whereas no such bubbles were observed in water at $88^{o}C$.

Graphs were plotted of bubble radius as a function of time for bubbles formed in coolant at 28, 48, 70 and $88^{o}C$. These are reproduced in Figs 16 to 18. They show that the initial steam bubble takes 2.73 ms, 2.84 ms, 3.04 ms and 5 ms to expand and collapse for water temperatures of 28, 48, 70 and $88^{o}C$ respectively. Each bubble generated had similar dimensions.

4.2 Large Scale

4.2.1 Copper-Water Interactions

Molten copper in amounts varying between 0.91 kg and 4.54 kg

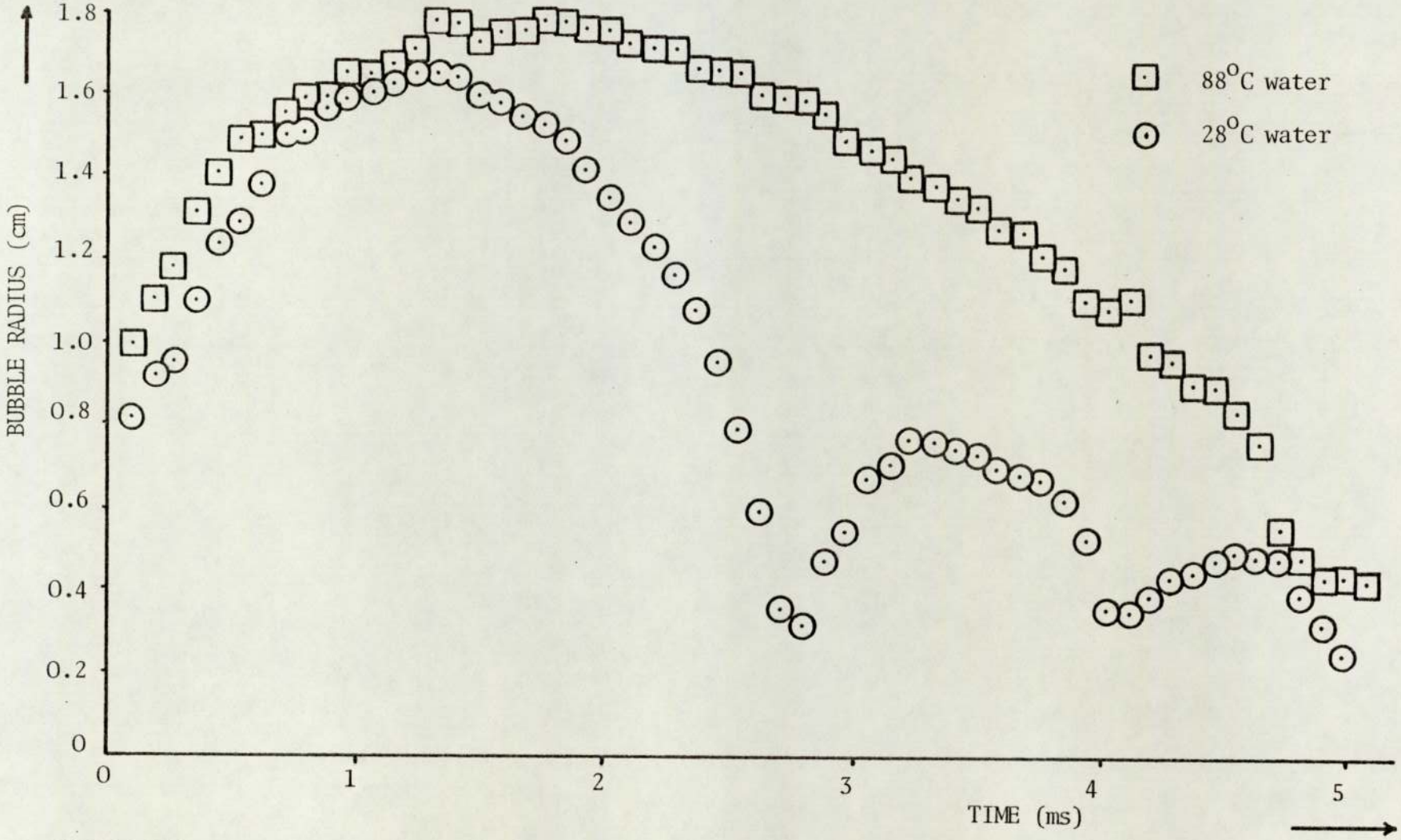

Fig 16 Characteristic features of a spark generated bubble formed in water at 28°C and 88°C

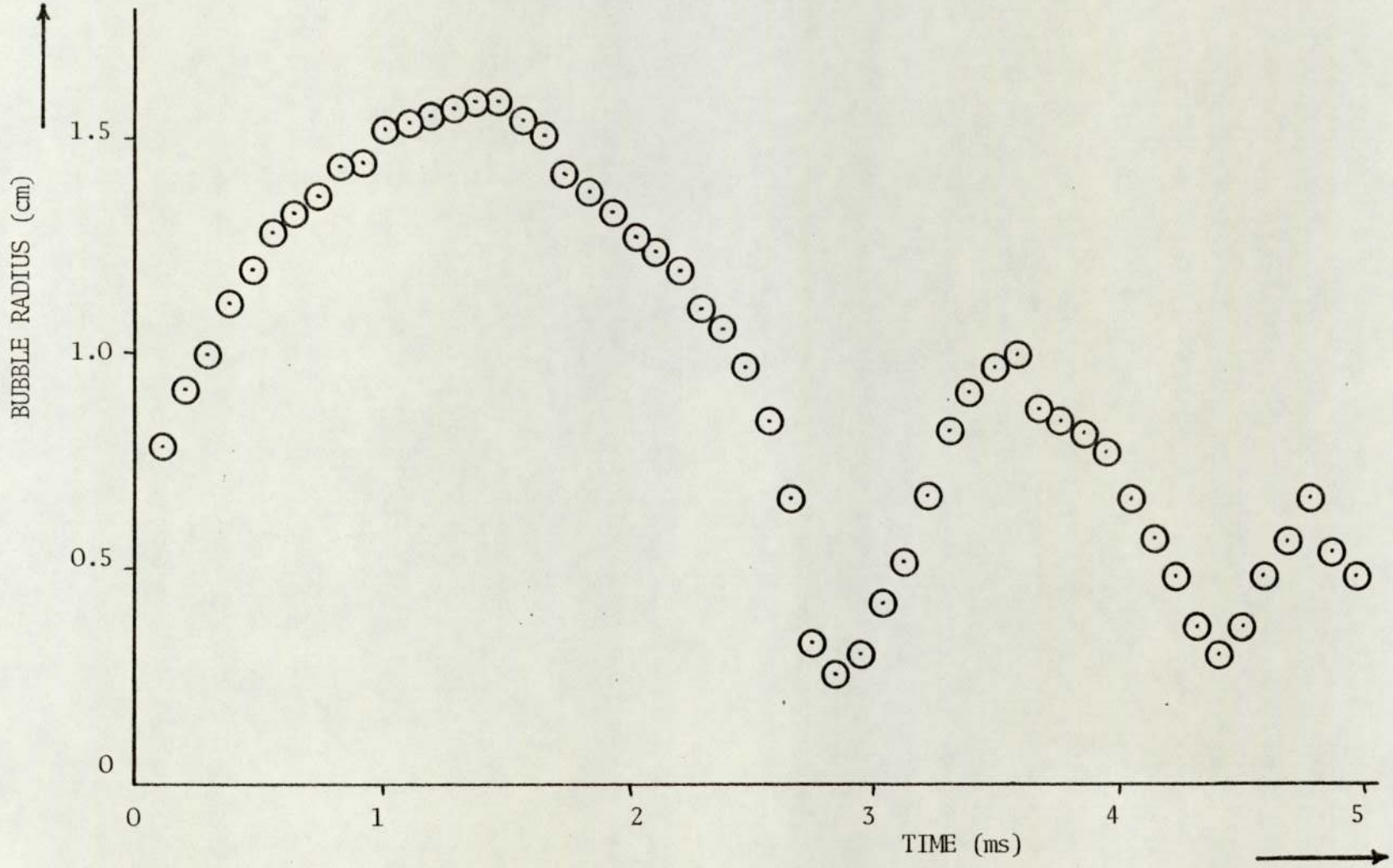

Fig 17 Characteristic features of a spark generated bubble formed in water at 48^{o}C

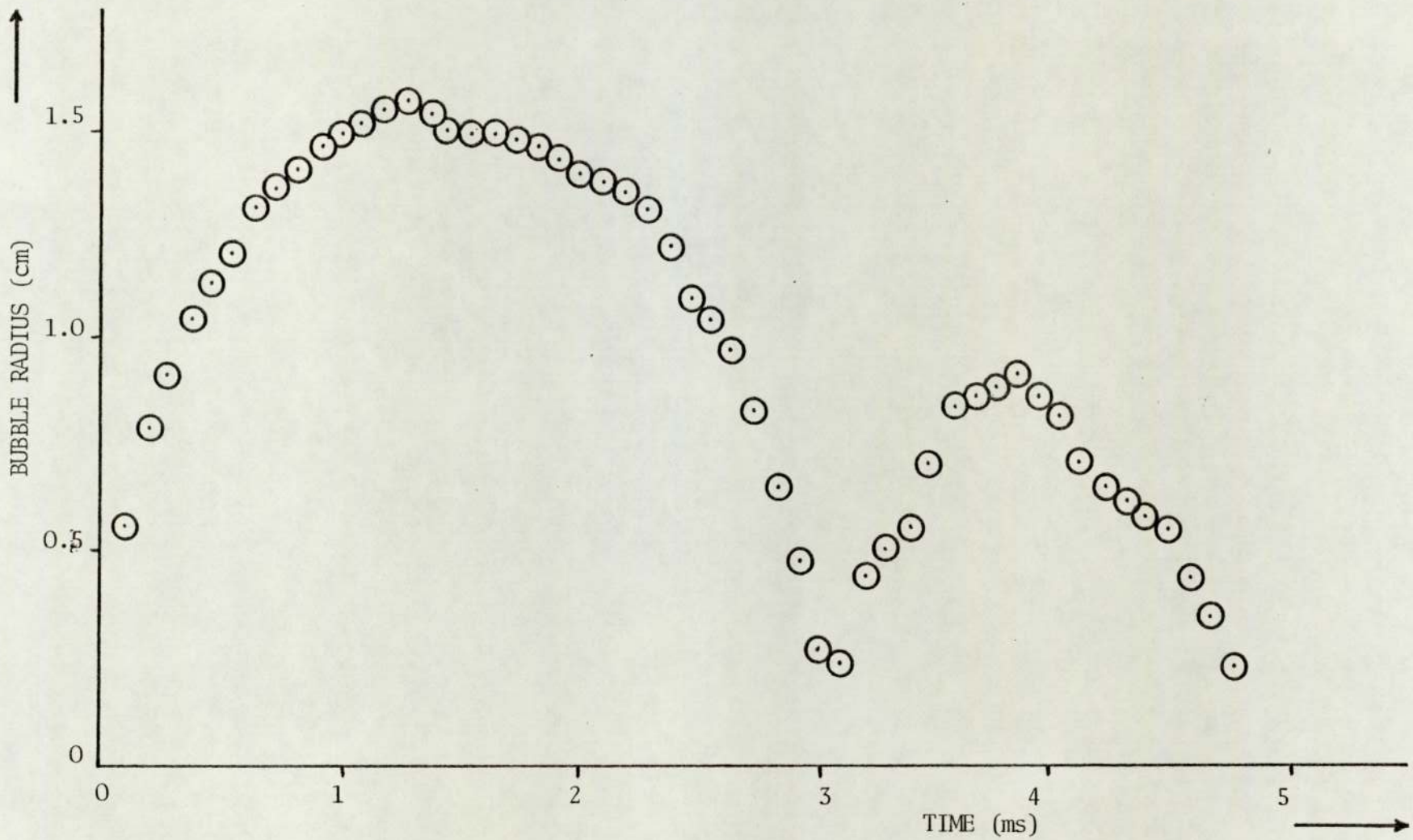

Fig 18 Characteristic features of a spark generated bubble formed in water at 70°C

were dropped into coolant tanks full of water. Explosions were never seen to occur as the metal fell through the water but only after it had come into contact with the base of the tank. A minimum mass of copper (1 kg) was required below which no explosion took place. The tank base also had to be rusty to sustain an explosive interaction. No such interaction was observed when the base was painted with a rustoleum coating to make it smooth. Some copper melt was poured into larger coolant tanks (2 ft cube) but this did not succeed in suppressing an explosion. Many reels of high speed film were taken of copper-water MCIs which showed that the explosive trigger took place in a very short space of time (much less than half a millisecond). A short sequence of high speed film is shown in Plate XVII. The debris collected after an explosion was very finely divided with metal particles below 10^{-2} cm in size being common.

4.2.2 Iron-Water Interactions

Crucibles of molten iron were poured into water to see if any explosive activity similar to copper occurred. The metal was melted using the minitoroidal burner to provide adequate superheat. Spontaneous explosions did not occur even after the metal had spread on the base of a rusty tank. Tests were then carried out to see how much a pressure wave in the water affected the cooling process. After deciding to use a small cordtex charge stuck onto the side of a water

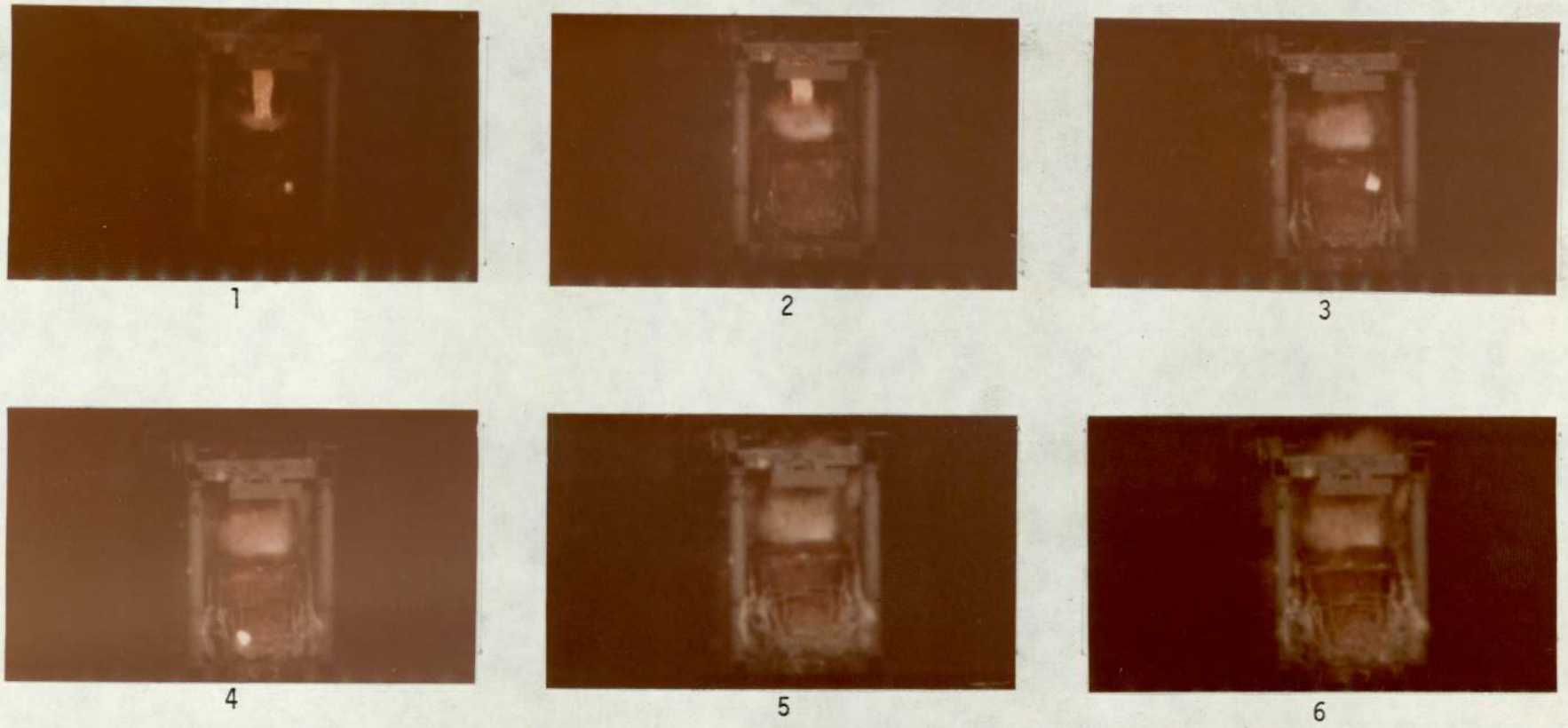

Plate XVII A high speed film sequence showing a large-scale explosion of copper in water (3000 frames per sec.)

tank to provide the shock wave, a film was taken to see how much effect the charge alone had on the tank. The cordtex moved the tank only slightly to one side so that any explosive MCI created would be easily identified. After initial synchronisation difficulties, a high speed film showing a pressure wave promoting an iron-water explosive interaction was taken. The cordtex charge had been detonated as the iron fell through the water so that no base involvement occurred. A sequence of this film is shown in Plate XVIII. The cavitation induced in the coolant soon clears to expose a rapidly expanding metal bolus the shockwave associated with which cracks the perspex window in the tank and eventually blows the whole tank apart. The molten iron is definitely an orange colour just before the cordtex charge is detonated. Subsequently, it assumes a grey colour which indicates a high heat transfer from the metal to the coolant in a very short space of time.

4.2.3 Molten Salt-Water Interactions

Common salt was heated to 1000^{o}C plus and then poured into cool water. A very loud noise was heard as a result but on examining the tipping rig and tank afterwards, no significant damage was caused. High speed films indicated that the molten salt did not fall through the water but reacted at the surface with the bolus breaking up considerably to spray the surrounding area with white streaks.

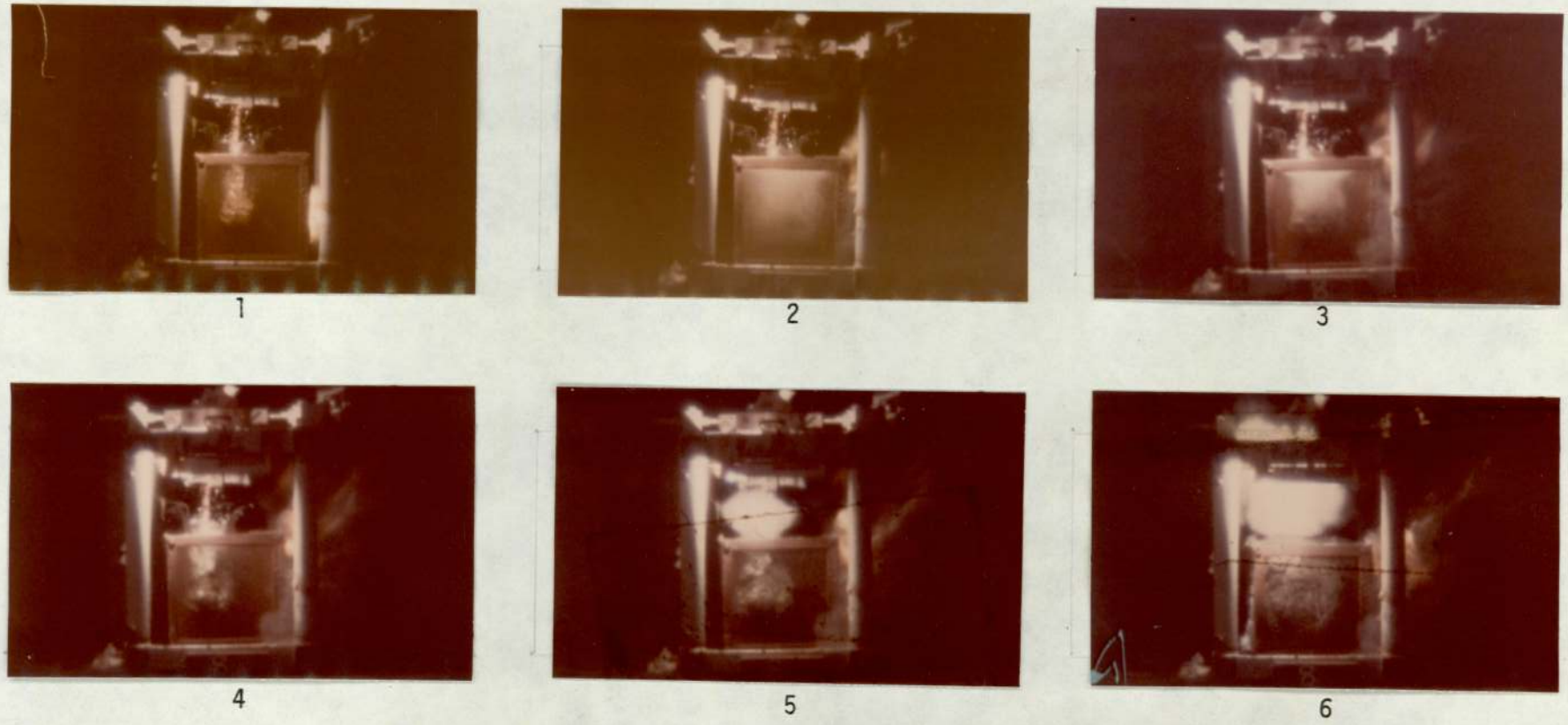

Plate XVIII A high speed film sequence showing how a shock wave promotes a large-scale explosion between cast iron and water (3000 frames per sec.)

4.2.4 Nickel-Water Interactions

Several pours of Nimonic 105 (a nickel alloy containing 15% chromium, 20% cobalt, 5% Molybdenum, 5% aluminium, 1.2% titanium) into water were made with the metal having been heated to between 1320 and 1550°C with the minitoroidal burner. No explosive interactions occurred and the metal was seen to cool down quietly on the tank base.

4.2.5 Magnox-Water Interactions

Magnox is an alloy containing 98.99% magnesium, 1% aluminium and 0.01% beryllium and has a low density (1.74 gm cm^{-3}). Quantities were melted, heated to between 700 and 800°C and poured into cubic foot tanks of water. Explosions took place and an examination of the high speed films taken of the interactions showed a definite two-stage process. On hitting the water surface, the magnox was seen to break up slightly with fragments being thrown upwards. The bulk of the metal, however, did fall through the coolant and after a while another more violent interaction took place. This second event whited out the film completely, suggesting that oxide was formed. It emanated from the base of the tank with the time between the first and second interactions being roughly 0.12 seconds (measured from films of two separate pours).

CHAPTER FIVE

DISCUSSION

The experiments carried out serve to bolster the evidence in favour of a vapour collapse theory for the fragmentation process. The data collected both from small and large scale work indicate that the film of vapourised coolant which separates the two liquids has to collapse or become disturbed for an explosive condition to exist. Certainly, the intimate mixing of melt and coolant which is generally considered to be a necessary precursor to an explosion can only take place once the vapour film 'barrier' between the melt and coolant has been removed.

5.1 Small Scale Work

The experimental system whereby small droplets of melt are made to fall into water provides results of a reproducible nature. The percentage disintegration curve for lead shows distinct similarities to that for tin which Konuray[128] obtained. Indeed, apart from Bradley and Witte's[18] experimental arrangement where melt is injected into the coolant, the droplet system is the only one to date which brings a standard size and shape of hot fluid into contact with a cold one.

When the higher melting point metals, namely copper (1083^{o}C)

and aluminium (660°C), were dropped into cool water, no spontaneous explosions occurred unlike many of the lower melting point metals, eg tin (232°C), lead (327°C) and Woods metal (70°C). Although complete fragmentation did not take place, some evidence of minor interactions was apparent. Some of the aluminium drops fell to form hollow spheres, the centres of which contained some gritty debris. This tends to indicate an entrainment of water (cf Groenveld[103], Schins[104]) rather than air on falling. Spheres of copper were also recovered (see Plate XIII).

Some copper and aluminium drops did show signs of minor fragmentation. However, by far the majority of drops cooled to form solid regularly shaped pieces of metal.

The solidification of the droplets took place within a 40 cm water depth at which time the stroboscopically illuminated photographs showed that the vapour film around them was still intact. Therefore, when film collapse finally did take place, at between depths of 50 cm and 60 cm, a droplet would be solid and unable to mix with coolant to provide an explosion.

The copper and aluminium drops which showed signs of fragmenting would have had the film of vapour surrounding them perturbed in some way. Indeed the hydrodynamic forces which are exerted on a vertically falling drop may create such a perturbation.

5.1.1 Water Entry

When a body falls into a liquid, it initially creates a vented cavity behind it and a splash at the surface. As the body progresses downwards, this cavity seals with the subsequent formation of two liquid jets, one upward and one downward (Worthington[131]). This latter jet is directed towards the body and is called the reentrant jet. Under some circumstances, this jet traverses the length of the cavity to strike the body with considerable force. Gilberg and Anderson[132] have stated that this occurs very often with vertical entry as opposed to oblique entry. The entry of a body into water is shown diagrammatically in Fig 19. A paper by May[133] supports the work of Gilberg and Anderson.

From this sequence of events, a copper drop would come under the influence of a reentrant jet on falling through water. Furthermore this jet might cause the vapour film around the drop to become distorted or perhaps broken so that liquid water could come into contact with molten copper. Such a temporary film breakdown might conceivably create the partial fragmentation of copper which is experimentally observed. A complete fragmentation of the drop would be prevented by a very rapid solidification of metal following this initial interaction.

Generally, however, both aluminium and copper drops would fall in water whilst being surrounded by a blanket of steam. The

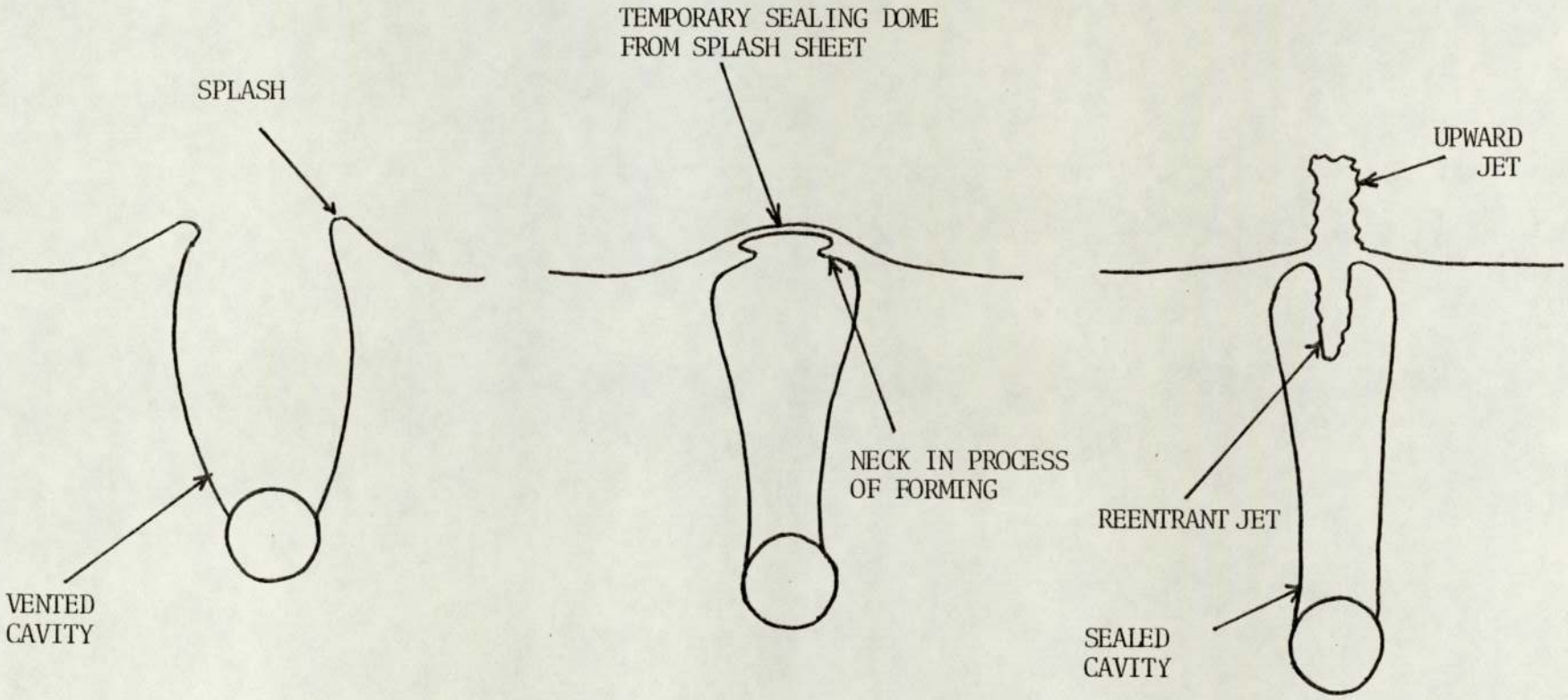

Fig 19 Schematic representation of hydrodynamic phenomena created by vertical water entry

temperature of the drops and their thermal conductivity would provide sufficient heat energy to maintain such a blanket until well below the solidification temperature. On the other hand, the film of vapour surrounding lower melting point metals would generally collapse before solidification and hence enable intermixing of melt and coolant to produce an explosion.

The more direct way of causing a collapse of the vapour blanket surrounding a cooling droplet was with a submerged pressure pulse. As may be seen in Plate X and Fig 20, an aluminium droplet acquires a stable boiling film very soon after water entry. So long as this film is disturbed whilst the metal is still molten, then an explosion will probably result. The experiments designed to fragment aluminium in this way were almost entirely successful. The spark generator electrodes which provided the pulse were positioned so that no drop passed through more than a 6 cm depth of water to ensure that the metal was still molten and fragmentation was usually total (see Plate XIII).

The effect of a shock wave on a cooling copper droplet was not quite as predictable. As a droplet was not made to explode, this infers that contact between liquid water and liquid copper did not take place. The copper was, however, definitely molten because it went to form smaller regularly shaped globules. One possible interpretation of this is that instead of breaking the film down, the shock wave was transmitted through the film

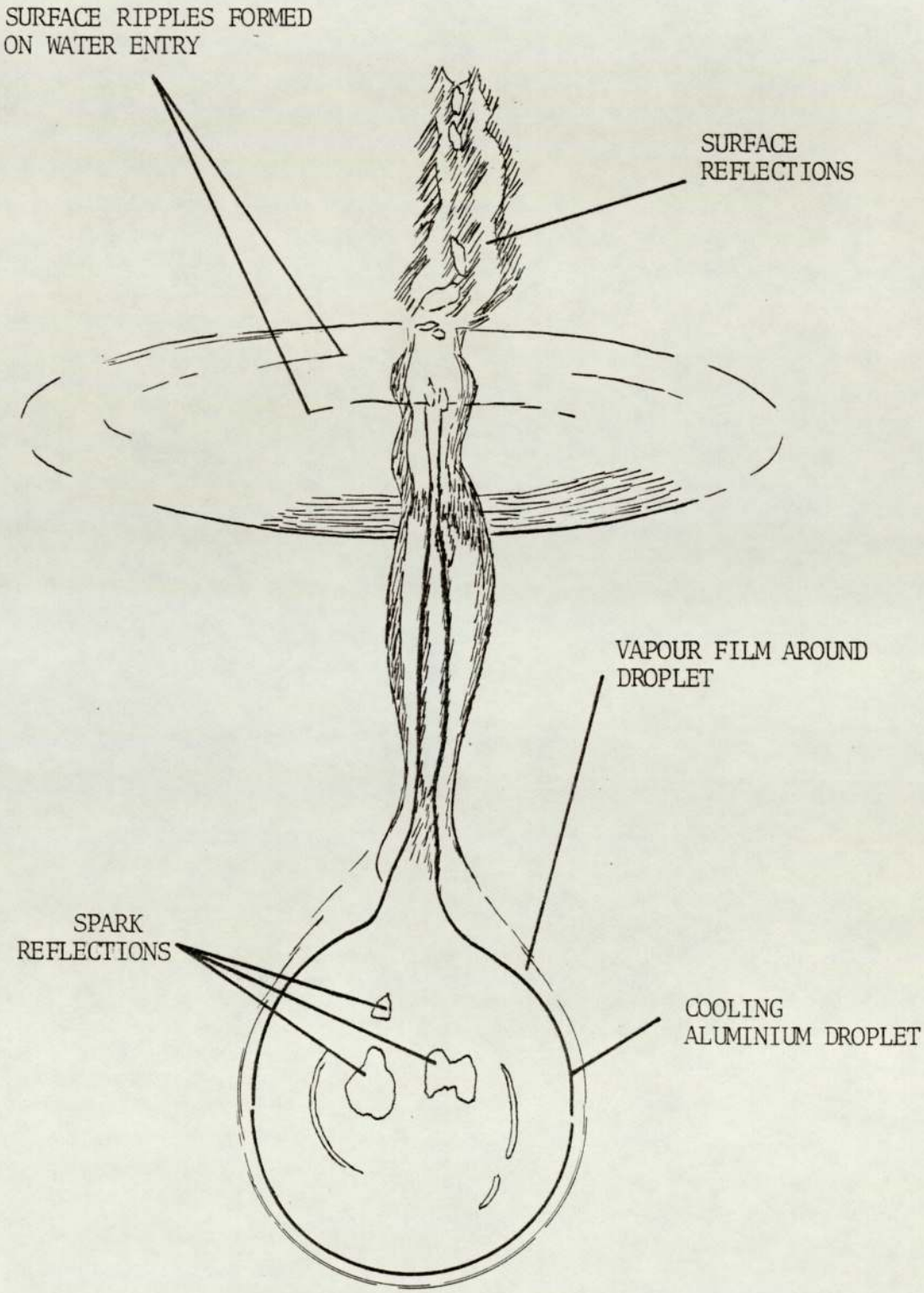

Fig 20 Tracing of Plate X showing major features

and broke up the meltdrop subsequently. Only in this way would the two liquids maintain their separation and an explosive condition be averted.

A third shock wave effect was observed when an aluminium drop passed near to the spark generator electrodes. The high speed film of the incident appeared to show that the thickness of the vapour film surrounding the drop was increased but no explosion induced. This apparent thickness increase (see Fig 9) is of the order of a millimetre or so and is very noticeable on projected cine film. It occurred at the point of rebound of the spark generated bubble (see theory of vapour bubble collapse, Chapter 2).

Firstly there is no definite evidence that the metal drop was molten. In the earlier experiments, some aluminium drops had solidified very soon after water entry, so it may have been this that prevented an explosion. Also, what appeared to be an increase in the vapour film thickness around the drop may have been something else. The film had been push processed and was very 'grainy' (not sharp) as a consequence. What seemed like a vapour film thickness increase could have been the formation of a large number of small bubbles at the liquid water-vapour interface.

In general, it seems that a shock wave does indeed disturb the film of vapour around a cooling droplet. This disturbance need

not necessarily, however, lead to the drop exploding.

The experiments performed using other coolant liquids demonstrated their inability to sustain an explosion with molten tin. It was observed that the film of vapour which surrounded the melt on passing through these coolants was maintained for longer than a fall through ordinary water. In addition, the tin shapes recovered afterwards resembled those obtained after the metal had fallen through water above the critical temperature. A disc-like form was created as opposed to the distinct pear drop shape produced when tin just above its melting point had fallen into water (see Plate XIV). The conclusion may be drawn that a disc-like shape is formed when the melt remains molten for a longer time. The aluminium drops generally showed a similar form to this with a stable steam blanket around the drop enabling heat to be transferred less rapidly to the coolant than by an explosion.

Carbonated water, formamide and propan-1-ol all provided stable vapour films around cooling tin droplets which persisted until well after the metal had solidified. Once film collapse did take place, there was no molten metal present to intermix explosively with liquid coolant. If the boiling curves of these other coolants were compared to that of water, the most noticeable difference would be their ability to sustain stable film boiling around a hot body at much lower superheats.

The non-metallic melts investigated showed explosive behaviour with water. The tendency for sodium chloride and copper (I) iodide not to explode was only found in hot water (greater than $85^{o}C$). These salts differ from metals in many respects, an important one being thermal conductivity. For example, salt's thermal conductivity is 0.09 W cm^{-1} $^{o}K^{-1}$ whereas that of copper is 3.5 W cm^{-1} $^{o}K^{-1}$.

The thermal conductivity differential can explain their difference in behaviour with water. On being dropped into the coolant, both the salt and the metal establish a blanket of steam around them. However, the thermal gradient within either melt globule is quite different. As heat is freely conducted through a liquid metal, the temperature of a droplet varies gradually from the centre to the metal-vapour interface. The heat transferred to the bulk water is determined by the vapour film and when the metal's melting point is reached, the whole droplet solidifies almost immediately thereby denying an explosive situation. For a salt droplet cooling from a similar high temperature, its centre remains molten even after solidification has taken place at the surface. This is because heat from the centre is not efficiently conducted to the surface of the droplet and a thin shell of solid salt forms around a molten core. When film boiling ceases in the surrounding coolant, the hydrodynamic forces produced are easily able to permit water to penetrate this surface layer and mix explosively with the melt inside. A diagram showing the temperature profiles in and around cooling drops, both metallic

and non-metallic is given in Fig 21.

When salt falls into hot water, the vapour layer around a droplet persists longer than in coolant which is more subcooled. This enables a greater part of the droplet to solidify before film collapse so that a non-explosive situation results. As demonstrated experimentally, the steam blanket surrounding a salt drop in hot water readily supports the molten mass. By the time the Leidenfrost point is reached at the salt vapour interface, a large proportion of the droplet has crystallised and no contact takes place between the melt and liquid water. As Board et al[87] have demonstrated, liquid water at high temperatures may sustain explosions when intimately mixed with melt. Once again, it seems that it is the vapour film barrier which prevents contact between the hot and cold fluid and thereby an explosion.

The measurements made hydrophonically within the coolant on the tin/water system are worthy of some discussion. In the earlier experiments, without the transient recorder, comparisons were made between the explosive intensities created by tin at different temperatures. Not surprisingly, an increase in metal temperature resulted in the generation of a peak pressure pulse which also increased in amplitude (see Figs 10-12). The conclusion to be drawn is that the thermal energy stored by the tin droplets is transformed into the mechanical shock wave energy created by the subsequent explosion in water. These

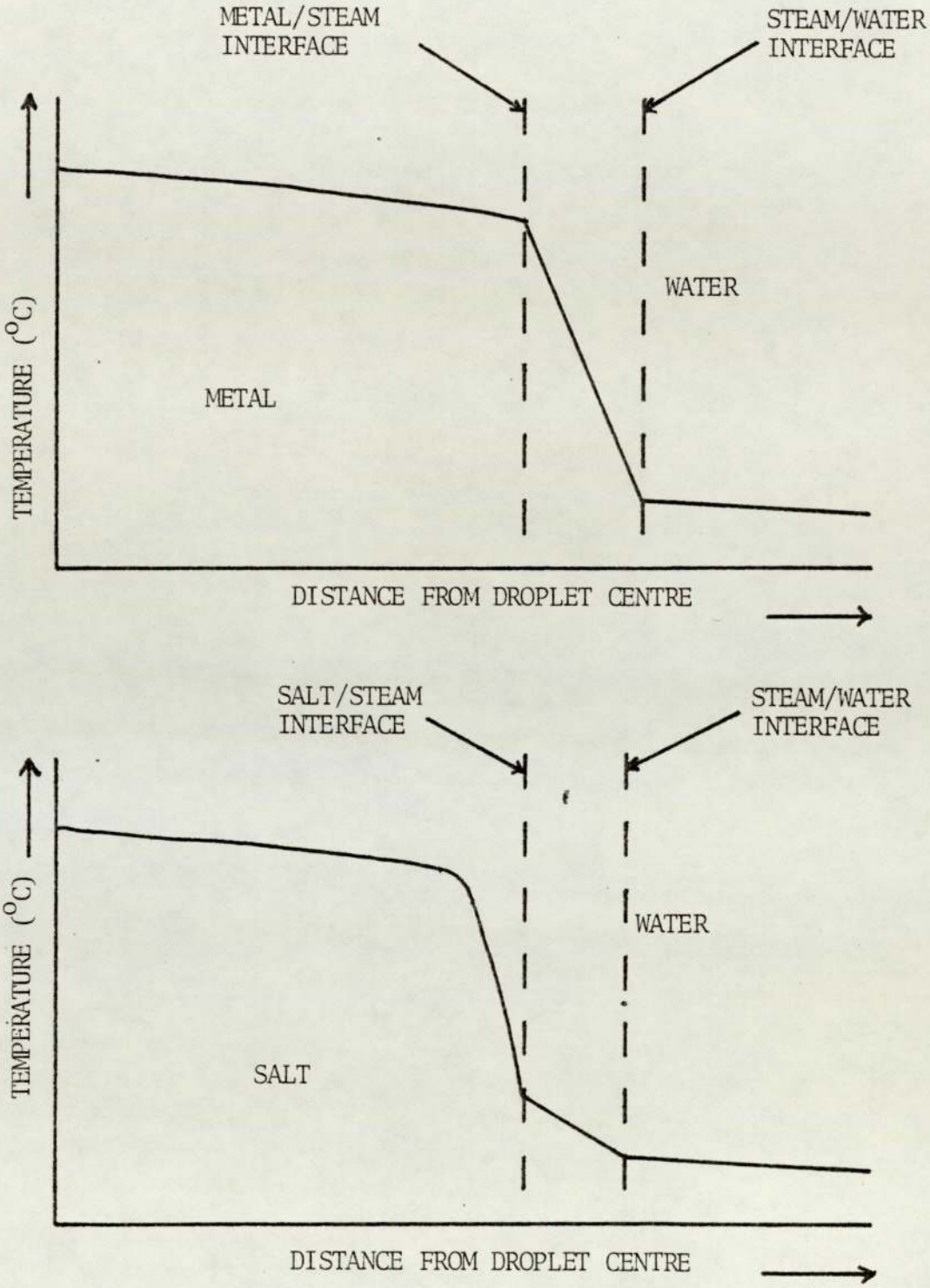

Fig 21 Diagram showing the thermal profiles of a liquid metal and a molten salt which exist when in contact with coolant water

earlier tests also show a distinct spread in time over which a pressure disturbance is produced for tin at 400°C compared to that for tin at 500°C and 600°C. A correlation may be made here between Konuray's[128] percentage disintegration curve for tin which shows less probability of fragmentation for tin at 400°C than for tin at 500°C and 600°C. A non-fragmenting tin drop would fall to generate weaker shock waves within the water. These are readily identifiable from Fig 10.

The information gathered when the transient recorder was introduced, namely that dwell time increased as water temperature went up, continue to reinforce the experimental evidence in support of a vapour film collapse theory prior to fragmentation. If the vapour film surrounding a cooling tin drop is considered to be a steam bubble inside which there is a sustaining heat source, then it is when the bubble contracts onto the surface of the drop that fragmentation is likely to occur. This contraction takes place over a time period which is very much a function of the coolant subcooling. In other words, for a complete contraction to occur in water at 80°C, more time is required than in water at 20°C. The less subcooled the water, the longer it takes for the boiling film to contract towards the metal. As the dwell time values demonstrate, for water at 0°C, the vapour film takes only 0.833 ms to break down whereas for water at 60°C, the vapour film exists for 2.65 ms. The subsequent fragmentation and the formation of a pressure pulse takes a matter of microseconds. Indeed, an estimate of the time

taken to reach peak pressure (the pressure peak rise time) was made from a pressure trace and found to be between 20 and 30 μs.

To see whether the timescales involved in the film contractions were realistic, measurements on spark generated steam bubbles were made. From these results, as expected, a bubble took longer to expand and collapse in hot water than in cool water. In fact, at 28°C, a bubble took approximately 2.7 ms to form and collapse. This time rose to over 3 ms at 70°C. Furthermore, for a bubble generated at 88°C, this expansion and collapse cycle took about 5 ms, and the bubble shape was less regular than at lower temperatures. Such a result may help to explain the existence of a coolant critical temperature above which no spontaneous explosions are experienced. By the time a surrounding vapour film has contracted sufficiently, melt solidification almost certainly will have taken place under these conditions, thereby preventing an explosive interaction. Obviously, the steam bubbles created by a spark and surrounding a cooling tin drop are not exactly identical. However, although a spark creates a high temperature (20,000°K) it lasts only for a matter of microseconds whereas a hot tin drop (500°C) retains its heat for a great deal longer. Therefore, the similarity in lifetimes which was measured may be taken as a rough guide to the vapour film behaviour around a cooling molten drop. Some notes on spark generated steam bubbles may be found in the Appendix.

5.2 Large Scale Work

The results of work carried out in the field by dropping larger masses of melt into water have tended to back up the small scale experiments performed in the laboratory. As higher melting point metals were generally used on the large scale, spontaneous free-contacting explosions were not produced. Only in the case of molten salt did such an explosion occur and as previously discussed, this may be explained by salt's low thermal conductivity and therefore its inability to sustain a film of vapour around it as a sort of protection.

Molten copper exploded only after it had spread on the rusty base of the coolant container (see Plate XVII). Such an irregular surface would nucleate any trapped water quite readily and promote rapid vapour expansion in the way Long proposed after his original aluminium observations. The likelihood of his entrapment hypothesis being valid is borne out by a lack of explosive activity after copper had spread on a smooth, rustoleum painted base. Further work on the base triggered MCI is required to test Long's hypothesis.

The observation made in the laboratory that molten copper drops are capable of sustaining a vapour film around them until after they have solidified in water is in definite agreement with the large scale evidence. Even when molten copper was dropped into larger tanks, only after base spread had occurred did any

explosion take place.

Nimonic 105 failed to explode in water even after it had spread on the rusty base of a coolant tank. It did, however, form a distinctly cellular shape on solidifying unlike the flatter pancake-shaped masses which were retrieved when no explosion occurred with molten copper. From the evidence, it seems likely that some very coarse intermixing of nimonic 105 and water did occur or perhaps of nimonic 105 and steam, and an explosion may well have been prevented by a rapid solidification of metal. Such a cellular form was also created when cast iron fell into water. However, the promotion of an explosion by a shock wave in the water as iron fell through it is of great interest.

As the high speed cine film of this event shows (see Plate XVIII), when the cordtex charge on the tank side is ignited (Frame 1), metal is still well away from the tank base. The cavitation created after the charge has been ignited (Frame 2) by the rarefaction wave completely obscures the iron bolus from sight. When it does reappear, its colour has changed from an orange to a grey which indicates a very rapid loss of heat energy over a short space of time. The bolus of metal proceeds to increase in volume presumably as steam within it expands. The powerful nature of the expansion is seen when the tank's perspex window cracks (Frame 6). Steam may also be seen rising in a funnel shape from the coolant container.

The immediate temptation is to compare this shock-induced explosion to the ones in the laboratory involving aluminium drops. The explanation on the small scale was that the vapour blanket surrounding a cooling metal drop was prematurely collapsed by the pressure disturbance. The subsequent contact between water and molten aluminium led to the fragmentation. Certainly, on the large scale, a great deal of heat energy was quickly removed from the iron bolus and this could well have resulted from direct contact between water and molten iron. What may have assisted in the large scale test is the containment of the pressure wave within the sturdy coolant container. This would have focussed the triggering shock wave onto the iron bolus and caused a collapse of the vapour layer all around the metal, thereby providing more contact area between molten iron and water.

The magnox interactions were unlike any other MCIs observed. When dropped into water, the metal appeared to break up twice, once at the water surface and again upon reaching the container base. Magnox is a magnesium alloy and has a fairly low density (1.74 g c c^{-1}) making it particularly susceptible to Weber number deformation. When the metal was poured into water, it fell in a long tongue shape the first part of which seemed to fragment on reaching the water surface. This initial interaction did not involve any steam generation however and was a consequence of the Weber number effect. The major part of the melt fell through the water and onto the container base. It is here that the second, more energetic interaction, took place. With the

high speed cine film 'whiting out' a great deal of oxide was produced, and the way in which it was probably formed has been outlined by Maischak and Feige[11]. The oxygen-containing compounds are most likely to be the base contaminants such as rust.

Finally, the large masses of molten salt which were dropped behaved just as predicted in the laboratory. Whilst their explosive interaction with water was far louder than many of the metal-water explosions, damage was minimal in comparison. Such behaviour may be explained in either of two ways. First, any solidified salt would not have restricted the growth of expanding water vapour as much as a hard crust of solidified metal. Second, the heat transferred from the molten salt to liquid water may not have been as rapid as that transferred from a molten metal (taking thermal conductivity differentials into account).

5.3 Suggestions for Further Work

The method of obtaining spark-illuminated photographs of cooling melt droplets may be improved upon still further. Rather than manually firing the spark generator, the photoelectric circuit used in the earlier hydrophone experiments might be incorporated to provide photographs at predetermined stages of the droplet's fall into coolant. Such an experimental system could well be capable of capturing an explosive triggering event on film. Also, the electrodes used to date have been machined from

stainless steel rod. A reduction in exposure time (to well below 35 μs) could result from a harder, less easily eroded metal such as zirconium.

The different way in which copper and aluminium drops seem to be affected by a pressure pulse within the coolant warrants more experimental work. Perhaps more high speed films of these metals would determine why aluminium drops usually explode but copper drops break up without fragmentation.

The hydrophonic arrangement has provided results of a reproducible nature. It has been the introduction of the transient recorder which has improved the recording of pressure waves within the coolant - something Konuray[128] was unable to achieve successfully. So far, measurements have been made on only the tin/water system. A logical extension of this work is to apply it to such systems as lead/water, bismuth/water and Woods metal/water - all of which give spontaneous explosions to see whether the dwell time trends exist here also. Consideration may also be given to molten salt/water systems to see if any meaningful hydrophonic data is obtainable. Also, with respect to the tin/water system, dwell times for fuel droplets falling through varying distances before water entry could be measured. Work currently being carried out at the University of Aston points towards a critical velocity range between meltand coolant within which a stable vapour film forms most readily.

Another photographic technique could well provide a visual record of the pressure waves created by an explosive MCI in the laboratory. Shadowgraphy is a widely used technique in the aerodynamics industry and relies on parallel light rays being refracted more by denser media such as are present in shock wave fronts. To supplement the strength measurements of pressure waves produced by MCIs by information on where they emanate from during an interaction would be desirable.

A variation in the large-scale testing would be to use coolant containers of differing geometries. Early large scale tests in the field indicated that the geometry might have a significant effect on whether an explosion occurred. Such a geometrical effect may well have its foundation in the way a trigger pulse is contained prior to an explosive event.

APPENDIX

Notes on Spark Generated Steam Bubbles

The approximation first made by Judd[135,135] may be used. Writing:

T_W - initial temperature of water, ^oK

T_S - temperature of water at the bubble surface, ^oK

T - temperature at a point radius r from the bubble centre, ^oK

K - thermal conductivity of water, W m^{-1} K^{-1}

C - specific heat of water, J kg^{-1} K^{-1}

ρ - density of water, kg m^{-3}

R - bubble radius, m

The heat conduction equation is not solved in the region near the bubble surface, instead the temperature is assumed to be given by the equation:

$$T-T_W = (T_S-T_W) \frac{R}{r} \exp\left[\frac{-(r-R)}{\lambda}\right]$$

where λ is a time-varying skin depth for the heated region of the bubble surface. The following quantities may be expressed as a function of λ:

heat flux at bubble surface $\phi = K \left[\frac{\partial T}{\partial r}\right]_{r=R}$

$$\phi = -K(T_S - T_W)\left(\frac{1}{\lambda} + \frac{1}{R}\right) \text{ , W m}^{-2} \qquad \ldots(1)$$

total heat content of the heated bubble surface

$$Q = \rho C \int_R^{\infty} (T - T_W)\, 4\pi r^2\, dr$$

$$Q = 4\pi\rho C(T_S - T_W)\lambda R(R + \lambda) \qquad \ldots(2)$$

The electrical power delivered to the spark, W, which heats the water, vaporises the water and then heats the steam, is supplied over the time interval $0 < t < \tau$ and is of the form:

$$W = W_{max} \operatorname{Sin}^2 \left(\frac{\pi t}{\tau}\right) \qquad \ldots(3)$$

where τ has been taken as $10\mu s$.

This is taking the current wave to be of damped sinusoidal form with period $20\mu s$ and the peak current reduced by a factor of 2 in one period. The above assumption means that the spark has a constant resistance and all the heating takes place in the first half-period of the oscillation.

The steam is assumed to behave as a perfect gas. Writing:

G - gas constant per unit mass of steam, $J\ kg^{-1}\ K^{-1}$

p - pressure of steam, Nm^{-2}

Tg - temperature of steam, ^{o}K

M - mass of steam in bubble, kg

$$\text{then} \quad p = \frac{GMTg}{\frac{4}{3}\pi R^3} \qquad \ldots(4)$$

An approximate formula for the internal energy per unit mass of steam is used.

The vapour pressure p_v of steam (Nm^{-2}) in thermal equilibrium with water at a temperature T_c (^{o}K) is given by:

$$p_v = 4.97703 \times 10^{10} \exp\left(-\frac{4889.98}{T_c}\right) \qquad \ldots(5)$$

Inverting equation (5), for a pressure p, the thermal equilibrium temperature is given by:

$$T_c = \frac{4889.98}{\log_e\left(\frac{4.97703 \times 10^{10}}{p}\right)} \qquad \ldots(6)$$

The superheat temperature difference, ΔT, is given by:

$$\Delta T = Tg - T_c \qquad \ldots(7)$$

A formula is now sought to express, approximately, the internal

energy per unit mass of steam, U ($J\ kg^{-1}$) in terms of ΔT only. Such a formula is:

$$U = 2.190 \times 10^{6} + 1.540 \times 10^{3}\Delta T + 1.842 \times 10^{6} \frac{\Delta T}{594.2 + \Delta T} \quad \ldots(8)$$

This formula has been devised so that at large values of ΔT, the value for U is as for a gas with the ratio of specific heats $\gamma = 1.300$.

The mass flux of steam, j, ($kg\ m^{-2}\ s^{-1}$) condensing at the bubble wall is given by the formula referred to by Collier[136]:

$$j = \left(\frac{2\sigma}{2-\sigma}\right) \frac{1}{(2\pi G)^{\frac{1}{2}}} \left[\frac{p}{Tg^{\frac{1}{2}}} - \frac{p_v}{T_s^{\frac{1}{2}}}\right] \quad \ldots(9)$$

where σ is a constant, which for steam is 0.04.

Computation of Bubble Dynamics

Writing:

p_e - external (atmospheric) pressure, Nm^{-2}

The equation of bubble motion first derived by Rayleigh is:

$$R\frac{d^2R}{dt^2} + \frac{3}{2}\left(\frac{dR}{dt}\right)^2 = \frac{p-p_e}{\rho} \qquad \ldots(10)$$

The solution of equation (10) may be regarded as the simultaneous solution of the equations:

$$\frac{dR}{dt} = Z \qquad \ldots(11)$$

$$\frac{dZ}{dt} = \frac{p-p_e}{\rho R} - \frac{3}{2}\frac{1}{R}Z^2 \qquad \ldots(12)$$

For the bubble there are also the equations:

$$\frac{dQ}{dt} = 4\pi R^2 \emptyset \qquad \ldots(13)$$

$$\frac{dM}{dt} = -4\pi R^2 j \qquad \ldots(14)$$

The equations (11), (12), (13) and (14) are solved using the second order Runge-Kutta method as described by Lance[137]. Taking a series of time intervals, Δt_n such that

$$t_{n+1} = t_n + \Delta t_n$$

and writing R_n for $\left[R\right]_{t=t_n}$. First a set of approximate values R', Z', Q' and M' for the quantities R_{n+1}, Z_{n+1}, Q_{n+1} and M_{n+1} are obtained from the equations:

$$R' = R_n + Z_n \Delta t_n,$$

$$Z' = Z_n + \left(\frac{p_n - p_e}{\rho R_n} - \frac{3}{2} \frac{Z_n^2}{R_n} \right) \Delta t_n,$$

$$Q' = Q_n + 4\pi R_n^2 \phi_n \Delta t_n,$$

$$M' = M_n - 4\pi R_n^2 j_n \Delta t_n.$$

From R', Z', Q' and M' all the other quantities characterising the physical state of the bubble may be calculated and in particular, p', Q' and j'. More accurate values of R_{n+1}, Z_{n+1}, Q_{n+1} and M_{n+1} may then be obtained from the equations:

$$R_{n+1} = R_n + \tfrac{1}{2} (Z_n + Z') \Delta t_n,$$

$$Z_{n+1} = Z_n + \tfrac{1}{2} \left(\frac{p_n - p}{\rho R_n} - \frac{3}{2} \frac{Z_n^2}{R_n} + \frac{p' - p}{\rho R'} - \frac{3}{2} \frac{Z'^2}{R'} \right) \Delta t_n$$

$$Q_{n+1} = Q_n + \tfrac{1}{2} (4\pi R_n^2 \phi_n + 4\pi R'^2 \phi') \Delta t_n,$$

$$M_{n+1} = M_n - \tfrac{1}{2} (4\pi R_n^2 j_n + 4\pi R'^2 j') \Delta t_n$$

From R_{n+1}, Z_{n+1}, Q_{n+1} and M_{n+1}, new values, p_{n+1}, Q_{n+1} and j_{n+1} may be calculated and the computation continued for the next step. The error in the calculated increment $R_{n+1} - R_n$ is of the form function $(R_n, Z_n, Q_n, M_n) \times (\Delta t_n)^3$.

This error may be calculated and the time step Δt_n adjusted to obtain the required accuracy.

The calculation of all other physical quantities for the bubble, when R_n, Z_n, Q_n and M_n are known, is now described.

Writing:

E_T - Energy delivered by the electrical circuit, J

$E_p = \frac{4}{3}\pi R^3 p_e$ - work done against external pressure, J

$E_K = 2\pi R^3 \left(\frac{dR}{dt}\right)^2$ - kinetic energy in water surrounding the bubble, J

U = Internal energy (thermodynamic) per unit mass of steam in the bubble, J kg^{-1}

From the conservation of energy,

$$E_T = Q + E_p + E_K + MU$$

$$\therefore U = (E_T - Q - E_p - E_K)/M \qquad \ldots(15)$$

Inverting equation (8) of the previous section to give ΔT in terms of U

$$T = 3.24675 \times 10^{-4} \left[-(4.94707 \times 10^6 - U) + \sqrt{(16.4575 \times 10^{12} - 6.23387 \times 10^6\, U + U^2)} \right] \qquad \ldots(16)$$

From equations (4), (6) and (7)

$$Tg = \Delta T + \frac{4889.98}{\log_e(2.08477 \times 10^{11} \frac{R^3}{GMTg})} \qquad \ldots(17)$$

✳ ✳ See page 144

The case when U=0 and Q=0 has been solved by Theofanous et al[138]. Writing the maximum bubble radius R_{max} and considering the subsequent motion of the bubble, equation (15) becomes:

$$\frac{4}{3}\pi R_{max}^3 \, p_e = \frac{4}{3}\pi R^3 p_e + 2\pi\rho R^3 \left(\frac{dR}{dt}\right)^2$$

Writing $\frac{R}{R_{max}} = y$, this equation can be expressed as an integral

$$t = R_{max}\sqrt{\left[\frac{3\rho}{2p}\right]}\int_{R/R_{max}}^{1} \frac{y^{3/2}\,dy}{\sqrt{1-y^3}}$$

In particular, the time to complete collapse,

$$t_c = R_{max}\sqrt{\left[\frac{3\rho}{2p}\right]}\int_{0}^{1} \frac{y^{3/2}\,dy}{\sqrt{1-y^3}}$$

$$= 0.9115\, R_{max}\sqrt{\left[\frac{3\rho}{2p_e}\right]}$$

As the bubble motion radius against time is symmetrical,

about $R=R_{max}$, the bounce time t_B from bubble initiation until bubble collapse is given by:

$$t_B = 2t_c = 1.8231\, R_{max} \left[\frac{3\rho}{2p_e}\right]$$

This result agrees with experimental measurement at lower water temperatures. However, at higher temperatures the bubble pressure is nearer the external pressure and motion ceases to be governed entirely by the external pressure p_e. With all the quantities known but Tg, equation (17) is solved by a method of trial and error to give Tg.

* *

Writing

L - latent heat of evaporation of steam, J kg^{-1}

Cp - specific heat of steam at constant pressure, J kg^{-1} K^{-1}

then $$\emptyset = j\left[L + Cp\,(Tg-T_S)\right]$$

Using this equation together with equations (1), (5) and (9),

$$\frac{K(T_S-T_W)\left(\frac{1}{R}+\frac{1}{\lambda}\right)}{L + Cp(Tg-T_S)} - 0.0835102\,\frac{MTg^{\frac{1}{2}}}{R^3} + 3.77252 \times 10^7 \exp\frac{\left(\frac{-4889.98}{T_S}\right)}{T_S^{\frac{1}{2}}} \qquad \ldots(18)$$

Inverting equation (2)

$$\lambda = \tfrac{1}{2}\left[\sqrt{\left\{R^2 + \frac{Q}{\pi C(T_S - T_W)P_r}\right\}} - R\right] \qquad \ldots(19)$$

Equations (15), (16) and (17) may be solved to give successive values of U, ΔT and Tg. A method of trial and error is used to solve equations (18) and (19). A trial value of T_S enables λ to be calculated from (19) and this then substituted into (18), a series of trials being made until equation (18) is satisfied.

REFERENCES

1 Raistrick A, 'The Coalbrookdale Ironworks; a short history', Ironbridge Gorge Museum Trust, 1975

2 Letter in the Sheffield City Archives, 26 July 1820

3 Wakabayashi K, Toyama University

4 Private Communication

5 Lipsett S G, 'Explosions From Molten Materials and Water', Fire Technology, 2, 118-126 (1966)

6 Witte L C, Cox J E and Bouvier J E, 'The Vapour Explosion', J of Metals, 22, 39-44 (1970)

7 Rengstorff G W P et al, Review of knowledge on explosions between aluminium and water, Aluminium Association, USA, April 1967

8 Health and Safety Executive, 'The Explosion at the Appleby-Frodingham Steelworks, Scunthorpe, 4 November 1975', HMSO, 1976

9 Long G, 'Explosions of Molten Aluminium in Water - Cause and Prevention', Metal Progress, 71, 107-112 (1957)

10 Laber D and LemmonJnr A W, 'Explosion of Molten Aluminium and Water', Annual Summary Report to the Aluminium Association, December 1970

11 Maischak K D and Feige W, 'Causes and Prevention of Aluminium Water Explosions', Neue Huette, 15, 662-665 (1970)

12 Epstein L F 'Analytical Formulations for the Reaction Rate of Metal-Water Reactions', USAEC Report, GEAP3272, 1958

13 Brauer F E, Green N W and Mesler R B, 'Metal-Water Explosions' Nucl Sci and Eng, 31, 551-554 (1968)

14 Flory K, Paoli R and Mesler R, 'Molten Metal-Water Explosions', Chem Eng Prog, 65, 50-54 (1969)

15 Genco J M and Lemmon Jnr A W, 'Physical Explosions in Handling Molten Slags and Metals', Trans of the American Foundrymen's Society, 78, 317-323 (1970)

16 Witte L C, Vyas T J and Gelabert A A, 'Heat Transfer and Fragmentation during Molten Metal-water Interactions', J Heat Transfer, 95, 521-527 (1973)

17 Zyszkowski W, 'Thermal Interaction of Molten Copper with Water', Int J of Heat Mass Transfer, 18, 271-287 (1975)

18 Bradley R H and Witte L C, 'Explosive Interaction of Molten Metals Injected into Water', Nucl Sci Eng, 48, 387-396 (1972)

19 Paoli R M and Mesler R B, 'Explosions of Molten Lead in Water', Proc of the 8th International Conference on High Speed Photography, Stockholm, Sweden, John Wiley and Sons, NY (1968)

20 Jennings A J D, 'The Physical Chemistry of Safety', Chem Eng (London), 290, 637-641 (1974)

21 Keey R B, 'Hazards of Heating Immiscible Liquids', Institute Chem Eng Symp Series No 49, 147-152 (1977)

22 Hughes J R, 'Storage and Handling of Petroleum Liquids: Practice and Law', Griffin, pages 145 and 220, 2nd Ed (1970)

23 Burgess D S, Murphy J N and Zabetakis M G, 'Hazards Associated with the Spillage of Liquid Natural Gas on Water', Report of Investigations 7448, US Department of the Interior Bureau of Mines, November 1970

24 Enger T and Hartman D E, 'Rapid Phase Transformation during LNG Spillage on Water', Proc 3rd Conference on LNG, Washington DC, 1972

25 Enger T and Hartman D E, 'Explosive Boiling of Liquified Gases on Water', Shell Pipe Line Corp R and D Lab, Houston, Texas 1972

26 Boyle G T, 'Vapour Production from LNG Spills on Water', Shell Research Ltd, UK, 1973

27 Rausch A H and Levine A D, 'Rapid Phase Transformations Caused by Thermodynamic Instability in Cryogens', Cryogenics, 224-229, April 1973

28 Katz D L and Sliepcevich C M, 'LNG Water Explosions, Cause and Effect', Hydrocarbon Processing, 50, 240-244 (1971)

29 Board S J, Hall R W and Brown G E, 'The Rate of Spontaneous Nucleation in Thermal Explosions: Freon/Water Experiments', CEGB Report no RD/B N-3007, June 1974

30 Enger T and Hartman D E, 'LNG Spillage on Water, 1 Exploratory Research on Rapid Phase Transformations', Shell Pipe Line Corp Technical Progress Report no 1-71, February 1971

31 Sallack J A, 'An Investigation of Explosions in the Soda Smelt Dissolving Operation', Pulp and Paper (Canada), 56, 114-118 (1955)

32 Nelson W and Kennedy E H, 'What Causes Kraft Dissolving Tank Explosions, I Laboratory Experiments', Paper Trade Journal, 140, 50-56 (1956)

33 Nelson W and Kennedy E H, 'Waht Causes Kraft Dissolving Tank Explosions, II Mill Investigations', Paper Trade Journal, 140, part 30, 30-32 (July 1956)

34 Osborne M J, 'Summary Report on the Activities of the Black Liquour Recovery Boiler Advisory Committee', TAPPI, 53, 2311-2313 (1970)

35 Taylor M L and Gardner H S, 'Causes of Recovery Boiler Explosions', TAPPI, 57, no 11, 76-78 (November 1974)

36 Hurst D G, 'The Accident to the NRX Reactor', AECL-233 (1953)

37 Epstein L F, 'Metal-Water Reactions, VII Reactor Safety Aspects of Metal-Water Reactions', USAEC Rep No GEAP-3335 (January 1960)

38 USAEC 'IDO Report on the Nuclear Incident at the SL-1 Reactor, Jan 3 1961', IDO 19302 (1962)

39 USAEC,'IDO Final Report of SL-1 Recovery Operation' IDO-19311, July 1962

40 Thompson T J, and Beckerley J G, 'The Technology of Nuclear Reactor Safety' MIT Press 1964

41 Hatfield G W, 'A Reactor Emergency with Resulting Improvements', Mech Eng, 77, 124-126 (1955)

42 Miller R W, Spano A H, Dugone J, Wieland D D and Houghtaling J E, 'Experimental Results and Damage Effects of Destructive Test', Trans Am Nucl Soc, 6, 137-144 (1963)

43 Elgert J O and Brown A W, 'In-pile Molten Metal-Water Reactions', US Atomic Energy Commisssion Publications, 10016257 (1956)

44 Cronenberg A W and Grolmes M A, 'Fragmentation Modelling Relative to the Breakup of Molten Uranium Dioxide in Sodium' J Nucl Safety, 16, 683-700 (1975)

45 Brittan R O, 'Analysis of the EBR-1 Core Melt Down', Proc of the 2nd UN Conference on Peaceful Uses of Atomic Energy, 12 (1958)

46 Gunnerson F S and Cronenberg A W, 'A Prediction of the Inert Gas Solubilities in Stoichiometric Molten Uranium Dioxide', J Nucl Materials, 58, 311-320 (1975)

47 Anderson R P and Armstrong D R, 'R-22 Vapour Explosions', Annual ASME Winter Meeting : Nuclear Reactor Safety, Heat Transfer Section, Atlanta, Georgia, 31-45 (1977)

48 Fauske H K, 'On the Mechanism of Uranium Dioxide-Sodium Explosive Interactions', Nucl Sci Eng, 51, 95-101 (1973)

49 Fauske H K, 'The Role of Energetic Mixed Oxide Fuel-Sodium Thermal Interactions in LMFBR Safety', Proc of the 3rd Specialist Meeting on Sodium/Fuel Interactions in Fast Reactors, Tokyo, Japan (1976)

50 Ergen W K et al, Emergency Core Cooling Report of Advisory Task Force on Power Emergency Cooling, USAEC (1966)

51 Ivins R O and Baker L, Chemical Engineering Division Argonne National Laboratory, Semi-Annual Report, ANL-6900 (Jan-June 1964)

52 Ivins R O et al, 'Reaction of Water as Initiated by a Power Excursion in a Nuclear Reactor (TREAT)' Nucl Sci Eng, 25, 11-140 (1966)

53 Colgate S A and Sigurgeissen T, 'Dynamic Mixing of Water and Lava', Nature, 244, 552-555 (1973)

54 Fishlock T P, 'Expel-A Computing Model For Molten Fuel Coolant Interactions in Fast Reactor Sub-assemblies', AEEW, R1029, October 1975

55 Caldarola L, 'A Theoretical Model for the Molten Fuel-Sodium Interaction in a Nuclear Fast Reactor', Nucl Eng and Design, 22, 175-211 (1972)

56 Cole R, 'Boiling Nucleation, Adv in Heat Transfer, 10 85-166 (1974)

57 Wismer K L, 'The Pressure-Volume Relation of Superheated Liquids', J Phys Chem, 26, 301-315 (1922)

58 Hall W B and Harrison W C, 'Transient Boiling of Water at High Temperatures', Proc 3rd Int Heat Transfer Conference, Inst of Mech Eng, Chicago, 193-203 (1966)

59 Tachibana F, Akiyama M and Kawamura H, 'Heat Transfer and Critical Heat Flux in Transient Boiling', J Nucl Sci Tech, 5, 117-126 (1968)

60 Yessin A O and Jeffers D E, 'Bubble Growth in Transient Pool Boiling', J Br Nucl Eng Soc, 8, 267-274 (1969)

61 Rogers T F and Mesler R B, 'An Experimental Study of Surface Cooling by Bubbles during Nucleate Boiling of Water', AI Ch EJ, 10, 656-660 (1964)

62 Cichelli M T and Bonilla C F, 'Heat Transfer to Liquids under Pressure Trans AI Ch EJ, 41, 755-787 (1945)

63 Cryder D S and Finalborgo A C, 'Heat Transmission from Metal Surfaces to Boiling Liquids: Effect of Temerature of the Liquid on Film Coefficient', Trans Am Inst Chem Eng, 33, 346-362 (1937)

64 Zuber N, 'On the Stability of Boiling Heat Transfer', Trans ASME Paper No 57, HT-4 (1958)

65 Forster H and Zuber N, 'Growth of a Vapour Bubble in a Superheated Liquid', J App Phys, 25, 474-478 (1954)

66 Berenson P J, 'Experiment on Pool Boiling Heat Transfer', Int J Heat Mass Transfer, 5, 985-999 (1962)

67 Bankoff S and Mehra V S, 'Quenching Theory for Transition Boiling', Ind Eng Chem Fundamentals, 1, 38-40 (1962)

68 Westwater J W and Santangelo J G, 'Photographic Study of Boiling', Ind Eng Chem, 47, 1605-1610 (1955)

69 Bradfield W S, 'Liquid Solid Contact in Stable Film Boiling', I and E C Fund, 5, 200-204 (1966)

70 Leidenfrost J G, 'De Aquae communis nonnullis qualitatibus tractatus (a tract about some qualities of common water), Disburg on Rhine, 1756

71 Spiegler P, Hopenfeld J, Silberberg M, Bumpus Jnr C F and Norman A, 'Onset of Stable Film Boiling and the Foam Limit', Int J Heat Mass Transfer, 6, 987-989 (1963)

72 Bromley L A, 'Heat Transfer in Stable Film Boiling', Chem Eng Prog, 46, 221-227 (1950)

73 Berenson P, Paper No 18, Heat Transfer Conference, Buffalo NY 1960

74 Hsu Y Y and Westwater J W, 'Approximate Theory for Film Boiling on Vertical Surfaces' Chem Eng Prog Symp Ser, 56, No 30, 15-24 (1962)

75 Dhir U K and Purohit G P, 'Subcooled Film Boiling Heat Transfer from Spheres', ASME paper 77-HT-78 (1977)

76 Purohit G P and Dhir U K, 'Vapour Film Collapse and its Application to Molten Metal Coolant Interaction', Trans Am Nucl Soc, 27, 665-666 (1977)

77 Walford F J, 'Transient Heat Transfer from a Hot Nickel Sphere Moving Through Water', Int J Heat Mass Transfer, 12, 1621-1625 (1969)

78 Stevens J W and Witte L C, 'Destabilisation of Vapour Film Boiling Around Spheres', Int J Heat Mass Transfer, 16, 669-678 (1973)

79 Board S J, Clare A J, Duffey R B, Hall R S and Poole D H, 'An Experimental Study of Energy Transfer Processes Relevant to Thermal Explosions', Int J Heat Mass Transfer, 14, 1631-1641 (1971)

80 Burmeister L C, 'Effect of Pressure Fluctuations on Laminar Film Boiling', PhD Thesis, Purdue University, 1966

81 Paschkis V and Stolz Jnr G, 'Quenching as a Heat Transfer Problem', J Metals, 8, 1074-1075 (1956)

82 Paschkis V and Stolz Jnr G, 'How Measurement Leads to Efficient Quenching', The Iron Age, 178, 95-97 (1956)

83 Paschkis V, 'The Coefficient of Heat Transfer during Quenching (in German)', Hart Techn Mitt, 15, 189-193 (1960)

84 Paschkis V and Stolz Jnr G, 'Research and Development with Respect to Heat Transfer Quenching, Armed Forces Tech. Information Agency Report No AD281854, Arlington, USA

85 Hinze J O, 'Forced Deformation of Liquid Globules' App Sci Res A1,263-272 (1949)

86 Hinze J O, 'Critical Speeds and Sizes of Liquid Globules' App Sci Res A1, 273-288 (1948)

87 Board S J and Hall W B, 'Propagation of Thermal Explosions, 1 Tin-Water Experiments', CEGB Report RD/B/N2850, 1974

88 Ivins R O, 'Interaction of Fuel, Cladding and Coolant', Argonne National Laboratory Report, ANL-7399 (1965)

89 Magarvey R H and Taylor B W, 'Free Fall Breakup of Large Drops' J App Phys, 27, 1129-1135 (1956)

90 Zuber N, 'On the Stability of Boiling Heat Transfer', Trans ASME, 80, 711-720 (1958)

91 Taylor G I, 'The Instability of Liquid Surfaces when Accelerated in a Direction Perpendicular to their Planes, I,' Proc Roy Soc, London, Ser A, 201, 192-196 (1950)

92 Swift D, Argonne National Laboratory Chemical Engineering Division Semi-Annual Report, ANL-7125 July-Dec 1965,

93 Epstein M, 'Thermal Fragmentation - A Gas Release Phenomena', Nucl Sci Eng, 55, 462-467 (1974)

94 Shiralkar G, 'An Investigation of the Fragmentation of Molten Metal Dropped into Cold Water', MIT 600-2781-7TR, 1976

95 Epstein M, Armstrong D R, Cho D H, Hauser G M and McDaniel R L, 'Reconsiderations of Gas Release in Molten Metal Fragmentation', Trans Am Nucl Soc, 27, 669-670 (1977)

96 Buxton L D and Nelson L S, 'Impulse Initiated Gas Release - A possible Trigger for Vapour Explosions', Trans Am Nucl Soc, 26, 398-399 (1977)

97 Hsiao K H, Cox J E, Hedgcoxe P G and Witte L C, 'Pressurisation of a Solidifying Sphere', J App Mech, 39, 71-77 (1972)

98 Cronenberg A W, Chawla T C and Fauske H K, 'A Thermal Stress Mechanism for the Fragmentation of Molten Uranium Dioxide upon Contact with Sodium Coolant', Nucl Eng and Design, 30, 443-453 (1974)

99 Armstrong D R, Goldfuss G T and Gebner R H, 'Explosive Interaction of Molten Uranium Dioxide and Liquid Sodium', Argonne National Laboratory Report, ANL-76-24 (1976)

100 Knapp R B and Todreas N E, 'Thermal Stress Initiated Fracture as a Fragmentation Mechanism in Uranium Dioxide-Sodium FCI', Nucl Eng and Design, 35, 69-76 (1975)

101 Swift D L and Baker Jnr L, 'Experimental Studies of the High Temperature Interaction of Fuel and Cladding Materials with Liquid Sodium', Proc of the Conference on Safety, Fuel and Core Design in Large Power Reactors, Argonne National Laboratory, ANL-7120, 1965

102 Fast, J D, 'Causes of Porosity in Welds', Philips Technical Review, 11, 101-110 (1949)

103 Groenveld P, 'Explosive Vapour Formation', J Heat Trans Trans ASME Series C, 94, 236-238 (1972)

104 Schins H, 'The Consistent Boiling Model for Fragmentation in Mild Thermal Interaction - Boundary Conditions', EURATOM Report: EUR/C-IS/699/73e (1973)

105 Kazimi M S, 'Theoretical Studies on Some Aspects of the Molten Fuel-Coolant Thermal Interaction', Science Doctorate Thesis, MITNE-154 MIT,May 1973

106 Bernath L, 'Theory of Bubble Formation in Liquids', Ind Eng Chem 44, 1310-1313 (1952)

107 Cronenberg A W and Grolmes M A , 'A review of Fragmentation Models Relative to Molten Uranium Dioxide Breakup when Quenched in Sodium Coolant' ASME paper: 74-WA/HT-42 (1974)

108 Flynn H G, 'Physics of Acoustic Cavitation in Liquids', Physical Acoustics,1(B), New York: WP Mason,Acad Press, 1964

109 Parsons C A and Cook S S, 'Investigations into the Causes of Corrosion or Erosion of Propellers', Trans Inst Nav Arch 61, 233-240 (1919)

110 Rayleigh, Lord (Strutt,John William), 'On the Pressure Developed in a Liquid During the Collapse of a Spherical Cavity', Phil Mag, 34, 94-98 (1917)

111 Harrison M, 'An Experimental Study of Single Bubble Cavitation Noise', DTMB report 815 (1952)

112 Peterson F B, 'Light Emission from Hydrodynamic Cavitation', PhD Thesis, Northwestern University, 1966

113 Kornfeld M and Suvarov L, 'On the Destructive Action of Cavitation', J App Phys, 15, 495-506 (1944)

114 Benjamin T B and Ellis A T, 'The Collapse of Cavitation Bubbles and the Pressures thereby Produced Against Solid Boundaries', Phil Trans Roy Soc, London, A260, 221-240 (1966)

115 Naudé C F and Ellis A T, 'On the Mechanism of Cavitation Damage by Non-Hemispherical Cavities Collapsing in Contact with a Solid Boundary', Trans ASME, 83, Ser D, J Basic Eng, 648-656 (1961)

116 Shutler N D and Mesler R B, 'A Photographic Study of the Dynamics and Damage Capabilities of Bubbles Collapsing Near Solid Boundaries', Trans ASME, 87, Ser D, J Basic Engineering, 511-517 (1965)

117 Floreschuetz L W and Chao B T, 'On the Mechanics of Vapour Bubble Collapse - A Theoretical and Experimental Investigation', Trans ASME, 87, Ser C, J Heat Transfer, 209-220 (1965)

118 Gibson D C, 'The Collapse of Vapour Cavities', PhD Thesis, Churchill College, Cambridge, 1967

119 Plesset M S and Chapman R B, 'Collapse of an Initially Spherical Vapour Cavity in the Neighbourhood of a Solid Boundary', J Fluid Mech, 47, 283-290 (1971)

120 Board S J, Farmer C L and Poole D H, 'Fragmentation in Thermal Explosions', Int J Heat Mass Transfer, 17, 331-339 (1974)

121 Buchanan D J, 'A Model for Fuel-Coolant Interactions', J Phys, D-7, 1441-1457 (1974)

122 Buchanan D J and Dullforce T A, 'Mechanism for Vapour

Explosions', Nature, 245, 32-34 (1973)

123 Hancox N L and Brunton J H, 'The Erosion of Solids by the Repeated Impact of Liquid Drops', Phil Trans Roy Soc, London, A260, 121-139 (1966)

124 Henry R E, Fauske H K and McUmber L M, 'Vapour Explosion Experiments with Simulant Fluids', Proc of the American Nuclear Soc Conference on Fast Reactor Safety, Chicago 1976

125 Henry R E and McUmber L M, 'Vapour Explosive Behaviour at Elevated Ambient Pressure', Argonne National Laboratory Report, ANL-77-34, 113-120, 1976

126 Henry R E and Fauske H K, 'Nucleation Characteristics in Physical Explosion', Proceedings of the 3rd specialist meeting on sodium/fuel interactions in fast reactors, Tokyo,596-623, 1976

127 Board S J and Hall R W, 'Recent Advances in Understanding Large Scale Vapour Explosions', Proceedings of the 3rd specialist meeting on sodium/fuel interactions in fast reactors, Tokyo,249-284, 1976

128 Konuray M M, 'The Interactions of Hot Spheres and Volatile Liquids', PhD Thesis, University of Aston in Birmingham, 1975

129 Chesterman W D, 'The Photographic Study of Rapid Events', Oxford,1951

130 Board S J, Farmer C L and Poole D H, CEGB Report, RD/B/N2423 (1972)

131 Worthington A M, A Study of Splashes, Longmans, Green and Co (1908)

132 Gilbarg D and Anderson R A, 'Influence of Atmospheric Pressure on the Phenomena Accompanying Entry of Spheres into Water', J App Phys, 19, 127-139 (1948)

133 May A, 'Vertical Entry of Missiles into Water', J App Phys, 23, 1362-1372 (1952)

134 Judd A M, UKAEA Report No AEEW-M792 (1966)

135 Judd A M, UKAEA Report No AEEW-M813 (1968)

136 Collier J G, Convective Boiling and Condensation , McGraw-Hill (UK) Ltd, p 309 (1972)

137 Lance G N, Numerical Methods for High Speed Computers, Iliffe and Sons Ltd, p 52 (1960)

138 Theofanous T G, Biasi L, Isbin H S and Fauske H K, 'Nonequilibrium Bubble Collapse: A Theoretical Study', Chem Eng Prog Symp Ser 66(102), 37-47 (1970)

"INTERACTION OF DROPS FALLING INTO VOLATILE LIQUIDS"

(Submitted for Ph.D degree)

G. POOL

DWELL-TIME MEASUREMENTS ON A MOLTEN TIN/WATER SYSTEM

Abstract

Measurements were made of the time taken for a molten tin drop at 500^{o}C to explode after entering water coolant. This 'dwell-time' was recorded by observing the pressure fluctuations within the coolant using a hydrophone and transient recorder device. On increasing the entry velocity of the molten drop, the dwell-time increased, and it also increased when the temperature of the water was raised. Such results are consistent with the vapour film collapse theory regarding explosive melt-coolant interactions (MCI's).

Introduction

Melt-coolant interactions (MCI's) have been the subject of widespread research during the past twenty years or so. The explosive possibilities associated with such interactions have prompted the sponsorship of many programmes of investigation aimed at minimising the risks involved when a hot melt is cooled in another liquid.

A violent MCI is caused by a rapid vaporisation of the coolant within the melt which tends to create a damaging shock wave. The manner in which the liquid coolant becomes intermixed with the melt has still to be fully determined and many theories have been proposed. However, the precursor to an explosion is generally considered to be direct contact between the melt and the liquid coolant.

On dropping a sufficiently hot liquid into water, boiling takes place around the melt and a film of vapour is created. It is across this film that heat is transferred from the hot liquid to the coolant

until the melt can no longer provide enough heat energy to maintain it. At this point, the film collapses to enable melt and liquid coolant to come into contact with one another. This preliminary formation of a vapour film and its subsequent collapse takes place over a time period commonly known as the 'dwell-time'. Previous measurements of dwell-time have been made using 10 - 15 gm of melt tipped from a crucible, whereas the work reported here has been carried out using small, reproducibly shaped droplets of melt. The results demonstrate how the dwell time may vary depending upon the the water temperature and also the velocity with which the melt enters the coolant.

Apparatus and Method

Droplets of molten tin at 500^{o}C were generated using a cylindrical melting tube made from graphite placed in an electrical furnace. At the lower end of the tube, a small hole enabled discrete droplets to form and fall under the weight of tin in the tube. The furnace was positioned so that the droplets were able to fall through a predetermined distance and enter a perspex tank full of coolant water. This enabled a variation of entry velocity to be made and dropping distances used were 3 cm, 6 cm, 12 cm, 18 cm and 24 cm. A standard measuring hydrophone type 8100 (supplied by Brüel and Kjaer of Denmark) was suspended in the coolant to monitor pressure waves. Its sensitivity (26.6 $\mu v/Nm^{-2}$) meant that very small fluctuations could be recorded and the pressure waves created by a droplet on entry into the coolant could be easily distinguished from those produced by an explosive event. The cable from the hydrophone was connected directly to the input/trigger terminal of a transient recorder (Datalab type DL 905). This instrument was able to store information gathered over a small time period and

display it on a CRO screen for analysis. The time sweeps used in this work were 2 ms and 5 ms, the resolution associated with which was 2 μs and 5 μs respectively.

A diagram of the experimental apparatus is given in Fig. 1.

The type of trace obtained when a droplet enters the water and explodes is shown in Fig. 2. The dwell-time is marked and represents the time between the first vibrations being sensed due to droplet entry and the subsequent explosive pressure peak.

The data collected was based upon the average dwell-time values obtained after 30 droplets had fallen under identical conditions into the coolant . For the system under examination, it was found that there were no explosions produced when tin drops fell into water above 61^{o}C.

Results and Discussion

The results obtained are shown graphically in Fig. 3. It may be seen that dwell time increases both with entry velocity and with water temperature. Values in excess of 2.5 ms are encountered as the water temperature is raised towards 60^{o}C.

An interpretation of such data may be made by considering the formation and collapse of the boiling film around the tin droplet prior to explosive interaction. The growth of such a film takes place at a linear velocity comparable to that reported by Forster and Zuber[1] of around 10 ft/sec. or 300 cm/sec. Such a growth rate becomes impeded when the entry velocity of the hot tin droplet is taken into account. In addition, after heat has been transferred across the film so that the melt temperature drops to the Leidenfrost point, then this entry velocity assists in the collapse of the film.

High speed cinephotography and short exposure spark illuminated photography[2] indicate that the boiling film thickness is of the order of 0.05 cm. and varies only marginally with coolant temperature. This being so, the time taken for a vapour film to be established around a cooling tin droplet at rest is approximately 0.16 ms. When an entry velocity is introduced, say 217 cm/sec., then this growth cycle takes 0.60 ms.

In broad outline, the dwell-time may be split into three parts and represented by

$$t = \underbrace{\frac{s}{(v_o - v)}}_{\text{(GROWTH)}} + \underbrace{\frac{s}{(v_o + v)}}_{\text{(COLLAPSE)}} + t'$$

where t is the total dwell-time,

s is the film thickness,

v_o is the growth and collapse rate of the boiling film,

v is the entry velocity,

t' is the time for which the fully established boiling film exists.

t' is dependent upon the coolant subcooling and also the entry velocity in that the speed of entry affects the heat transfer rate to the coolant.

It should be remembered that the dwell time values obtained for this tin/water system are quite short and that even at an entry velocity of 217 cm/sec, the droplet penetrates the water surface by only 6.5 mm. in 3 ms. Therefore, a boiling film which completely surrounds a tin droplet never becomes established.

The reproducibility of tin droplet size is depicted by a histogram in Fig. 4.

Conclusion

The data collected has been interpreted by considering the behaviour of the vapour film around a cooling tin droplet at 500°C. Values for

the dwell times are of an order of magnitude which agree well with observed growth rates for liquid-vapour interfaces and boiling film thicknesses.

An extension of the experimental technique would be to apply it to other metallic melts which are known to explode when in free contact with water coolant, such as bismuth, Wood's metal and lead. If it were possible to generate droplets in excess of 1 gm. mass, then this would increase dwell time and enable a boiling film to develop completely around a melt sample.

References

1. Forster, H. K. and Zuber, N., "Dynamics of Vapour Bubbles and Boiling Heat Transfer", AIChEJ, 1, 531-535, (1955)
2. Pool, G., Interaction of Drops Falling into Volatile Liquids, Ph.D Thesis, University of Aston in Birmingham, 1980.

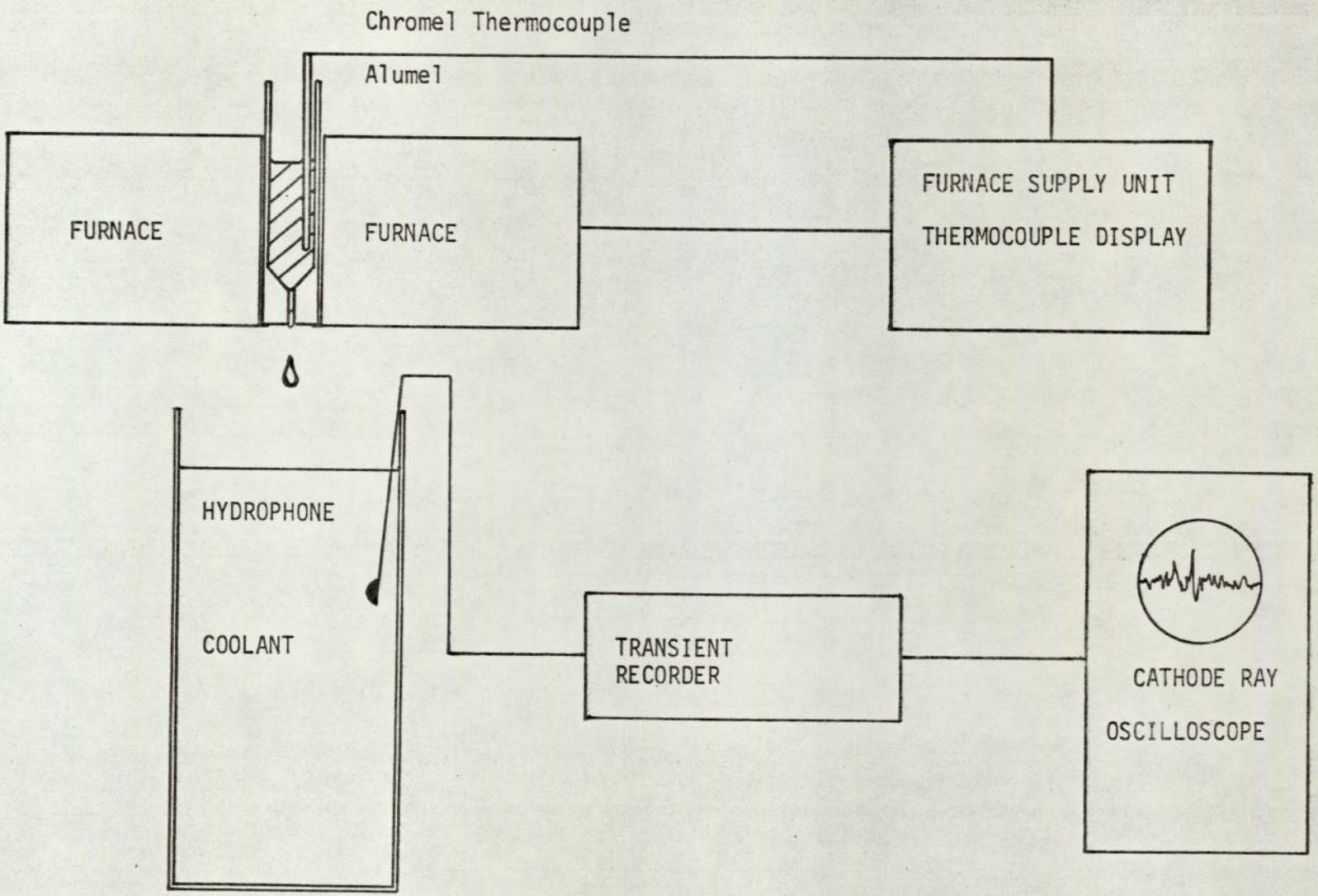

FIGURE 1. SCHEMATIC REPRESENTATION OF EXPERIMENTAL APPARATUS

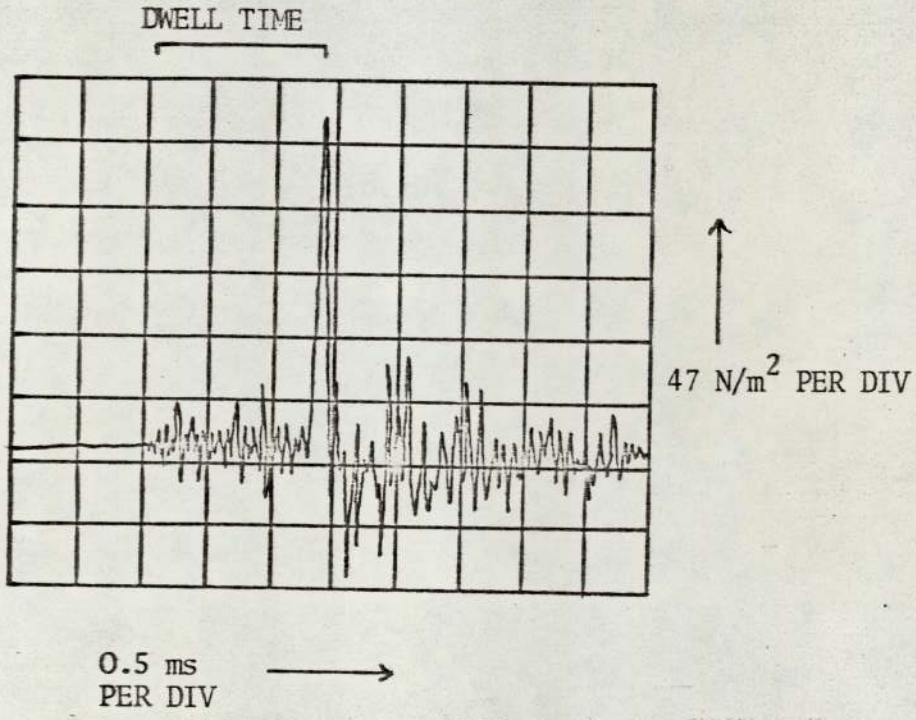

FIGURE 2. Pressure wave monitored using the transient recorder showing dwell time

FIGURE 3. DWELL TIME AS A FUNCTION OF WATER TEMPERATURE AND ENTRY VELOCITY OF DROPLET.

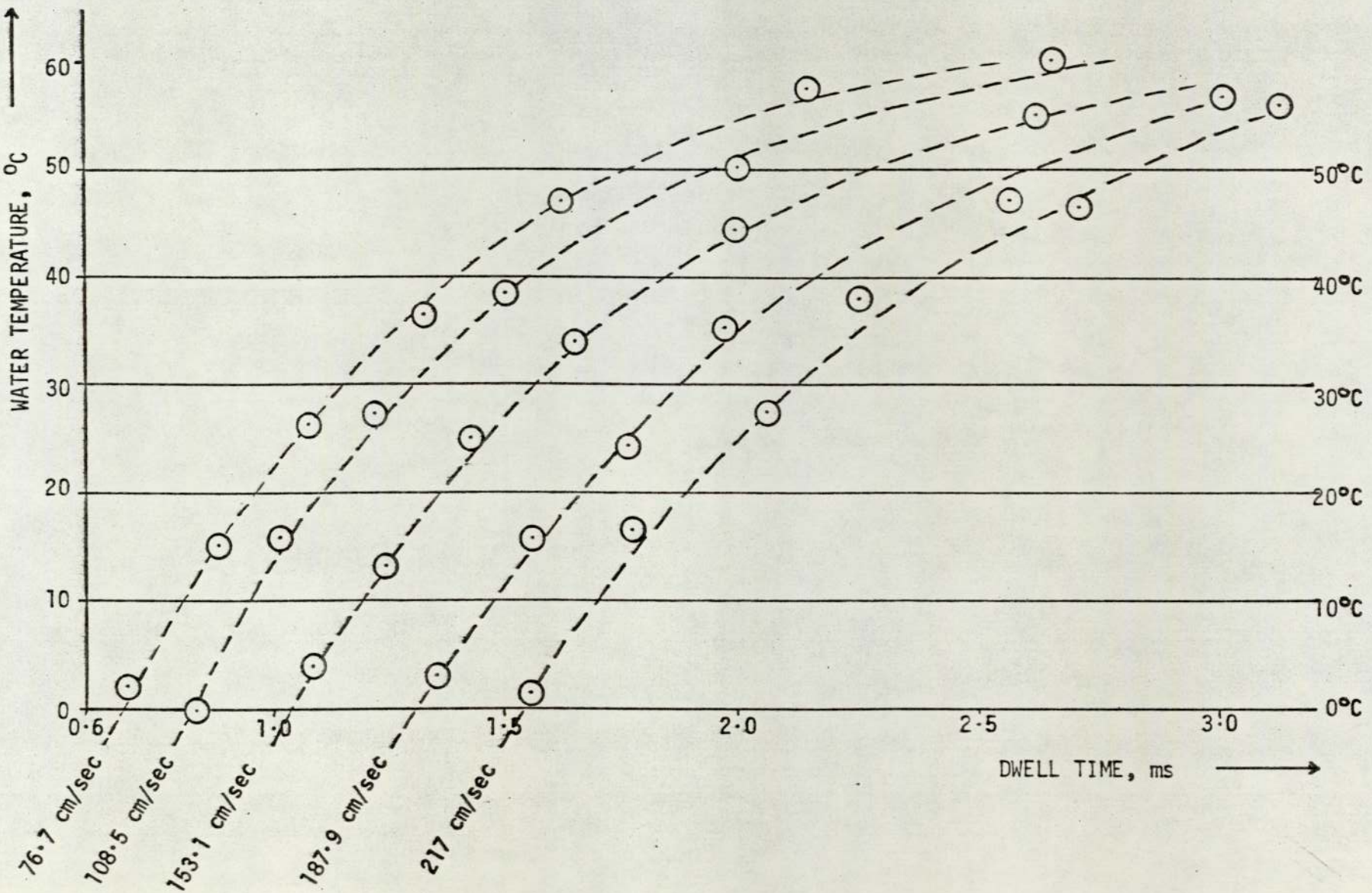

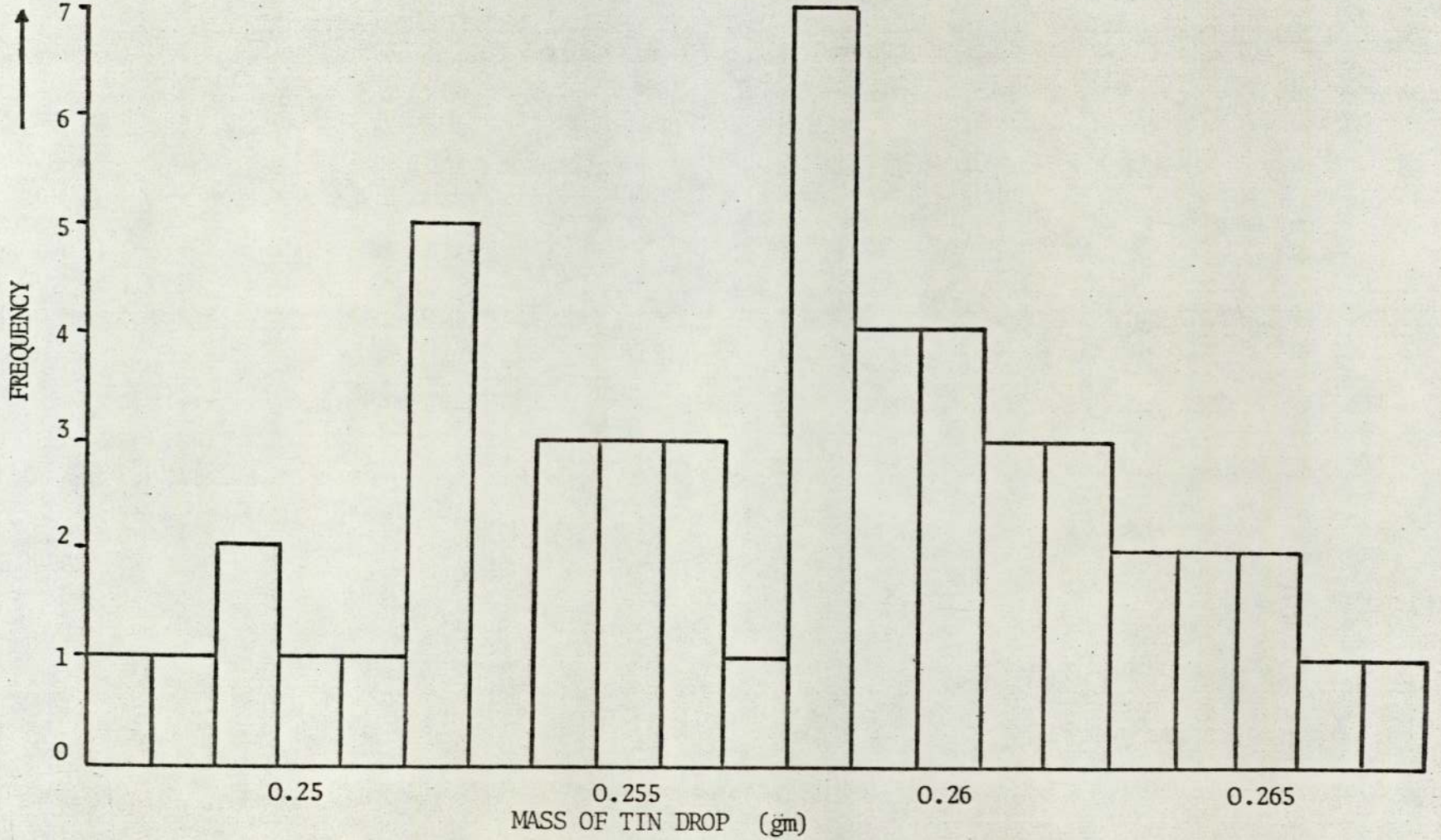

FIGURE 4. Weight distribution of tin drops